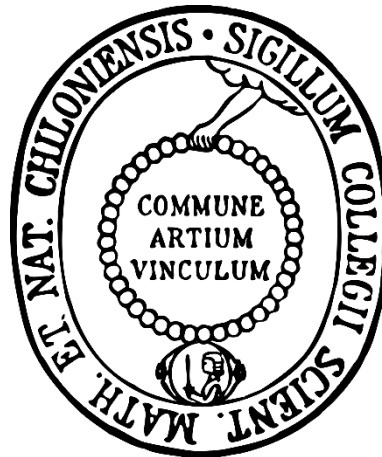


# ADVANCED POWDER CHARACTERIZATION TECHNIQUES FOR INHALATION POWDER MIXTURES



DOCTORAL THESIS  
SUBMITTED IN FULFILLMENT OF THE REQUIREMENTS  
FOR THE DEGREE OF  
DOCTOR IN NATURAL SCIENCE  
AT THE  
CHRISTIAN ALBRECHT UNIVERSITY,  
KIEL, GERMANY

BY

**EIKE CORDTS**

KIEL 2014

Referee: Prof. Dr. Hartwig Steckel  
Co-Referee: Prof. Dr. David Morton

Date of exam: 20.05.2014  
Accepted for publication: 20.05.2014

sgd. Prof. Dr. Wolfgang J. Duschl (Dean)

### **Research articles contributing to this thesis:**

- Buttini, Francesca; Colombo, Paolo; Chiapponi, Veronica; Balducci, Anna Giulia; Cordts, Eike; Steckel, Hartwig (2014): The Influence Of Energy Input During Dry Powder Blending on Dynamic Flow Properties, Powder Aerosolization and Dissolution of Dry Powders for Inhalation. In: Respiratory Drug Delivery 2014, Vol. 3, p. 697–702.
- Cordts, Eike; Steckel, Hartwig (2012): Capabilities and limitations of using powder rheology and permeability to predict dry powder inhaler performance. In: European Journal of Pharmaceutics and Biopharmaceutics 82 (2), p. 417–423.

### **Review articles:**

- Cordts, Eike; Steckel, Hartwig (2014): Formulation Considerations for Dry Powder Inhalers. In: Therapeutic Delivery, accepted for publication

### **Conference contributions:**

- Cordts, Eike; Steckel, Hartwig; Freeman, Tim (2013): Optimising the Performance of Dry Powder Inhaler Formulations through improved Powder Characterisation Techniques. Inhalation Asia. Hong Kong, China, 2013
- Cordts, Eike; Grasmeyer, Floris; van der Wel, P.; Dekens, Bert; de Boer, Anne H.; Steckel, Hartwig (2012): The influence of mixing time and intensity on blend homogeneity and dispersion performance. Drug Delivery to the Lungs 23. Edinburgh, UK, 2012.
- Cordts, Eike; Steckel, Hartwig (2011): Powder rheology analysis as tool for the characterisation of interactive powder mixtures. Drug Delivery to the Lungs 22. Edinburgh, UK, 2011.
- Cordts, Eike; Steckel, Hartwig (2011): The use of powder rheology to understand de-aggregation of inhalation powders. Powder Flow. London, UK, 2011.



*“The fundamental cause of the trouble is that in the modern world  
the stupid are cocksure while the intelligent are full of doubt”*

Bertrand Russell

Lack of a specific mark or a reference to a trademark or a patent does not imply that this work or part of it can be used or copied without copyright permission.

---

**TABLE OF CONTENTS**

<b>1. INTRODUCTION AND OBJECTIVES .....</b>	<b>1</b>
1.1 Introduction.....	1
1.2 Objectives.....	2
<b>2. INHALATION THERAPY .....</b>	<b>4</b>
2.1 Physiological considerations for formulation development.....	4
2.2 General requirements for inhalation products.....	7
2.3 Drug application devices.....	8
2.3.1 Nebulizers .....	8
2.3.2 Pressurized metered-dose inhalers (pMDIs).....	9
2.3.3 Soft mist inhaler (SMI).....	10
2.3.4 Dry powder inhalers (DPIs).....	10
2.4 Requirements for dry powder inhalation products .....	11
2.4.1 Particle size.....	11
2.4.2 Powder formulation.....	12
2.5 Composition of an adhesive inhalation mixture .....	16
2.5.1 Ternary fines addition .....	17
<b>3. PART 1 – MIXING INFLUENCE ON POWDER DISPERSION.....</b>	<b>19</b>
3.1 Introduction.....	19
3.2 Materials and Methods.....	21
3.2.1 Sieving.....	21
3.2.2 Mixing.....	22
3.2.2.1 High shear mixer .....	22
3.2.2.2 Free-fall mixer .....	24
3.2.3 Sample analysis.....	26
3.2.3.1 Determination of content uniformity .....	26
3.2.3.2 Sample analysis for impaction measurements.....	26

3.2.4	Dispersion measurements .....	27
3.2.4.1	Laser diffraction analysis.....	27
3.2.4.2	Carrier residue measurements.....	28
3.2.4.3	Impaction analysis.....	31
3.2.5	Scanning electron microscopy (SEM).....	35
3.3	Results.....	36
3.3.1	Content Uniformity.....	36
3.3.2	Dispersion measurements .....	37
3.3.2.1	Particle size analysis .....	37
3.3.2.2	Carrier residue, CR.....	37
3.3.2.3	Impaction analysis .....	42
3.3.3	SEM images.....	45
3.4	Discussion.....	47
3.4.1	Blend homogeneity .....	47
3.4.2	Laser diffraction .....	47
3.4.3	Carrier residue .....	47
3.4.4	Impaction analysis.....	51
3.5	Conclusion.....	52
<b>4.</b>	<b>PART 2 – POWDER RHEOLOGY AS TOOL FOR ADVANCED POWDER CHARACTERIZATION.....</b>	<b>54</b>
4.1	Introduction.....	54
4.1.1	Ternary fines addition .....	56
4.2	Bulk powder properties .....	58
4.3	Test methodologies to assess bulk behavior .....	60
4.3.1	Methodologies of the Pharmacopoeia.....	60
4.3.2	Non-pharmacopoeia techniques to investigate powder flow .	62
4.3.3	Powder rheology .....	64
4.4	FT4 Powder Rheometer®.....	65
4.4.1	Platform.....	65
4.4.2	Sample preparation.....	67
4.4.3	Bulk properties .....	68

---

4.4.3.1	Conditioned bulk density (CBD) .....	68
4.4.3.2	Compressibility .....	69
4.4.3.3	Permeability .....	69
4.4.4	Dynamic flow measurements .....	71
4.4.4.1	Basic flowability energy .....	71
4.4.4.2	Stability studies.....	73
4.4.4.3	Specific energy.....	74
4.4.4.4	Variation to blade tip speed.....	75
4.4.4.5	Program sequence .....	75
4.4.4.6	Aeration measurements.....	76
4.4.5	Shear measurements .....	77
4.4.5.1	Shear cell measurements.....	78
4.4.5.2	Wall friction test .....	79
4.5	Preliminary considerations and tests.....	79
4.5.1	Test reproducibility .....	79
4.5.2	Differences between lactose qualities.....	82
4.6	Materials and Methods.....	84
4.6.1	Sample preparation.....	84
4.6.1.1	Binary (drug-free) mixtures .....	85
4.6.1.2	Ternary mixtures.....	85
4.6.2	Content Uniformity.....	86
4.6.3	Dispersion measurements .....	86
4.6.4	Powder rheology analysis .....	89
4.6.4.1	Dynamic flowability testing of non-aerated powders .....	89
4.6.4.2	Permeability .....	89
4.6.4.3	Aeration testing.....	89
4.7	Results and Discussion.....	90
4.7.1	Aerosolization behavior .....	90
4.7.2	FT4 Powder Rheometer® measurements.....	94
4.7.2.1	Dynamic flow behavior with non-aerated powder.....	94
4.7.2.2	Permeability .....	95
4.7.2.3	Dynamic Aeration Tests .....	98
4.7.3	Comparison of permeability, aeration, and impaction analysis results.....	101

---

4.8	Limitations of FT4 Powder Rheometer® analysis .....	104
4.9	Conclusion .....	108
<b>5.</b>	<b>PART 3 – MIXING INFLUENCE ON DISSOLUTION BEHAVIOR.....</b>	<b>111</b>
5.1	Introduction.....	111
5.2	Materials and Methods.....	112
5.2.1	Blend preparation.....	112
5.2.2	Content Uniformity.....	115
5.2.3	NGI analysis .....	115
5.2.4	Dynamic powder rheology analysis .....	115
5.2.5	Dissolution behavior.....	116
5.3	Results and Discussion.....	116
5.3.1	Content uniformity .....	116
5.3.2	Laser diffraction analysis.....	117
5.3.3	Cascade impaction analysis .....	118
5.3.4	Powder rheology .....	120
5.3.5	Dissolution .....	124
5.4	Conclusion .....	126
<b>6.</b>	<b>OVERALL CONCLUSION AND FUTURE PERSPECTIVES .....</b>	<b>128</b>
<b>7.</b>	<b>SUMMARY.....</b>	<b>130</b>
<b>8.</b>	<b>SUMMARY (GERMAN).....</b>	<b>133</b>
<b>9.</b>	<b>APPENDIX.....</b>	<b>137</b>
9.1	Methods.....	137
9.1.1	Quantification of salbutamol sulfate content – UV/VIS.....	137
9.1.2	Quantification of API content – HPLC.....	138
9.1.2.1	Salbutamol sulfate.....	138
9.1.2.2	Budesonide.....	138
9.1.2.3	Salmeterol xinafoate .....	139
9.2	Materials.....	140

9.3 List of abbreviations.....142

**10. REFERENCES..... 144**







# 1. INTRODUCTION AND OBJECTIVES

## 1.1 Introduction

Inhalation therapy for the treatment of respiratory diseases such as bronchial asthma, chronic obstructive pulmonary disease or cystic fibrosis was shown to be superior in terms of efficacy and occurrence of drug related side effects compared to other administration routes (oral, intravenous, transdermal, for example) (Anderson *et al.*, 1975; Labiris and Dolovich, 2003; Onoue and Yamada, 2013; Shaw *et al.*, 1982). For local treatments, drug particles are able to reach their therapeutic target directly through inhalation and, therefore, a rapid clinical response and higher specific drug concentration can be achieved accompanied by a reduction of systemic adverse effects. As a result, current guidelines of the Global Initiative for Asthma (GINA, 2013) and Global Initiative for Chronic Obstructive Lung Disease (GOLD, 2013) suggest the use of inhalation products as first line therapeutics. The inhalation route has also become attractive for systemic delivery of drugs. The lung exhibits a large surface area with usually high membrane permeability, while a first-pass metabolism can be excluded (Labiris and Dolovich, 2003). Recently, an inhalation formulation (Adasuve<sup>®</sup>, Alexza UK Ltd.) for the acute treatment of agitation associated with schizophrenia or bipolar disorder in adults was approved by the US Food and Drug Administration (FDA) and European Medicines Agency (EMA). Also, new developments are currently awaiting approval containing inhalable insulin (Afrezza<sup>®</sup>, MannKind Corp.) or ergotamine (Levadex<sup>®</sup>, Allergan Inc.). Obviously, new developments are aiming towards the systemic administration of peptides, antibiotics, vaccines, anti-cancer substances or

other drug classes and will broaden the inhalation market considerably in the near future.

However, the development of an inhalation product is a complex task and a large number of different variables need to be considered. Unlike to most other dosage forms, an additional application device (inhaler) is essential to deliver the drug to its target region, the lungs. Consequently, the successful administration of drug is dependent on the medication formulation, the inhalation device, and the interactions between the two (Friebel, 2010). Also, breathing patterns of the patients differ significantly depending on their age, size, or disease state, and complicates the reproducibility and reliability of drug administration to the lungs (Mitchell *et al.*, 2007).

### **1.2 Objectives**

This thesis focuses on formulation aspects of dry powders for inhalation and only strikes the topics of inhalation device design and patient related factors. Despite many years of research, there is still no profound knowledge about the complex mechanisms involved in the formulation and dispersion of carrier based mixtures for inhalation (de Boer *et al.*, 2012). Therefore, advanced powder characterization techniques to investigate drug detachment and rheological bulk behavior were investigated to obtain improved mechanistic understanding.

After a brief general introduction about different aspects of inhalation therapy, the first part of this work focuses on the mixing process of adhesive powder blends for inhalation and its impact on the subsequent aerosolization behavior. In addition to the typically used *in-vitro* cascade impaction measurements, a second approach based on the classifier

technology (de Boer *et al.*, 2003) was applied to obtain an advanced understanding of particle interactions within the adhesive blends.

Secondly, the rheological behavior of adhesive mixtures with different amounts of ternary lactose fines as performance modifying agents was investigated. Rather than trying to display effects on a particulate basis, powder rheology assessments measure the consequences for the overall bulk behavior. Therefore, it was tested, whether specific measures of the bulk characteristics can be linked to the *in-vitro* inhalation performance of adhesive inhalation mixtures. The addition of excipient fines is known to be capable of improving the aerosolization of such blends. However, the exact mechanisms are still unclear and, with that, a justified recommendation about an optimal concentration within the mixtures cannot be given. Therefore, it was tested whether data obtained from rheological measurements, which capture powder properties under different stresses, can be utilized to propose mechanistic relationships within the blends.

In the final section of this thesis, adhesive powder blends were investigated by means of dissolution testing. Again, the impact of differences to the mixing process, i.e. mixing intensity, was related to the aerosolization performance and subsequent drug dissolution. The bulk behavior of the blends was also tested by means of powder rheology analysis to verify whether this methodology was capable of exposing mixing related differences between the powders. Further, mechanistic understanding obtained from the previous 2 parts was utilized to explain the observed differences in aerosolization and dissolution behavior, which were believed to be related to re- or de-agglomeration processes of the drug particles within the mixtures.

## 2. INHALATION THERAPY

### 2.1 Physiological considerations for formulation development

The respiratory tract consists of three main parts. The upper section includes the nasal passages and throat or pharynx, whereas the respiratory airways comprise the larynx, trachea, bronchi, and bronchioles. Thirdly, the lungs include the respiratory bronchioles, alveolar ducts, alveolar sacs, and alveoli. The trachea divides up into two main bronchi just before entering the right and left lung, which branch out further 20 – 23 times until terminating in the blood vessel-covered and gas exchanging alveoli (Figure 2.1).

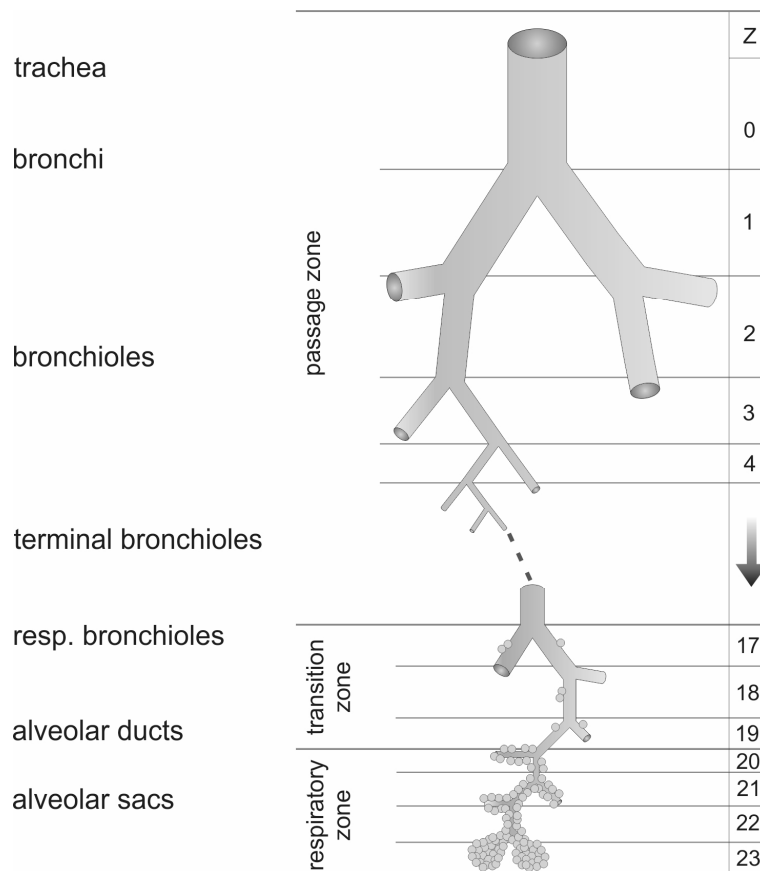


**Figure 2.1:** Division of the respiratory system, adapted from Mutschler *et al.* (2007)

Even though the cross-sectional area of each bronchus or bronchiole is decreasing consistently, the air resistance is lowered in the terminal branches due to the increase in total surface area (up to around 80 - 90 m<sup>2</sup> (Mutschler *et al.*, 2008)). More precisely, the highest air flow resistance and, hence, flow velocities are present in generations 6 - 8, before being reduced again dramatically in subsequent generations (Bossé *et al.*, 2010).

The lungs' primary function is the gas exchange between blood and air. It is the organ for atmospheric oxygen uptake and waste carbon dioxide release. However, the lungs also meet a number of auxiliary functions for respiration like cleaning, warming and moistening of the air. In particular the cleaning function is contrary to the intention of drug administration to the lower airways since drug particles or droplets may be filtered before reaching the lungs.

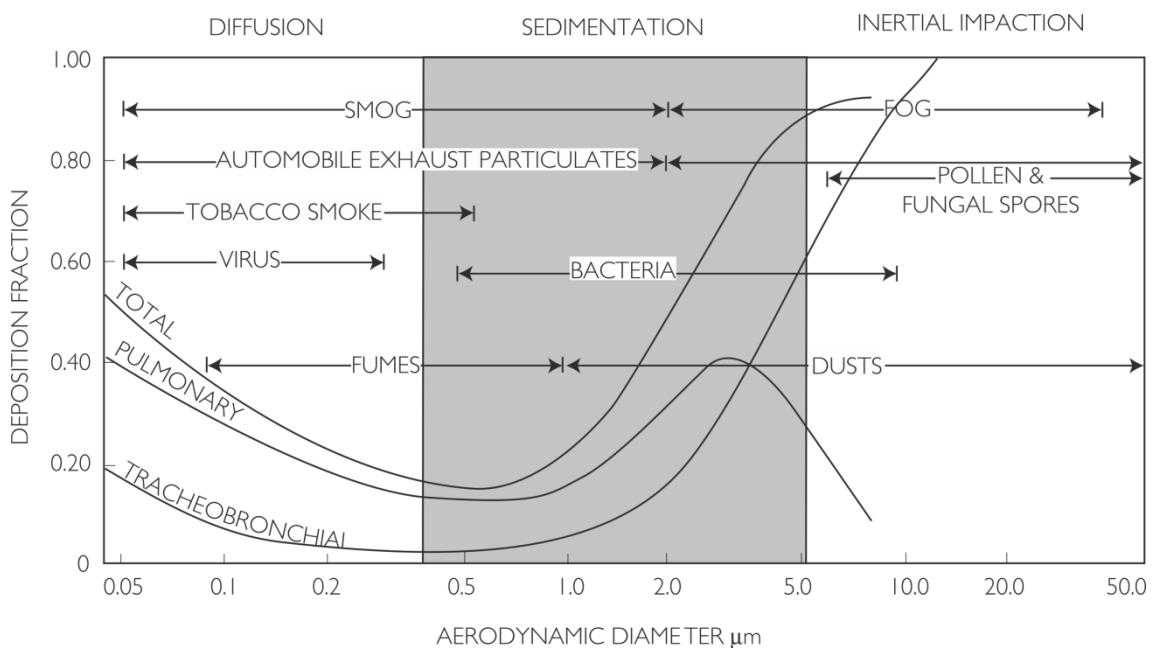


**Figure 2.2:** Relationship between particle size and lung deposition (reprinted from Labiris and Dolovich (2003))

The lungs filter particles mainly as a function of their aerodynamic size (see Figure 2.2). When inhaling an aerosol, which constitutes a disperse system of

dry or liquid particles in a gas phase, particles with an aerodynamic diameter  $> 5 \mu\text{m}$  predominantly deposit within the first decade of branches (“tracheobronchial” region) due to inertial impaction. Air flow velocity is comparably high and turbulent, which hinders large particles from following the airflow to lower lung regions (Figure 2.3a). Once impacted to the mucus covered walls, substances are removed mainly by ciliary clearance and are subsequently swallowed and digested. Objects in an aerodynamic size range between approximately  $0.4 \mu\text{m} - 5 \mu\text{m}$  are capable of penetrating the lower lung regions (“pulmonary” region) and deposit to the airway walls due to sedimentation (Figure 2.3b). Thirdly, particles  $< 0.4 \mu\text{m}$  may be affected by Brownian motion and, therefore, stick to the respiratory walls due to diffusion (Figure 2.3c). However, as a consequence of their low mass, small objects most likely will not remain in the lung tissue, but rather be exhaled again when breathing out.

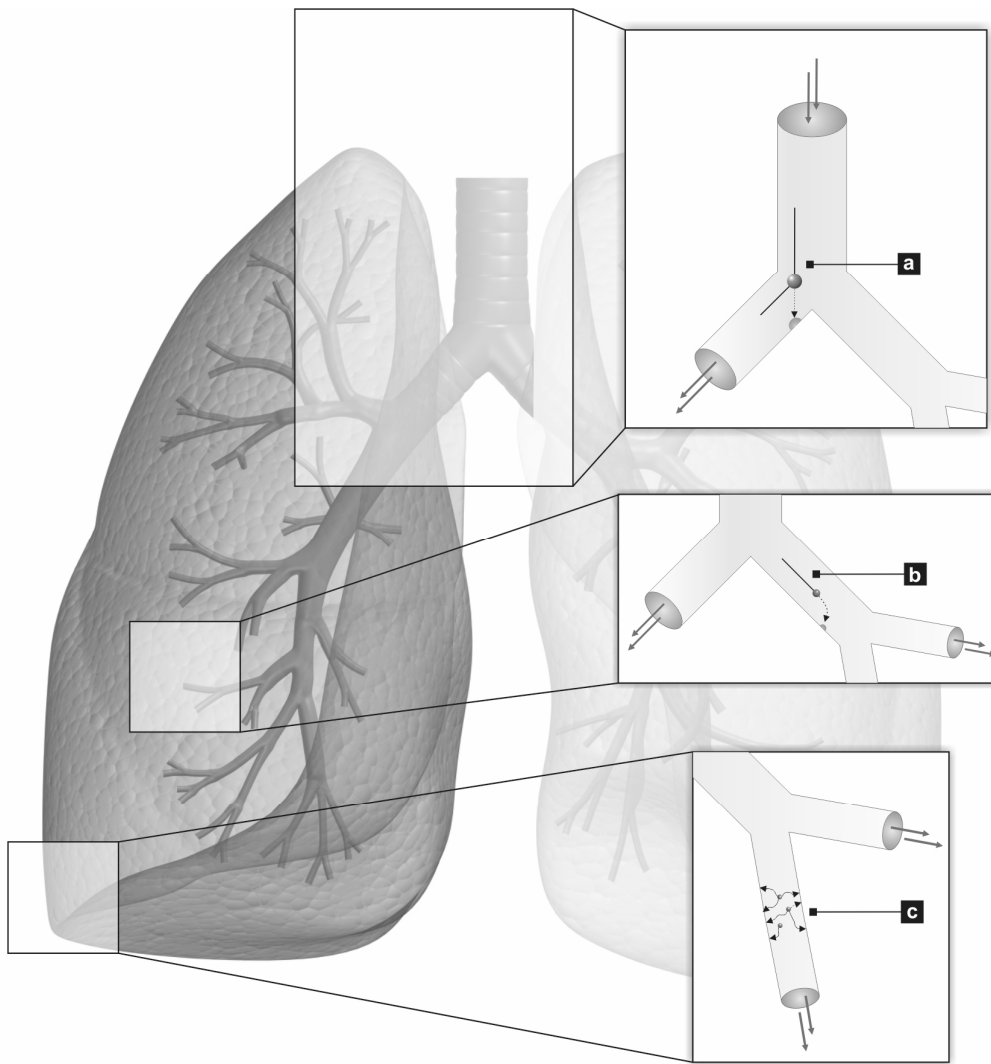


**Figure 2.3:** Deposition principles in the lung: **a)** inertial impaction, **b)** sedimentation, **c)** diffusion

## 2.2 General requirements for inhalation products

An inhalation product always consists of the drug containing formulation in combination with an appropriate dispersion device to generate the respirable aerosol cloud. Since the successful administration of medication is dependent on both, formulation aspects and device design, the requirements for the development of such a system may be of particular complexity.

In order to apply the desired amount of medication effectively to the lungs, particle size of the aerosolized formulation needs to be well controlled. Particles considerably larger than 5  $\mu\text{m}$  are prone to impact in the upper airways, which reduces treatment efficiency on the one hand and may increase adverse effects on the other hand. As described in section 2.1, drug particles in an aerodynamic size range between 1  $\mu\text{m}$  to 5  $\mu\text{m}$  are the most favorable for pulmonary delivery (see Figure 2.2).

### **2.3 Drug application devices**

Application devices can be classified into four distinct groups: active nebulizers, portable pressurized metered dose inhalers, soft mist inhalers, and the broad group of dry powder inhalers.

#### **2.3.1 Nebulizers**

Active nebulizers convert the drug solution or suspension into an aerosol either by a vibrating mesh, an ultrasonic transducer or by atomization (air jet nebulizer). The aerosol is then inhaled via a mouthpiece or a facemask until the solution has been fully aerosolized. As no specific coordination of the inhalation maneuver and device actuation is necessary, this type of administration is particularly suitable for small children or for ventilated patients. Also, multiple drug solutions may be applied at the same time (Kamin *et al.*, 2013). On the other hand, the need for a consistent power supply and the prolonged treatment time limit the usability in everyday life. Also, an inconsistent aerosolization has been reported as a shift in droplet size occurs over the nebulization duration (Phipps and Gonda, 1990; Steckel and Eskandar, 2003).

### 2.3.2 Pressurized metered-dose inhalers (pMDIs)

Portable pressurized metered-dose inhalers are suitable for drug solutions or suspensions and have been used since the 1950s with the introduction of the Medihaler (Anderson, 2005; Freedman, 1956). For this type of product, the drug is either dispensed in a solvent that is miscible with the propellant (for example, ethanol) or is dispersed in it to form suspensions. Additional stabilizing and/or performance modifying excipients may be added to the formulation before it is filled into a can with appropriate metering valve. The first MDI systems were based on chlorofluorocarbon propellants (CFCs), which have nowadays mostly been replaced by the less environmental harmful propellants of the hydrofluoroalkane-type (HFAs). Upon actuation the metered solution or suspension is forced through a spray orifice and gets torn apart into fine droplets, leaving solid particles in the micrometer range after the rapid evaporation of propellant. Advantages of this system such as low production costs and the generation of a very fine particle collective are opposed by stability issues and the high exit velocity of the aerosol cloud, which causes massive particle deposition in the oropharynx and typically results in a low respirable fraction. Also, issues including the correct coordination of MDI actuation and simultaneous inspiration (Khassawneh *et al.*, 2008), even in healthcare professionals (Baverstock *et al.*, 2010), result in an unsatisfactory MDI efficacy through reduced deposition of medication in the lungs (Price *et al.*, 2013). Lung doses of 21% (Brand *et al.*, 2008) or less were repeatedly found in various studies. With the use of spacers (Newman, 2004) or breath actuated systems, the coordination issues can be overcome; however, they are not yet implemented in the therapy on a routine basis.

### 2.3.3 Soft mist inhaler (SMI)

Another drug delivery option was introduced to the market with Boehringer Ingelheim's Respimat® soft mist inhaler. It eradicates many of the disadvantages of pMDIs by generating a more slowly moving aerosol cloud of longer duration and smaller droplet sizes out of the aqueous or ethanolic active pharmaceutical ingredient (API) solution. As a result, higher lung depositions can be obtained (Pitcairn *et al.*, 2005) even in patients with poor inhalation technique (Brand *et al.*, 2008). However, the current Respimat® is a non-reusable device, which ends up in a significant increase in cost of treatment. Further, the device is currently limited to the use of aqueous drug solutions and is therefore only useful for a low number of drug molecules..

### 2.3.4 Dry powder inhalers (DPIs)

These days, dry powder inhalers are widely accepted to deliver diverse types of medication. They first appeared in the 1970s when Bell *et al.* (Bell *et al.*, 1971) had developed Fisons Spinhaler®, a capsule-based inhaler to administer 20 mg of sodium cromoglycate. However, interest in the use of DPIs became especially evident with the ratification of the 1987 Montreal protocol, in which the participating countries agreed to phase out CFC-propellants as they were identified to accelerate ozone layer depletion. Consequently, existing pMDI formulations had to be reformulated to alternative systems.

Besides replacement for pMDIs, dry powder inhalers obliterate many limitations of the previously mentioned systems. They feature a portable device, for which the dispersion energy is generated by the patient's inhalation maneuver itself, rather than an external power supply or propellant. Therefore, today's marketed DPIs are breath actuated systems

that demand less coordination of the inhalation maneuver and dose actuation. Most of the DPIs on the market are built as multiple use devices, either equipped with a formulation reservoir and dose counter or the ability to insert new capsules or blisters prior to inhalation. By doing so, the inhaler can easily be adapted to improve stability issues of the formulation or be adjusted to patient demands.

## **2.4 Requirements for dry powder inhalation products**

The development of a DPI product is a very complex subject as the overall performance of the medication is influenced by a large number of factors and their interactions. These include, but are not limited to various properties of the drug itself, further formulation processes and considerations for the right choice of inhalation device.

### **2.4.1 Particle size**

Particle size is a driving factor with respect to the deposition site in the lungs. The smaller the aerodynamic diameter of the particles, the deeper they may penetrate into the airways (Carvalho *et al.*, 2011). In general, aerodynamic sizes between 1-5  $\mu\text{m}$  are recognized as suitable for targeting the lung tissue (see section 2.2). Dry particles in the respirable size range can be generated via various processing methods (fluid energy milling (micronization), spray drying, spray-freeze drying, super critical fluid processing). However, the physico-chemical properties of the obtained particles may vary considerably depending on the processing technique used. Extensive research has focused on particle processing and the related consequences on the dispersion efficiency of inhalation products (Chan and Chew, 2003; Chow *et al.*, 2007). A

more sophisticated view on the diverse processing techniques is out of this thesis' scope and it is referred to the cited literature for further details.

### **2.4.2 Powder formulation**

As a consequence of the need to use drug particles below 5  $\mu\text{m}$  in size, these powders are strongly cohesive and show very poor flowability (Thalberg *et al.*, 2004).

The relationship between particle size and increase in surface area is illustrated in Figure 2.4, in which particle count and total surface area are displayed as a function of particle diameter. The data is based on hypothetical, spherical lactose particles ( $\rho = 1,53 \text{ g/cm}^3$ ). It is apparent that there is an exponential increase in total surface area with decreasing diameters. The increase in surface area gives more opportunities for particle interactions and is thus one reason why powders with particle diameters especially below 10  $\mu\text{m}$  usually exhibit very poor flowability (Winkler, 2013). In addition, single particle mass (by gravitation) is massively reduced and, hence, interparticulate adhesive forces (e.g. van der Waals, capillary, or dielectric forces) dominate.

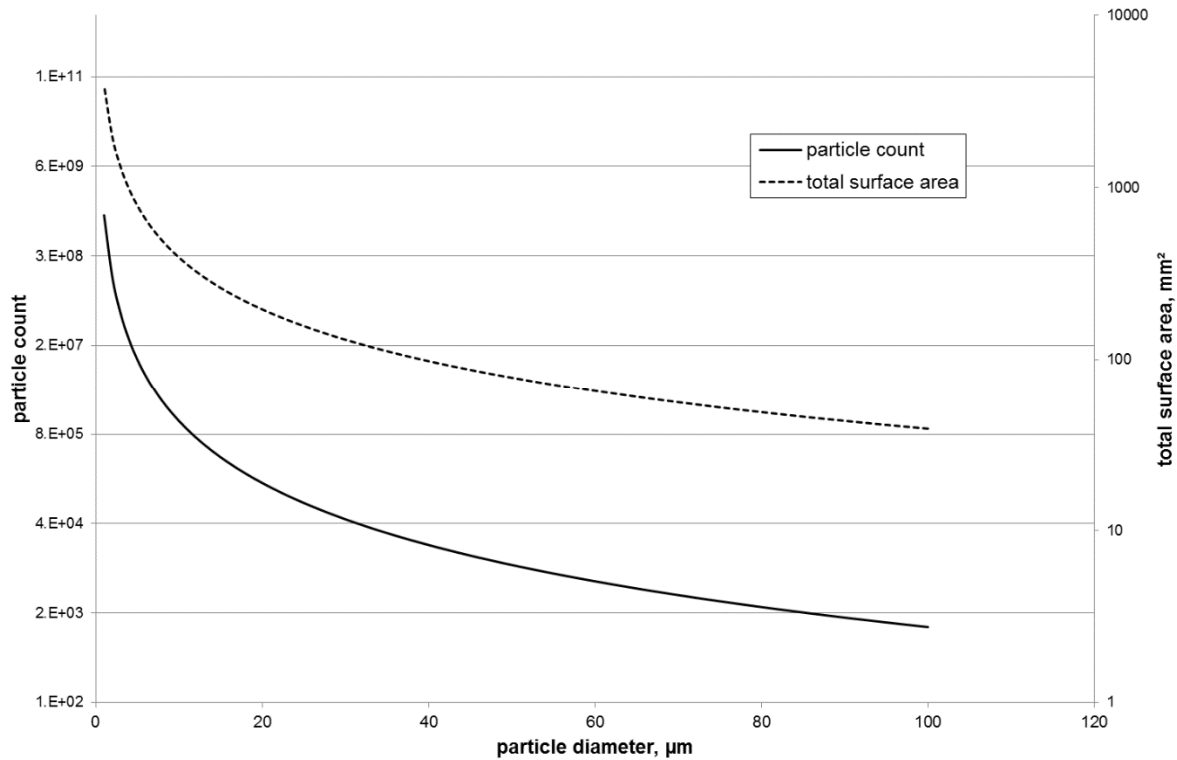


**Figure 2.4:** Hypothetical particle count and total surface area within 1 mg of lactose sample as a function of diameter, modified from Winkler (2013)

In order to achieve an accurate metering of the desired small quantities (sometimes as low as 6  $\mu\text{g}$  per dose), the drugs are either formulated with additional excipients or processed to soft spheres through spheronisation. The goal of both is to improve powder flowability, which is essential to allow volumetric filling of the device reservoir or capsules and blister cavities, respectively. The addition of coarse lactose increases the total mass and therefore the metering volume, leading to fewer variations in dosing. Further, the formation of an adhesive mixture improves the flowability significantly, as the used lactose is generally larger in size. A similar effect can be obtained through controlled agglomeration (spheronisation) of the micronized drug particles. The increase in agglomerate size goes in line with a decrease in inter-agglomerate forces and, hence, an increase in flowability.

Since micronization through milling of API is still, despite its lack of critical process parameter control (Rasenack and Müller, 2004), the most commonly used method to obtain particles in the respirable size range, further formulation steps to improve flowability are necessary. The aim is always to use the adhesive forces of the micronized powder to build up agglomerates that are larger in size and, therefore, exhibit improved powder flowability. For such a process, the control over agglomerate strength, i.e. the magnitude of interparticle forces, is fundamental. On the one hand, agglomerates need to be mechanically stable during storage, filling and dosing, on the other hand, the thorough dispersion into single particles upon inhalation is essential to achieve reasonable respirable fractions of the drug.

As mentioned before, agglomerates can be formed through spheronisation of pre-agglomerates (as obtained through sieving) of micronized materials. This approach was first patented by Fisons Limited (Bell, 1979), further developed by Astra Zeneca (Trofast and Falk, 1994) and is currently used for products in the Turbuhaler® and Twisthaler® devices. Likewise, Hartmann *et al.* (Hartmann *et al.*, 2008) developed a continuous process to produce comparable spheres through a vibration technique.

Most of the DPIs on the market, however, contain a powder formulation with additional carrier material. In theory, the micronized drug binds to the host crystal surfaces while blending and forms an adhesive mixture (Hersey, 1975); it gets separated again as individual particles during the inhalation maneuver (Figure 2.5).

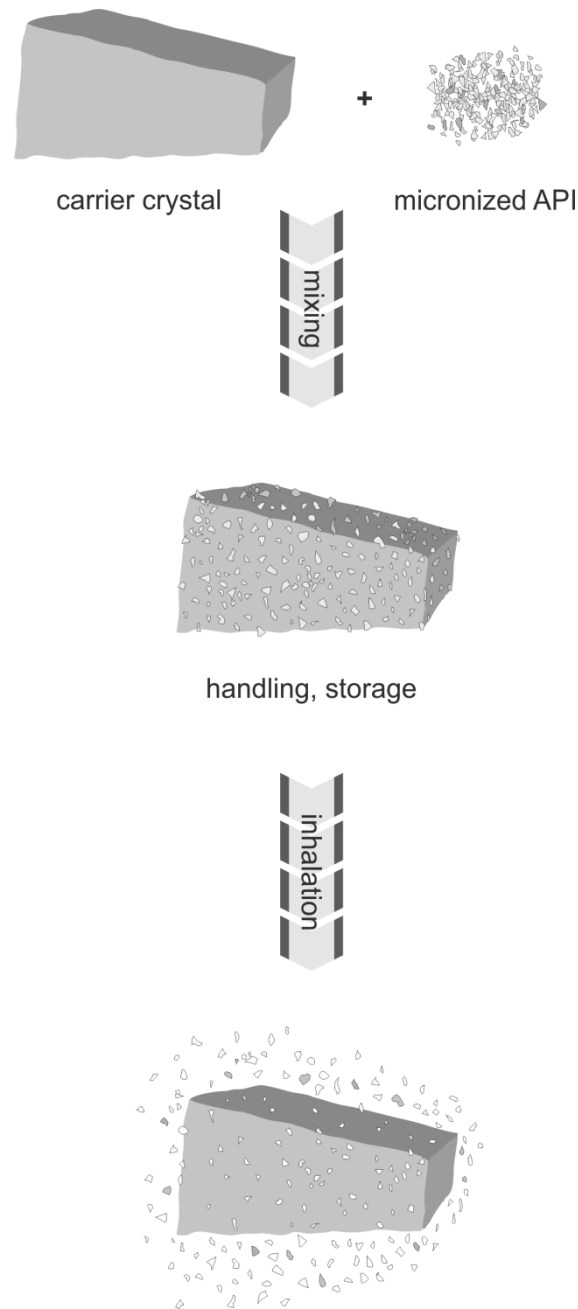


**Figure 2.5:** Adhesive mixture strategy for inhalation powders

As carrier material, different sugars and sugar alcohols like glucose monohydrate, mannitol, sorbitol, maltitol, xylitol, trehalose (Littringer *et al.*, 2012; Rahimpour *et al.*, 2013; Steckel and Bolzen, 2004; Tee *et al.*, 2000), and others have been tested. Nevertheless, alpha lactose monohydrate is presently the carrier of choice for almost all current DPis on the market (Pilcer and Amighi, 2010). The reasons for this are manifold; lactose has a

well-established safety and stability profile (generally recognized as safe (GRAS) excipient), production is inexpensive, various qualities are easily available on the market, it is less hygroscopic compared to alternative sugars, and the knowledgebase around its physico-chemical properties is quite extensive (Telko and Hickey, 2005). It presents a suitable carrier for the majority of API molecules; however, lactose may not be applicable for formulations containing substances that are incompatible with its reducing sugar function (especially peptides).

### **2.5 Composition of an adhesive inhalation mixture**

Generally, an adhesive powder mixture for inhalation purposes is composed of the micronized drug and excipient carrier material. A typical crystal carrier size ranges between 50 – 200  $\mu\text{m}$  in diameter and the payload of drug is usually between 0.1% - 4% by weight (Grasmeijer *et al.*, 2013) for currently available inhalation formulation. These two basic components are mixed together and the micronized drug is meant to detach from its host crystal upon inhalation through a DPI.

However, the de-agglomeration efficiency of the mixture is not only dependent on the drug and carrier sizes and quantities. Extensive research has been performed to study further influencing factors and their interactions. For instance, it was found that particle morphology, physico-chemical properties ((pseudo-) polymorphs (Traini *et al.*, 2008), amorphous content (Wittmann *et al.*, 2012)), dose (Grasmeijer *et al.*, 2013; Young *et al.*, 2005), and environmental conditions (Das *et al.*, 2009; Zhu *et al.*, 2008) also influence the de-agglomeration behavior significantly. A sophisticated review about the variety of impacting factors is out of the scope of this thesis, but it

needs to be mentioned and is concluded from the available literature that the very complex relationship between variables are still not fully understood.

### **2.5.1 Ternary fines addition**

Amongst others, one strongly influencing factor is the addition of a third component to the binary API/carrier mixtures. There are numerous publications about the increased respirable API fraction with the addition of a ternary fine (mostly micronized lactose) component. However, the exact mechanisms responsible for the performance modification are still unclear.

One supposed theory for the enhancement is the saturation of “active sites” on the carrier surface with excipient fines (regions of increased adhesive forces). It is proposed that excipient fines are likely to bind to these regions (passivation of active sites), thus shifting the micronized API particles towards lower energy binding sites (Staniforth, 1995, 1996). Consequently, drug/carrier adhesion decreases and a more thorough dispersion can be achieved upon inhalation. A second hypothesis includes the formation of drug/fine excipient agglomerates with beneficial overall dispersion properties. The formulation may result in a hybrid ordered system containing API/coarse carrier adhesion units and API/excipient fines multiplets. These multiplets detach more easily from the coarse carrier surface and, therefore, increase the extent of detached drug (Lucas *et al.*, 1998a; Lucas *et al.*, 1998b). Subsequently, the fine particle multiplets may be further dispersed in the air stream or remain intact and impact as agglomerates.

Both theories have been investigated by different groups in the past; however, conflicting findings have not led to a science-based explanation about the mechanisms involved in fines addition to a binary mixture. It needs

to be considered that the supplementation of fines is accompanied by an increased complexity of variables and interactions. It is referred to section 4, in which powder rheology techniques are investigated to gain an improved understanding of the overall powder behavior.

Different excipients may be used as ternary component, but amongst mannitol, sorbitol, trehalose, and others, alpha lactose monohydrate fines are the most commonly used in published literature. The optimal size range appears to be in the range of 5  $\mu\text{m}$  to 8  $\mu\text{m}$  (Jones and Price, 2006), however, a justified recommendation for the type of ternary component, size and morphology of the fine particles cannot be given at the moment. In particular, the ideal amount of added ternary component still remains unclear and demands further investigation.

It should also briefly be mentioned, that in contrast to the majority of marketed adhesive mixtures consisting of lactose and drug exclusively, the blends in FOSTER<sup>®</sup> NEXThaler<sup>®</sup> (Chiesi GmbH) include additional magnesium stearate particles as performance modifiers. Magnesium stearate has shown to decrease adhesive forces and thus improve the aerosolization performance (Guchardi *et al.*, 2008; Tay *et al.*, 2010).

### **3. PART 1 – MIXING INFLUENCE ON POWDER DISPERSION**

#### **3.1 Introduction**

Active pharmaceutical ingredients (APIs) for inhalation are mainly formulated as adhesive powder mixtures as a consequence of the requirements discussed in section 2.4. Many research groups have investigated and documented the impact of qualitative and quantitative differences in the blend composition on their de-agglomeration properties. The thorough understanding of particle processing and characterization is a key aspect when aiming towards improved powder de-agglomeration upon inhalation, i.e. fine particle fraction. However, concentrating on the qualitative and quantitative composition of the blends, the effects of variations to the mixing protocol itself (type of mixer, mixing time, and mixing intensity) have rather been neglected (de Boer *et al.*, 2012; Price, 2010). It is well known that the driving forces during mixing may affect particle ordering or randomization operations of constituents to different extents and may also influence re- or de-agglomeration tendencies of API particles. They (re-) distribute the micronized drug on the carrier surface and may induce tribocharging to the powder. Further, an increase in adhesion between drug substance and carrier particles is being discussed as a direct result of enhanced “press-on forces” (Dickhoff *et al.*, 2003; Podcizek, 1996). In contrast, possible weakening of adhesion forces may occur due to inertial separation forces during mixing.

Until today, no thorough knowledge of the unit operations and their interactions with other variables could be achieved. Underlying mechanisms responsible for the dispersion of carrier based powder mixtures are still not fully understood (de Boer *et al.*, 2012).

It can be expected that the process specifications during mixing of the raw materials directly affect parameters such as content uniformity or dispersion characteristics of the blend to different extents. Mixing is driven by the three principles diffusion, convection, and shearing (Egermann, 1991; Lacey, 1954) and the balance between these three is dependent on the choice of mixing equipment (free-fall mixer, high shear mixer). Consequently, subsequent effects like friction or impaction, which contribute to the overall result, are generated to a different extent as well.

For example, Hartmann (Hartmann, 2004) demonstrated in his work that in a high shear Diosna mixer an increase in mixing time had negative effects on the dispersion behavior, i.e. fine particle fraction, with a FlowCaps® device. This contrasts with findings from a study of Hagedoorn *et al.* (Hagedoorn *et al.*, 2011), in which they detected an increase in detached drug particles from the carrier with increasing mixing times in a Turbula® tumbler mixer at low inspirational flow rates.

In this study, binary inhalation powder blends of the same drug-lactose composition were produced with two different types of mixers. A small scale high shear mixer (Hosokawa Micron B.V. Picomix®) and a three-dimensional motion mixer (Turbula®) were used to prepare the mixtures and the results were compared by means of dispersion measurements and content uniformity tests. Finally, the data was analyzed to hypothesize on underlying mechanisms responsible for the observed dispersion behavior. The presented work was conducted in collaboration with the Department of Pharmaceutical Technology and Biopharmacy, University of Groningen, The Netherlands.

## 3.2 Materials and Methods

### 3.2.1 Sieving

$\alpha$ -Lactose monohydrate (Pharmatose 80M, DMV-Fonterra Excipients, Goch, Germany) served as carrier for the micronized API in the binary blends. The batch lactose was handled for 20 minutes on a vibratory sieve (Retsch AS 200 control, Haan, Germany) with an amplitude of 1.5 mm and the fraction between a 312  $\mu\text{m}$  and 250  $\mu\text{m}$  sieve was collected. Subsequent to this first step, the fraction was transferred to an air jet sieve (Hosokawa Alpine e200LS, Augsburg, Germany) with a 90  $\mu\text{m}$  mesh and treated for additional 10 minutes. The second sieving step served to remove any intrinsic lactose fines from the carrier surfaces.

With such a coarse particle size of the crystalline carrier material the impact of potential “press-on forces” during the mixing process and, with that, hypothetical effects on the aerodynamic characterization were hoped to be stressed (Grasmeijer *et al.*, 2013).

Micronized salbutamol sulfate (supplied by DFE Pharma, Goch, Germany) (see Table 3.1) was passed through a 90  $\mu\text{m}$  sieve to destroy any larger agglomerates before further use.

**Table 3.1:** Particle size parameters of used drug material (laser diffraction, dry dispersion, R3, 3 bar)

	$x_{10} \pm \text{SD}, \mu\text{m}$	$x_{50} \pm \text{SD}, \mu\text{m}$	$x_{90} \pm \text{SD}, \mu\text{m}$
salbutamol sulfate (SS10204002)	0.63 $\pm 0.00$	1.27 $\pm 0.01$	2.79 $\pm 0.01$

After sieving, the starting materials were allowed to stand for at least 24 hours to dissipate potential electrostatic charges.

### 3.2.2 Mixing

Two devices with different mixing principles (free-fall and high shear mixing, respectively) were used to prepare the model powder formulations.

#### 3.2.2.1 High shear mixer

The preparation of API blends was done with a Picomix<sup>®</sup> high shear mixer (Hosokawa Micron B.V., Doetinchem, The Netherlands) (Figure 3.1). The lab-scale equipment is based on the Cyclomix<sup>®</sup>-principle (see Figure 3.2) and with its maximum working volume of 180 cm<sup>3</sup> it provides the possibility to process powders in small batches. The rotational speed of the impeller is continuously variable in a range of 500 rpm to 6000 rpm. In a mixer based on the Cyclomix<sup>®</sup>-principle, the good gets affected by the impeller not only horizontally, but, in combination with the conical shaped vessel, rather experiences additional vertical acceleration, which results in an improved mixing efficiency (Ng *et al.*, 2007).



**Figure 3.1:** Picomix<sup>®</sup> high shear mixer

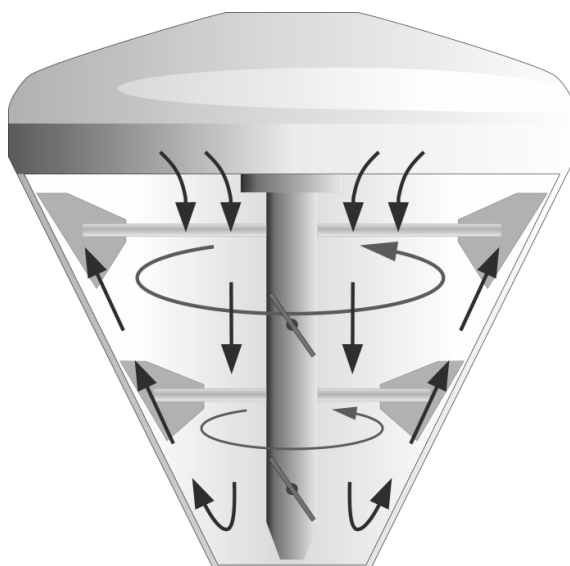


**Figure 3.2:** Cyclomix® principle – product flow pattern, adapted from HOSOKAWA MICRON B.V.

The micronized salbutamol sulfate was added to an initial load of carrier lactose (approximately half of total mass) in the mixing vessel and was covered with the remaining carrier powder. The total batch size for each blend in the high shear mixer was 60.0 g, which corresponds to a filling degree of about 45% (v/v).

The ambient temperature and humidity were monitored during the process; all mixtures were prepared at temperatures between 19.0 °C and 20.6 °C and a relative humidity between 41.5% and 67.5%.

Three compositions were prepared at different rotational speeds of the impeller (500 rpm, 750 rpm, and 1000 rpm, respectively). Samples were drawn at fixed time points (see Table 3.2) to check for content uniformity on the one hand (Section 3.2.3.1) and perform further aerodynamic characterization on the other hand (section 3.2.4).

**Table 3.2:** Mixing protocol and time points for sample drawing

total mixing time, s	mixing protocol	remaining powder mass after sample drawing
15	2 s (300 rpm) + 13 s (500 rpm)	approx. 57.0 g
30	+ 2 s (300 rpm) + 13 s (500 rpm)	approx. 54.0 g
60	+ 2 s (300 rpm) + 28 s (500 rpm)	approx. 51.0 g
300	+ 2 s (300 rpm) + 238 s (500 rpm)	approx. 48.0 g

The total mixing time summed up to 300 s and got interrupted three times to draw the appropriate samples. At each start of the mixing process, the powder was initially exposed to a rotational speed of 300 rpm for 2 seconds before the desired speed was established for the remaining time. This start sequence was necessary to bring the powder bed in the desired movement pattern within the mixing vessel (see Figure 3.2).

Drug content uniformity on the one hand and possible lactose particle comminution on the other hand were identified as critical process parameters. Preliminary tests had revealed that a mixing time of 15 s was sufficient in order to obtain homogeneous powder mixtures for all rotational speeds used. In addition, mixing for 300 s at a rotor speed of more than 1000 rpm showed an apparent particle size reduction, which was confirmed by particle size measurements using laser diffraction (see section 3.2.4.1).

Finally, the production of the three mixtures was repeated to obtain a total of six mixes for further testing.

### 3.2.2.2 Free-fall mixer

Two additional salbutamol sulfate/lactose blends were prepared with a T2C Turbula® free-fall mixer (WA Bachhofen, Basel, Switzerland). An appropriate stainless steel mixing vessel for small batches with a volume of 160 cm<sup>3</sup> was

used. The batch size was 25.0 g, which corresponds to a filling ratio of about 20% (v/v).

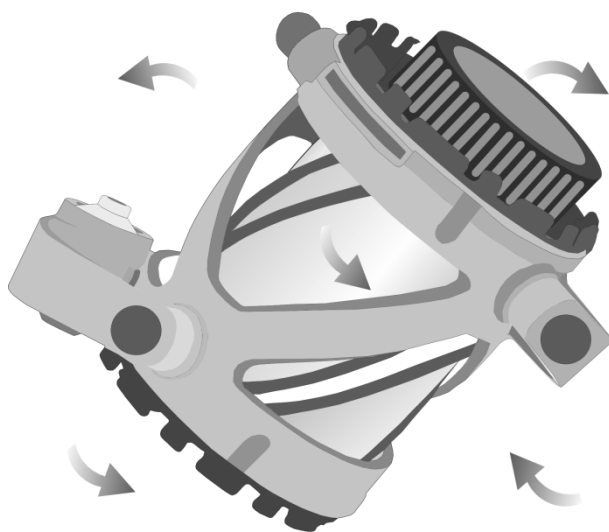


**Figure 3.3:** Movement of mixing vessel in the Turbula®

Filling of the raw materials was carried out in a similar manner as described for the Picomix® blends (see section 3.2.2.1).

Different rotational speeds were selected for the preparation of mixtures (20 rpm and 90 rpm, respectively). The total mixing time of 60 minutes was interrupted only once to draw samples at a time point of 0.5 minutes (for 90 rpm) or 5 minutes (for 20 rpm), respectively. The discrepancy of first time points for collecting the samples is the result of observations from preliminary experiments which had shown that at 20 rpm a mixing time less than 5 minutes would not be sufficient to distribute the drug homogeneously throughout the powder bed.

Again, the preparation was repeated, so that a total of four mixtures were produced by the free-fall mixer, and could be analyzed further.

### 3.2.3 Sample analysis

#### 3.2.3.1 Determination of content uniformity

The determination of the content uniformity was carried out by taking ten random samples at the indicated mixing times. The powder was spread on a sheet of paper and multiple samples of about 50 mg were drawn and collected in HPLC vials. Subsequently, 25 mg  $\pm$  1 mg were weighed accurately from each sample and mixed with about 15 g of demineralized water, also weighed accurately. After vortexing, the samples were set aside for about an hour to ensure that the salbutamol sulfate/lactose mixture had been fully dissolved. The sample size corresponded to the size of a single dose administered in the aerodynamic tests (see section 3.2.4.2). The drug concentration was measured using a UV/VIS spectrophotometer (Unicam UV-500, ThermoSpectronic, UK) at a wavelength of  $\lambda = 225$  nm. A coefficient of variation (CV) of less than 5% for the ten individual contents was set as the acceptance criteria for blend homogeneity.

#### 3.2.3.2 Sample analysis for impaction measurements

The samples from impaction measurements (see section 3.2.4.3) were analyzed via high performance liquid chromatography. The additional stage coating in the samples interfered with spectrophotometric analysis and made this change in methodology necessary. The impaction samples were dissolved in defined amounts of double distilled water (dd H<sub>2</sub>O) and analyzed by HPLC (see Appendix 9.1.2.1).

### 3.2.4 Dispersion measurements

#### 3.2.4.1 Laser diffraction analysis

A Helium-Neon Laser Optical System, HELOS® (Sympatec, Clausthal-Zellerfeld, Germany) with dry dispersion unit RODOS® was used to measure the volumetric particle size distribution of the binary blends and, thus, check for possible particle comminution as a result of the mixing process.

Briefly, a single particle diffracts a parallel laser beam and forms an according diffraction pattern (Figure 3.4). This pattern is dependent on the particle size and can be described mathematically by Fraunhofer or Mie theory. The distance from the center to the first minimum is recorded as  $r_0$  and can be recalculated as the particle diameter. The superposition intensity distribution of the diffracted light from a particle collective can now be captured through a Fourier lens and be recorded by a multi-element photo-detector. Calculation of the volumetric particle size distributions was performed with WINDOX 5 software (Sympatec, Clausthal-Zellerfeld, Germany). However, the obtained particle diameter refers to a sphere resulting in decreased measurement accuracy with increasing shape factors (de Boer *et al.*, 2002b).

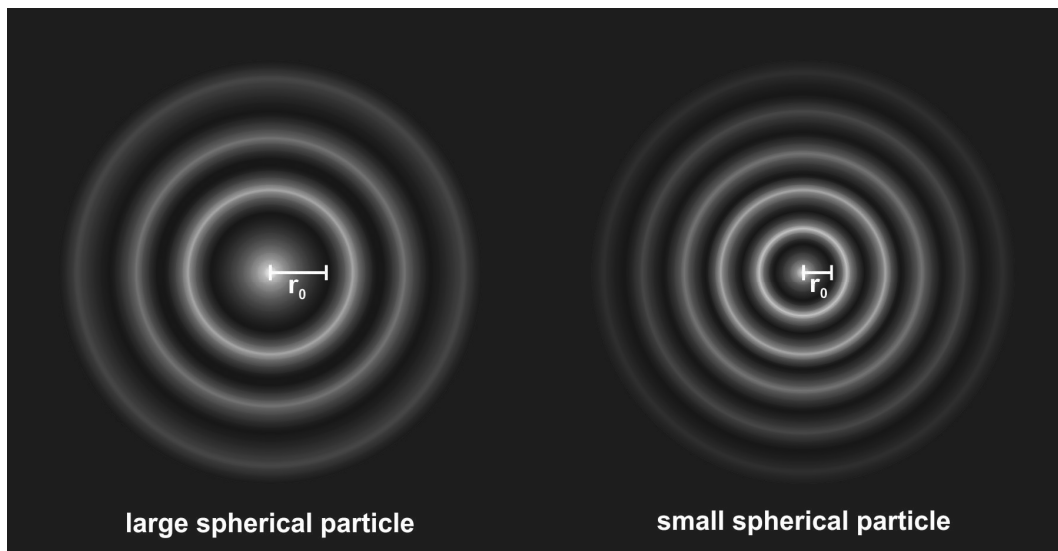


**Figure 3.4:** Laser light diffraction patterns of spherical particles

The RODOS<sup>®</sup> was set to operate at a pressure of 5 bar in order to disperse agglomerates of fine lactose particles that might have been formed during blending due to particle attrition. Approximately 9 g of sample was fed by means of a vibrational feeder (VIBRI<sup>®</sup>, Sympatec, Clausthal-Zellerfeld, Germany) and optical concentrations of around 20% were achieved for the measurements.

### 3.2.4.2 Carrier residue measurements

A special test inhaler developed by de Boer *et al.* (de Boer *et al.*, 2003) was used to determine the residual amount of salbutamol sulfate on the carrier surface after dispersion (see Figure 3.5). It is designed in a way that enables the possibility to classify particles according to their size (Air Classifier Technology, ACT). The adhesive powder mixture is filled into a cylindrical classifier chamber with tangential air supply channels, which gets sealed off by a lid with outlet channel (classifier discharge channel). By applying a certain inspiratory air flow at the mouthpiece (mouthpiece cylinder), the powder gets accelerated in the classifier chamber in a tangential direction.

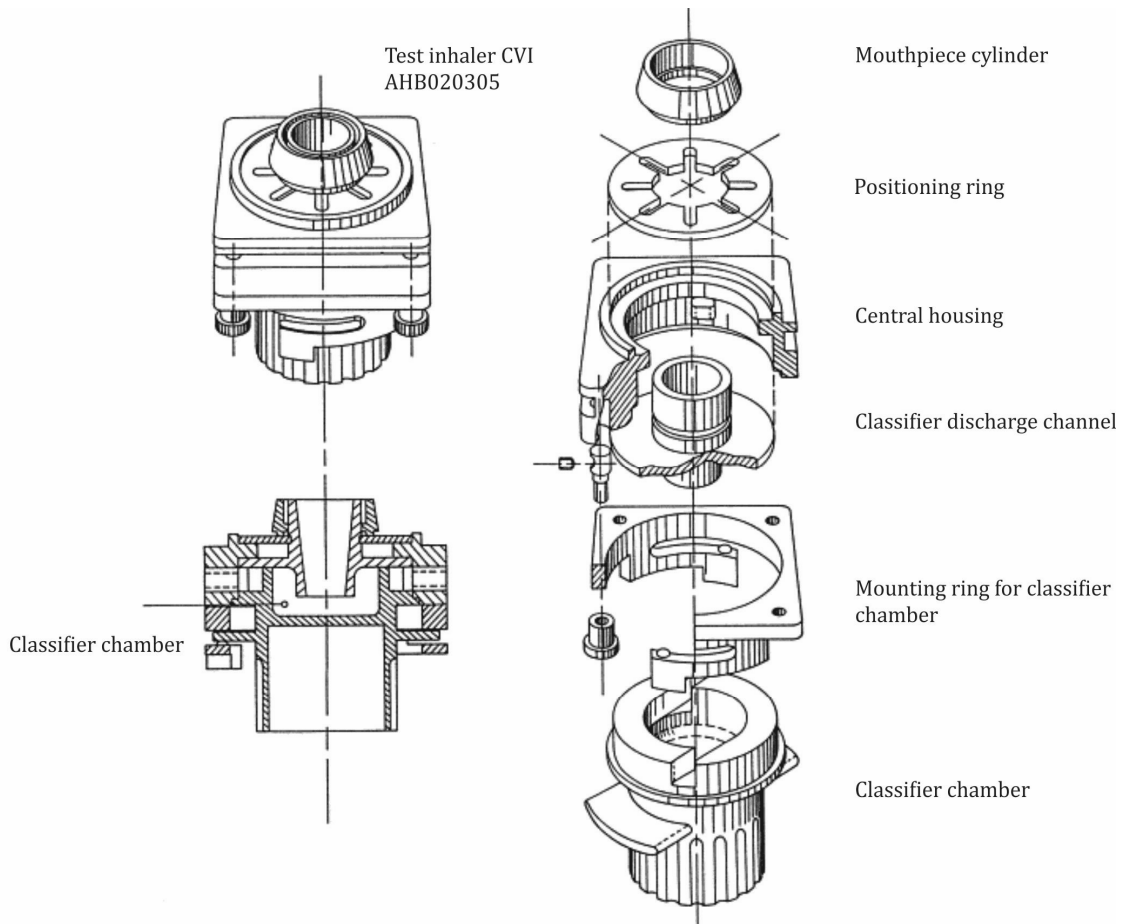


**Figure 3.5:** Schematic of “classifier” test inhaler (de Boer *et al.*, 2003)

In the device, particles are affected by two counter acting forces: drag force  $F_D$  and centrifugal force  $F_C$  (see Figure 3.6). The scale of drag forces ( $F_D$ ) occurring is directly proportional to the first power of the particle diameter and is especially dominant for the behavior of small particles. In contrast, large particles are particularly influenced by the centrifugal force ( $F_C$ ), as this effect is proportional to the third power of the diameter (de Boer *et al.*, 2003). Finally, fine particles (drug) overcome the forces of adhesion, detach from the lactose carrier, and are able to discharge from the inhaler through the central outlet opening. The coarse lactose particles (+ adhering fine particles) remain in the classifier chamber and may be recollected for further investigated.

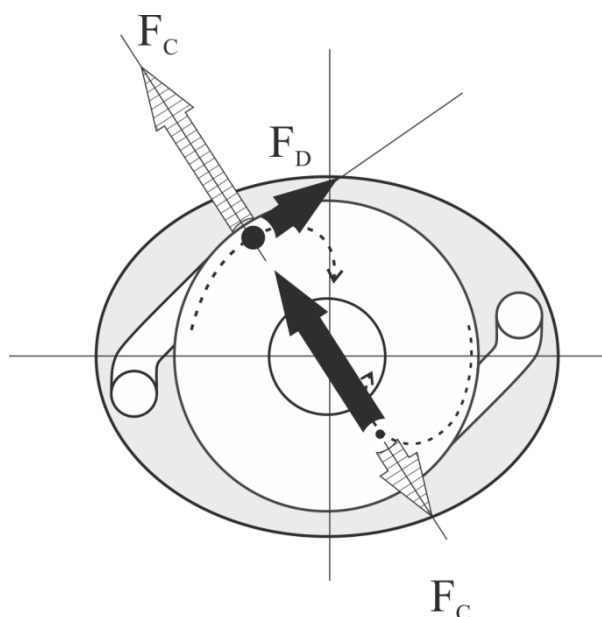


**Figure 3.6:** Schematic (top view) of acting forces on a particle in the classifier chamber (adapted from de Boer *et al.* (2003))

The test inhaler was operated at three different flow rates (20 L/min, 40 L/min, and 60 L/min, respectively). A mass of  $25 \pm 1$  mg was given into the classifier chamber and the appropriate air flow was applied for 3 seconds (flow-rate independent). Due to the device resistance of the test inhaler ( $0.056 \text{ kPa}^{0.5} \text{ min/L}$ ), corresponding pressure drops of 1.25 kPa, 5.02 kPa, and 11.29 kPa, respectively, were achieved. After 3 seconds, the inhaler was opened again and the non-discharged powder was collected and reconstituted with 5.0 g of demineralized water. Hence, the salbutamol sulfate particles that still adhered to the carrier surface were determined rather than the amount of detached drug particles which is the case for impaction analysis (see section 3.2.4.3). After complete dissolution of the samples, the drug content was measured spectrophotometrically at a wavelength of  $\lambda = 225 \text{ nm}$  (as described in section 3.2.3.1). The absorption values were corrected for the amount of a lactose reference.

The drug residue (hereinafter referred to as “carrier residue” or CR) was related to the initial sample mass and expressed as percentage for further comparison. CR is calculated as the average of 5 individual measurements.

### 3.2.4.3 Impaction analysis

Cascade impaction analysis was used to assess the aerodynamic particle size distribution (PSD) of the different formulation mixtures. The aerodynamic particle size refers to the diameter of a sphere with a unit density of  $1 \text{ g/cm}^3$ , having the same terminal settling velocity in still air as the particle in consideration (de Boer *et al.*, 2002a). It is related to its geometric diameter by the following Equation 3.1, in which  $\rho_p$  refers to the particle density and  $\rho_0$  to the sphere unit density ( $1 \text{ g/cm}^3$ ), respectively, and  $X$  is used as a shape factor ( $X = 1$  for spherical particles).

$$d_{ae} = d_{geo} \sqrt{\left(\frac{\rho_p}{\rho_0 X}\right)} \quad (3.1)$$

The aerodynamic PSD is a Critical Quality Attribute (CQA) and serves as an *in-vitro* measure for the performance of an inhalation product.

A Next Generation Pharmaceutical Impactor (NGI) (Copley Scientific, Nottingham, UK) with preseparator was used for the measurements in this work.

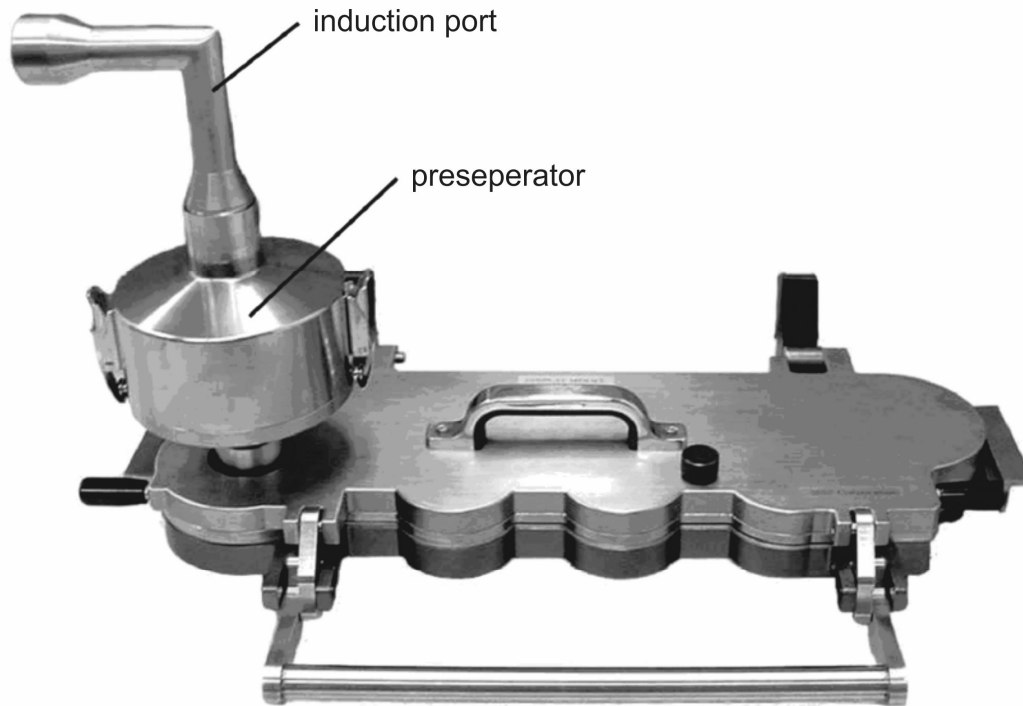


**Figure 3.7:** Closed NGI with preseparator and induction port

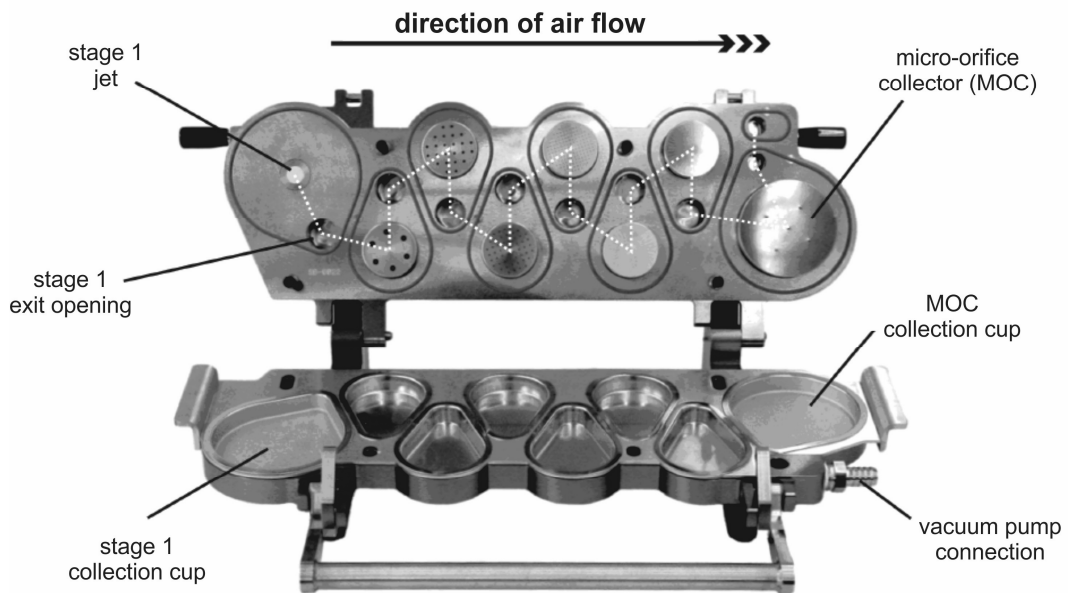


**Figure 3.8:** Opened NGI with collection cups

The NGI separates particles through inertial impaction at different stages in the equipment. The air flow passes through the impactor in a saw tooth pattern and its velocity increases continuously by forcing it through nozzles

of decreasing jet sizes. Subsequently, larger particles impact in the early stages of the NGI due to their increased inertial forces, whereas small particles are able to follow the air flow further down to later impaction stages (Figure 3.9). Each stage is assigned a specific cut-off diameter, which needs to be recalculated depending on the applied air flow.

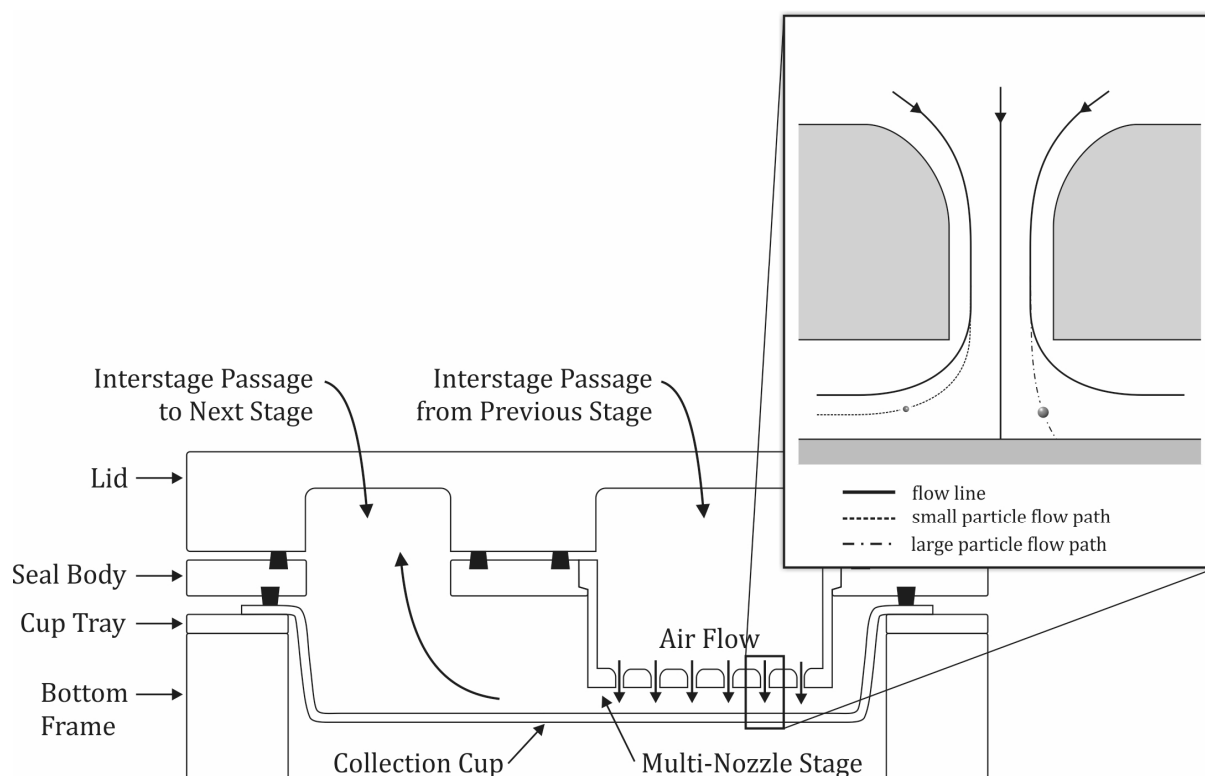


**Figure 3.9:** NGI stage layout adapted from USP (2013b) with flow lines and particle flow paths in a jet with deposition surface (modified from Wachtel (2009))

The particles deposited in each collection cup were dissolved with defined amounts of appropriate media and be analyzed via UV/VIS spectroscopy, HPLC, or other techniques. By plotting the amounts of drug particle remains on each stage as a function of cut-off diameter, the amount of API <math> < 5 \mu\text{m}</math> can be derived from the log-normal distribution. This amount is referred to as fine particle dose (FPD,  $\mu\text{g}</math>), or in conjunction with the recovered or total dose the fine particle fraction (FPF, %). For this work, the FPF is always expressed as the fraction <math> < 5 \mu\text{m}</math> of the recovered dose (including the device, induction$

port, and preseparator). For completeness, other size parameters that can be determined should be mentioned briefly, such as mass median aerodynamic diameter (MMAD,  $\mu\text{m}$ ), which describes the median of the distribution of airborne particle mass; and the geometric standard deviation (GSD,  $\mu\text{m}$ ), which is a measure for the width of an aerodynamic particle size distribution.

NGI analysis was performed according to the requirements of the European Pharmacopoeia's monograph 2.9.18 *"PREPARATIONS FOR INHALATION: AERODYNAMIC ASSESSMENT OF FINE PARTICLES"* (Ph. Eur., 2011) and according United States Pharmacopoeia's monograph *"<601> AEROSOLS, NASAL SPRAYS, METERED-DOSE INHALERS; AND DRY POWDER INHALERS"* (USP, 2013b).

An in-house constructed model inhalation device was used to apply powder doses of 25 mg to the apparatus (Figure 3.10). The airflow through the NGI was regulated to 80 L/min, which corresponds to the demanded pressure drop of 4 kPa in the device. A time controlled valve gets programmed to open for 3 seconds, i.e. until 4 L of air were drawn through the inhaler.

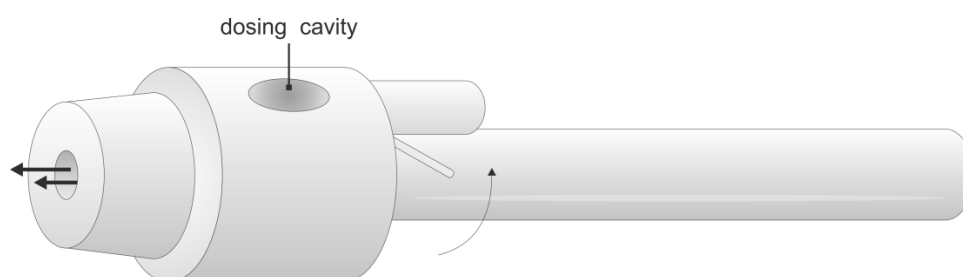


**Figure 3.10:** Model inhalation device

Before testing, the NGI stages and preseparator were prepared by applying a thin layer of coating solution to their surfaces. The stage coating consisted of 15 parts of Brij® 35 and 85 parts (m/m) of an ethanol/glycerol (6 + 4, m/m) mixture. The dried coating on the collection stages is meant to prevent

particle bouncing (Grasmeijer *et al.*, 2012) of already impacted particles, which may falsify the deposition towards lower stages. Upon impaction the dry powder particles now stick to the surface coating and, hence, cannot be carried on to lower separation stages.

10 doses (25 mg each) were administered to the NGI before opening the impactor and rinsing the collection cups with defined amounts of dd H<sub>2</sub>O. Since dispersion behavior is known to be influenced by changes in environmental temperature and moisture (Jashnani *et al.*, 1995; Young and Price, 2004), all measurements were performed under controlled ambient conditions (21 °C, 45%). Once the samples were dissolved, the drug content was determined via HPLC (see section 3.2.3.2).

Each run was performed in triplicate and the recovered amounts of drug were entered into CITDAS 3.0 software (Copley Scientific, Nottingham, UK) to calculate the corresponding FPD and FPF, respectively.

### **3.2.5 Scanning electron microscopy (SEM)**

To get a direct impression about the distribution of drug particles on the lactose carrier, scanning electron micrographs of the blends were recorded with a JSM-6301F microscope (Jeol, Japan). Therefore, the samples were fixed on an aluminum sample holder by means of adhesive double-sided carbon tape and any excess powder was removed by gentle tapping. Finally, a 20 nm gold-palladium coating was applied to the samples using a sputter coater (type 120B, Balzers AG, Liechtenstein) prior to measuring at an acceleration voltage of 3 kV.

### 3.3 Results

#### 3.3.1 Content Uniformity

All produced blends had a coefficient of variation significantly lower than 5% and can therefore be considered homogeneous. Table 3.3 and Table 3.4 list the average drug content and CV of the mixtures prepared in duplicate. A trend of decreased salbutamol sulfate content with increasing mixing intensity can be observed. This finding is consistent with impressions of visual inspections of the mixing vessel. With increasing mixing speed and time, a white film on the walls of the stainless steel vessel became evident.

**Table 3.3:** API content and CV of Picomix®-blends (target content: 0.4%)

rotational speed, rpm	mixing time, s	API, %	CV, %
500	15	0.39	1.93
	30	0.39	1.58
	60	0.39	1.35
	300	0.39	1.52
750	15	0.39	1.17
	30	0.39	1.63
	60	0.39	0.52
	300	0.37	1.01
1000	15	0.38	1.19
	30	0.38	3.84
	60	0.38	1.03
	300	0.35	1.87

**Table 3.4:** API content and CV of Turbula®-blends (target content: 0.4%)

rotational speed, rpm	mixing time, s	API, %	CV, %
20	5	0.39	1.25
	60	0.39	0.78
90	0.5	0.39	0.54
	60	0.37	0.73

### 3.3.2 Dispersion measurements

#### 3.3.2.1 Particle size analysis

Table 3.5 lists the  $x_{10}$ ,  $x_{50}$ , and  $x_{90}$  quantiles of the volumetric particle size distributions of the 300 s – Picomix® blends.

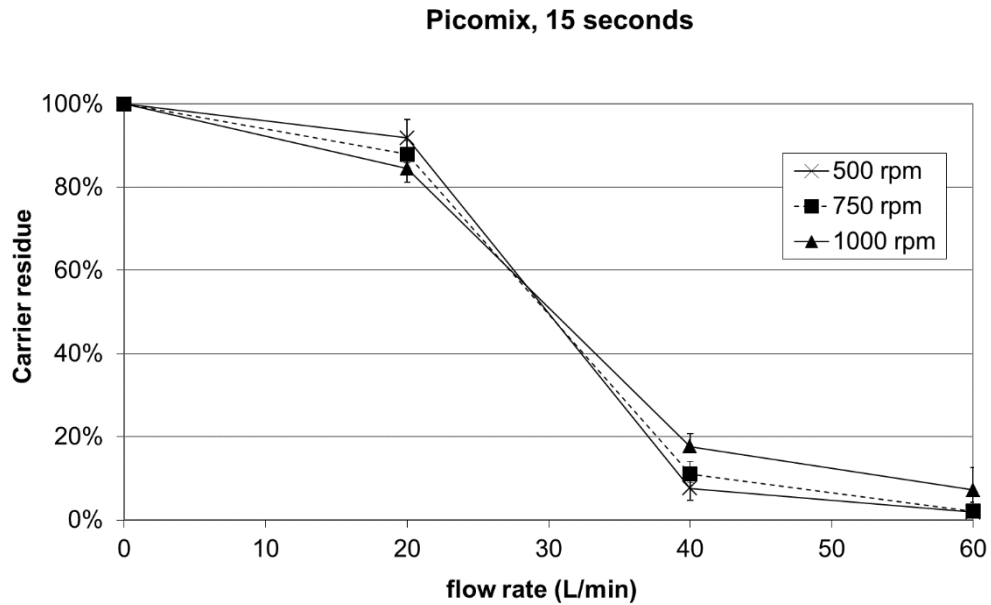
**Table 3.5:** PSD of mixtures (laser diffraction, dry dispersion 5 bar, lens R5)

mixing speed, rpm	mixing time, s	$x_{10} \pm SD, \mu\text{m}$	$x_{50} \pm SD, \mu\text{m}$	$x_{90} \pm SD, \mu\text{m}$
500	300	224.05 $\pm$ 0.27	334.40 $\pm$ 0.87	443.66 $\pm$ 7.02
750	300	222.60 $\pm$ 0.99	332.81 $\pm$ 1.34	432.89 $\pm$ 0.79
1000	300	219.04 $\pm$ 0.67	331.09 $\pm$ 1.33	433.30 $\pm$ 2.20

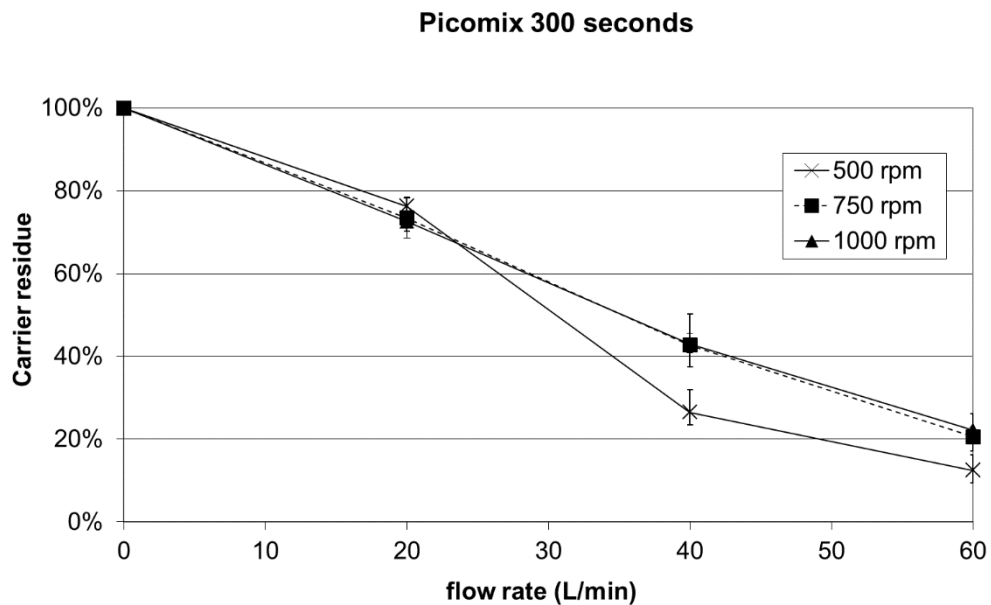
A slight trend towards smaller particle sizes is apparent for the  $x_{10}$  quantile values indicating a minor possible lactose carrier crystal abrasion.

#### 3.3.2.2 Carrier residue, CR

The drug residue on the lactose carrier after dispersion at 40 L/min (CR40) and 60 L/min (CR60) in the classifier increases significantly with prolonged mixing time and accelerated rotor speed (see Figure 3.11 to Figure 3.15).



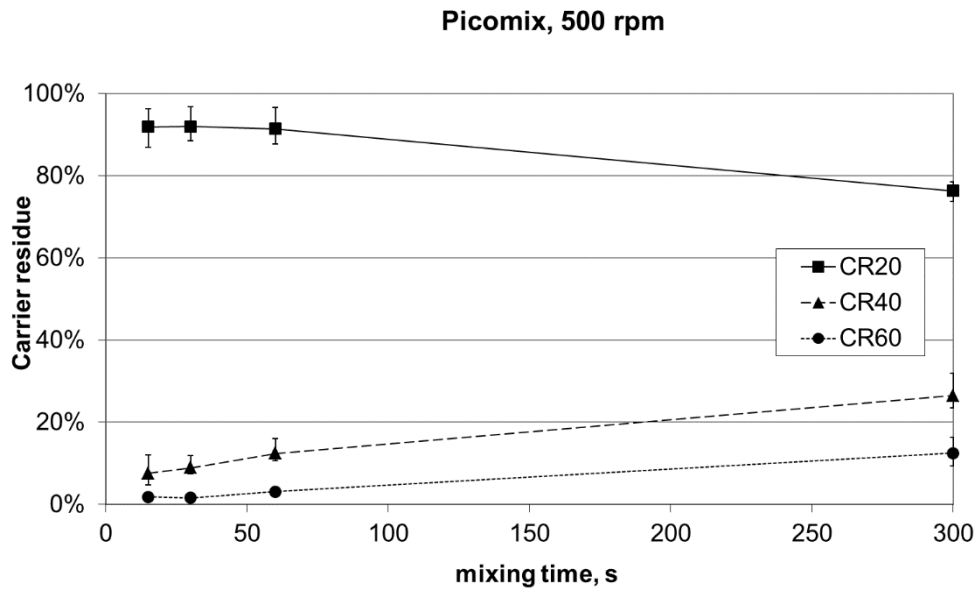
**Figure 3.11:** Carrier residue after mixing for 15 s (mean of 2 runs; n=5 per run; error bars present min/max-values)



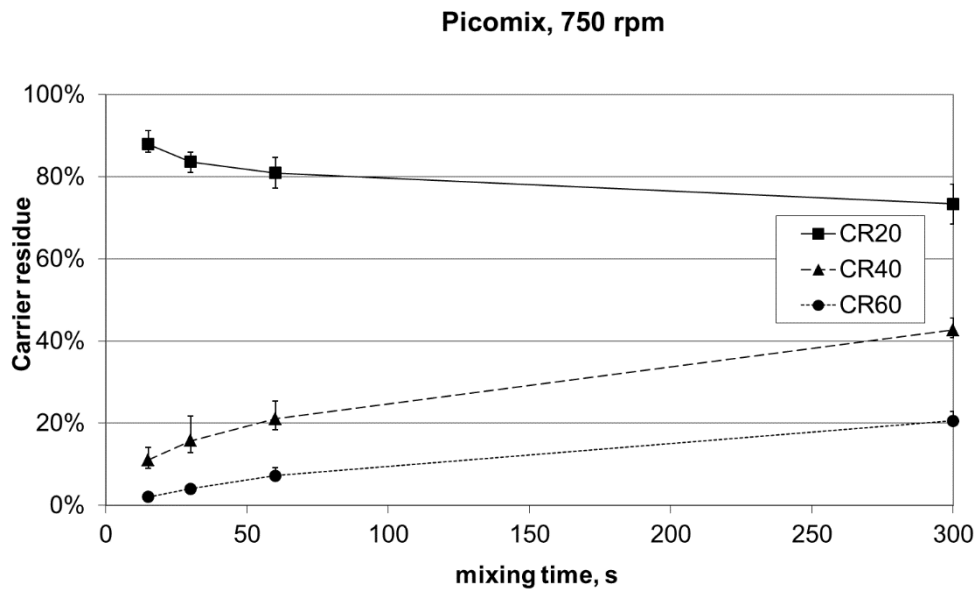
**Figure 3.12:** Carrier residue after mixing for 300 s (mean of 2 runs; n=5 per run; error bars present min/max-values)

A different behavior can be observed at a flow rate of 20 L/min (CR20). Rather than the expected increase in CR, dispersion tests reveal a significant

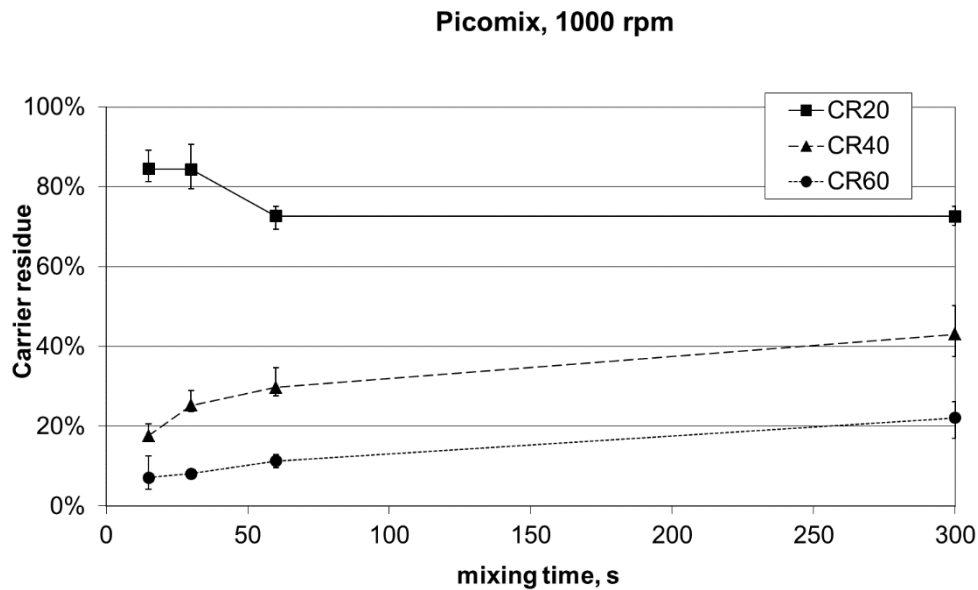
decrease of drug residue with prolonged and intensified mixing (see Figure 3.13 to Figure 3.15).



**Figure 3.13:** Carrier residue for blends treated at 500 rpm (mean of 2 runs; n=5 per run; error bars present min/max-values)



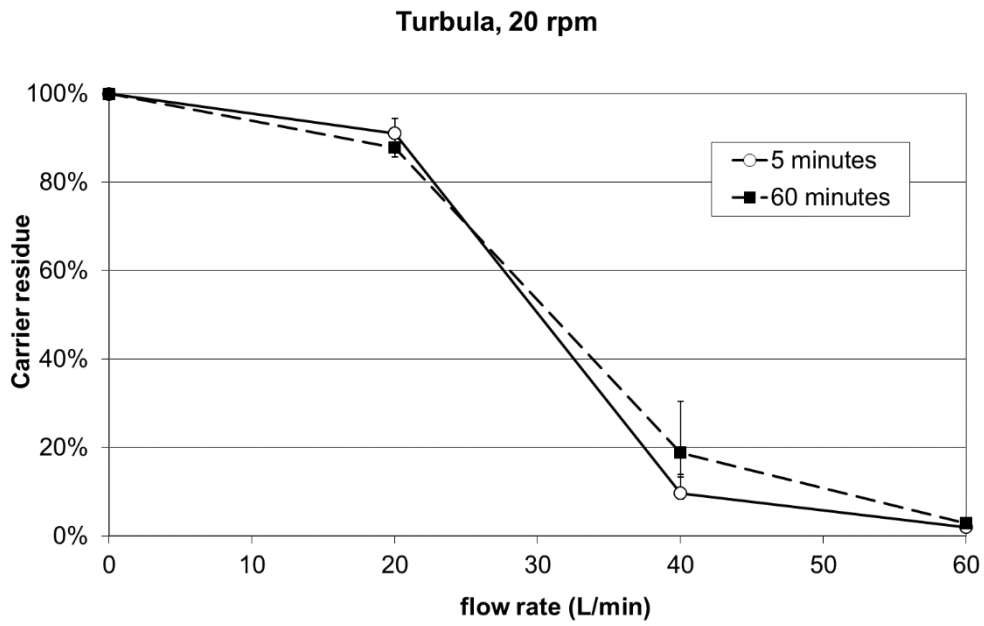
**Figure 3.14:** Carrier residue for blends treated at 750 rpm (mean of 2 runs; n=5 per run; error bars present min/max-values)



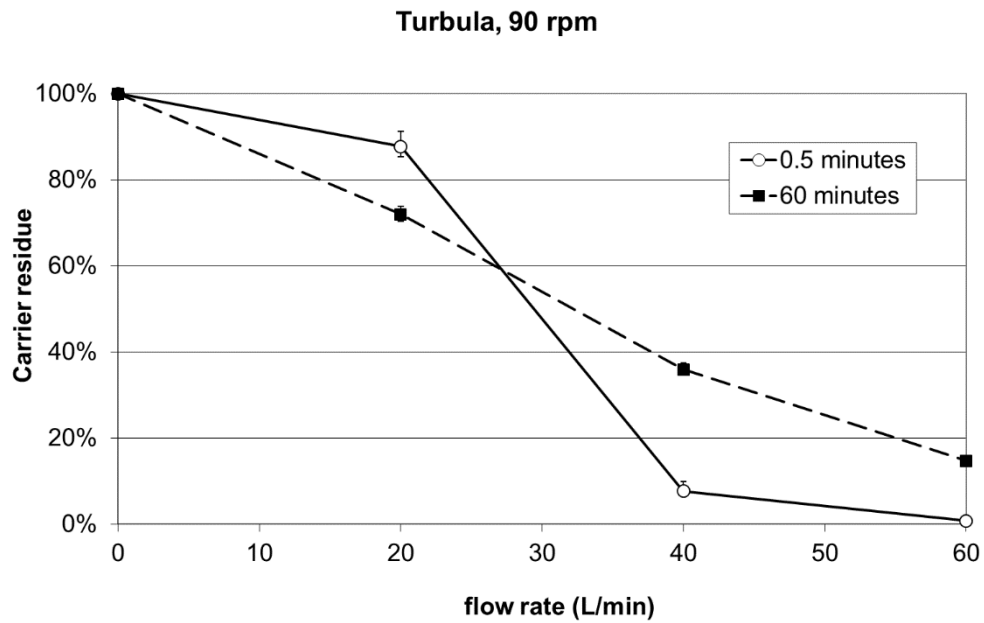
**Figure 3.15:** Carrier residue for blends treated at 1000 rpm (mean of 2 runs; n=5 per run; error bars present min/max-values)

It may be noted that under these experimental conditions, mixing time reveals a greater impact on the remaining amount of drug on the carrier than differences in mixing speeds.

A similar trend can be observed in the analysis of the Turbula®-mixtures (see Figure 3.16 to Figure 3.17). In fact, drug particles get almost separated completely from the lactose surface in mixtures that were prepared with 20 rpm and applied to a flow rate of 60 L/min, however, with process parameters above 60 minutes and 90 rpm, similar carrier residue values could be obtained as recorded for the Picomix®-blends.



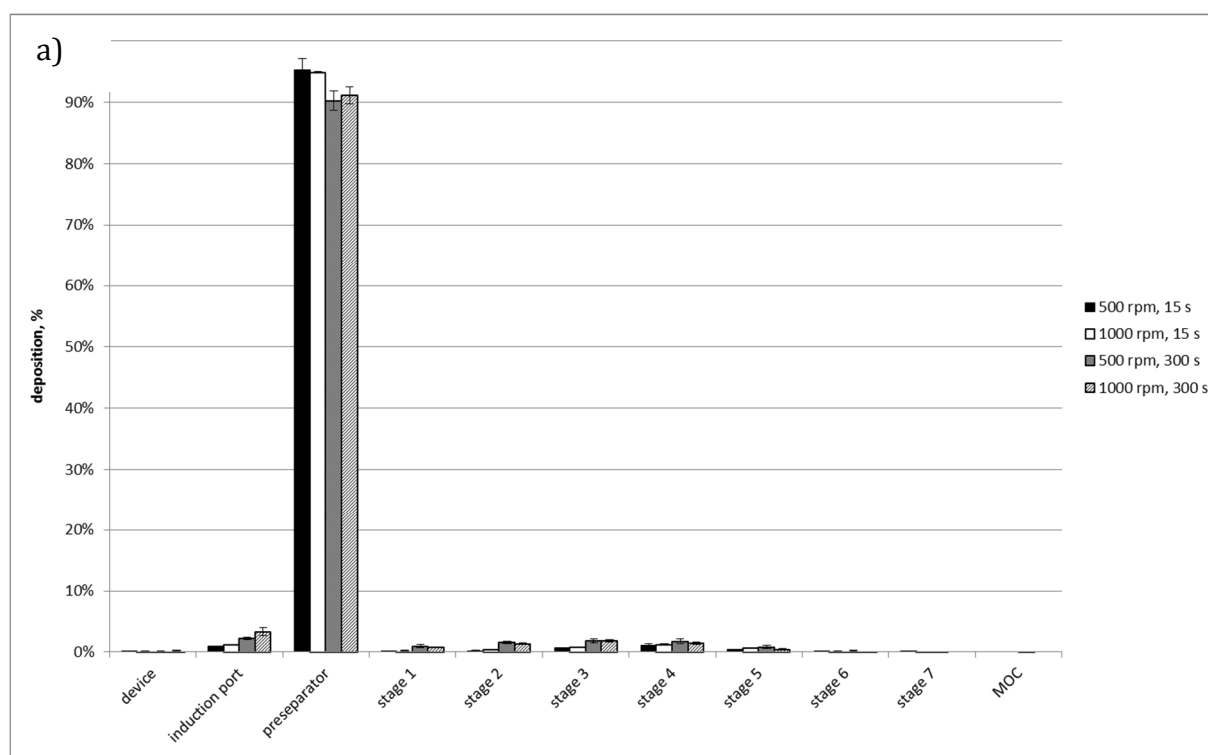
**Figure 3.16:** Carrier residue for blends treated at 20 rpm (mean of 2 runs; n=5 per run; error bars present min/max-values)



**Figure 3.17:** Carrier residue for blends treated at 90 rpm (mean of 2 runs; n=5 per run; error bars present min/max-values)

### 3.3.2.3 Impaction analysis

The results of the NGI impaction analysis show that for all blends prepared via high shear mixing the main fraction of drug (about 90%) impacted in the preseparator (Figure 3.18a). Nevertheless, despite the low deposition on the lower stages, significant differences between the formulations are apparent (Figure 3.18b). Similar to the findings of the carrier residue measurements the deposition patterns reveal that a change in mixing time has a greater influence on the impaction behavior than a change in rotor speed. Contrary to first expectations, a greater fraction of fine salbutamol sulfate particles detached from the lactose carrier with increasing mixing time.



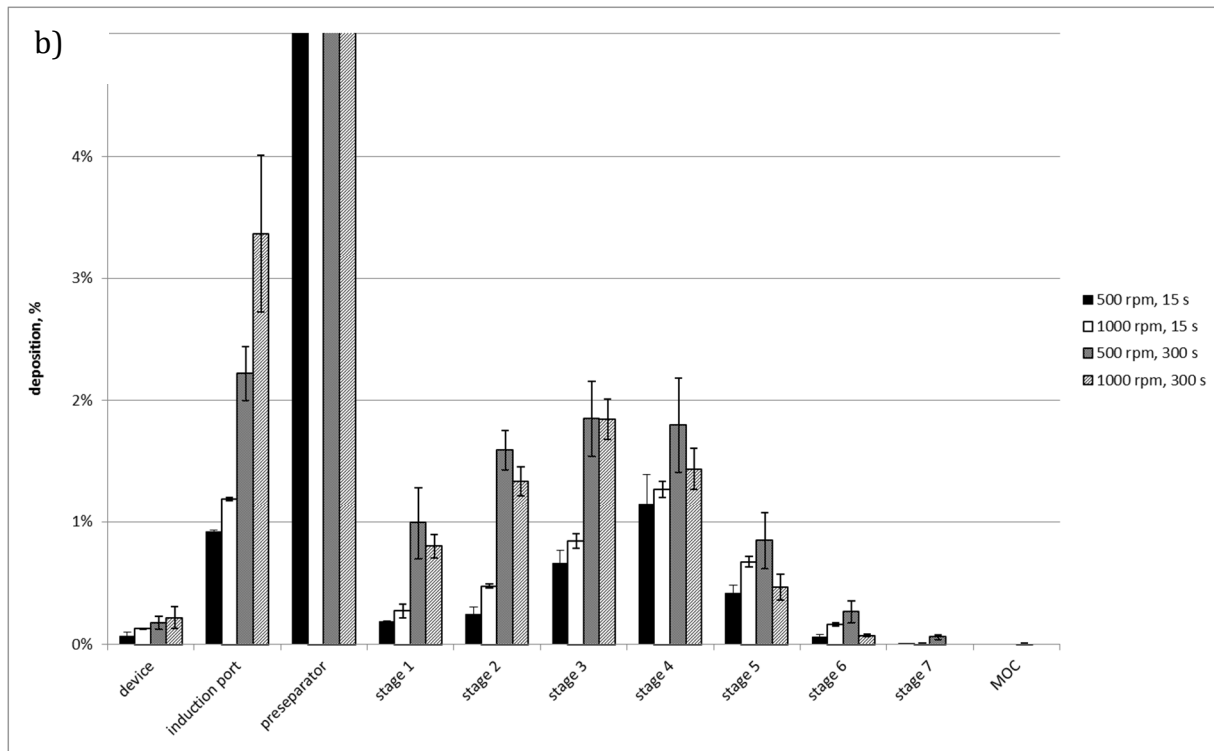


**Figure 3.18a and b:** NGI deposition patterns of Picomix®-blends

The mixtures prepared with the Turbula® also showed a very large preseparator fraction of about 95% (Figure 3.19a). An exception is apparent for the mixture of the most intense process conditions. The increase in the mixing time and speed led to a clear shift in the drug deposition from preseparator towards smaller separation stages (Figure 3.19b).

### 3.3 RESULTS

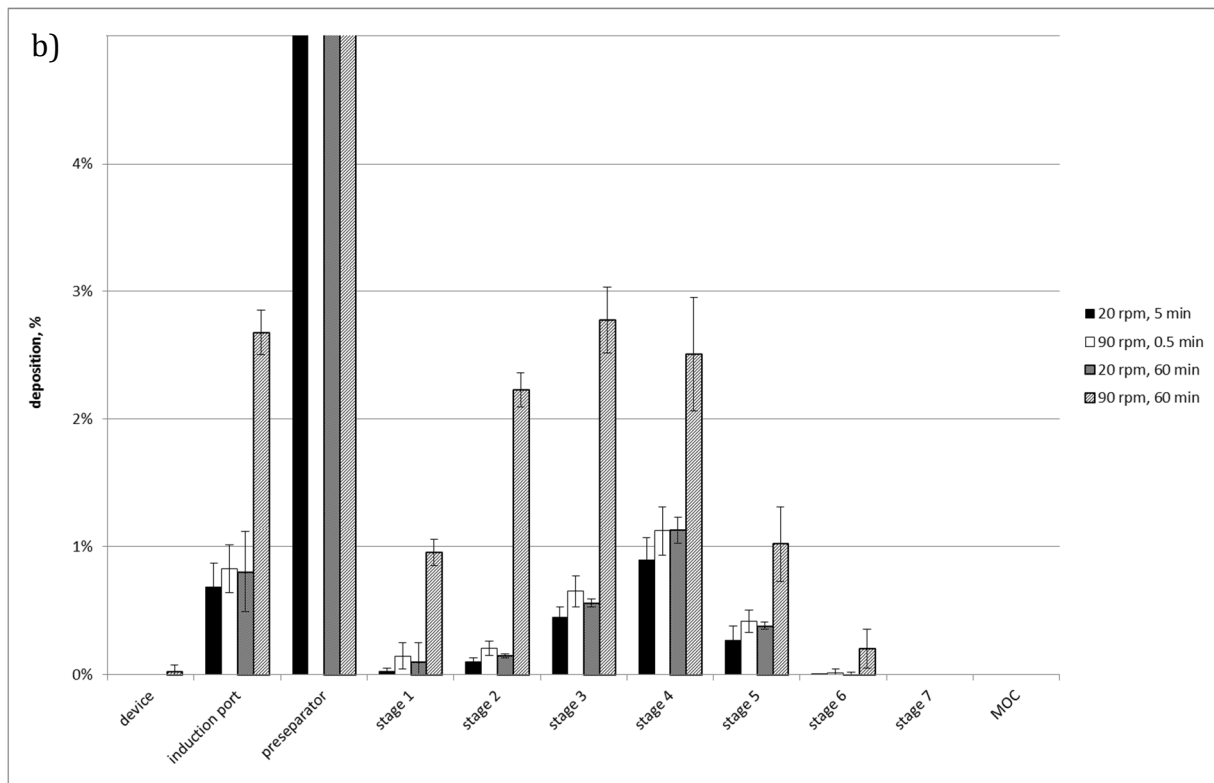
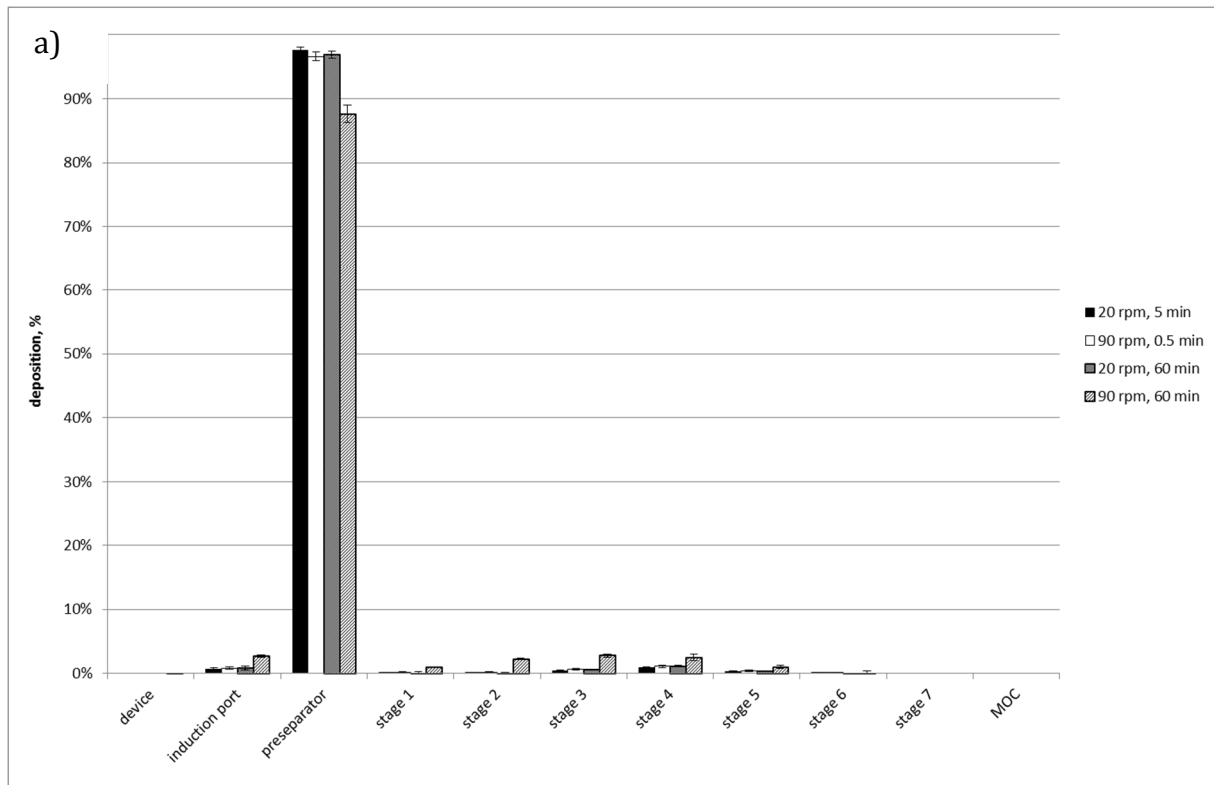


**Figure 3.19a and b:** NGI deposition patterns of Turbula®-blends

The calculated fine particle fractions (see Table 3.6) confirm the impression that, contrary to expectations, longer mixing times lead to increased fine

particle dispersion. Again, the influence of mixing time appears to be dominant over changes in rotational speed.

**Table 3.6:** mean values and standard deviations of fine particle fraction calculations

process paramteres	fine particle fraction, %	standard deviation, %
Picomix®		
500 rpm, 15 s	2.46	± 0.51
500 rpm, 300 s	5.66	± 1.10
1000 rpm, 15 s	3.19	± 0.10
1000 rpm, 300 s	4.50	± 0.36
Turbula®		
20 rpm, 5 min	1.66	± 0.40
20 rpm, 60 min	2.17	± 0.15
90 rpm, 0,5 min	2.32	± 0.45
90 rpm, 60 min	7.13	± 1.10

### 3.3.3 SEM images

The scanning electron microscope images of the Picomix® mixtures at 500 rpm and 1000 rpm show that fine particles preferably adhere to surface discontinuities/irregularities of the lactose carrier. Also, more intense mixing conditions (1000 rpm, 300 s) seem to promote fine particle agglomeration on the lactose surface as more aggregates become visible on these SEM images (compare Figure 3.20a to Figure 3.21a).

After dispersion of the mixtures with the classifier at 60 L/min remaining fine particles can predominantly be found in places where they find shelter like defects in the smooth lactose surface such as cracks or other cavities (see Figure 3.20b and Figure 3.21b, respectively).

### 3.3 RESULTS

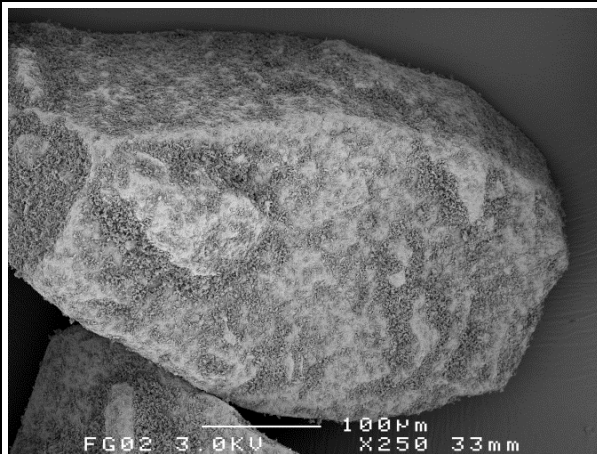


**Figure 3.20a:** 500 rpm, 15 s

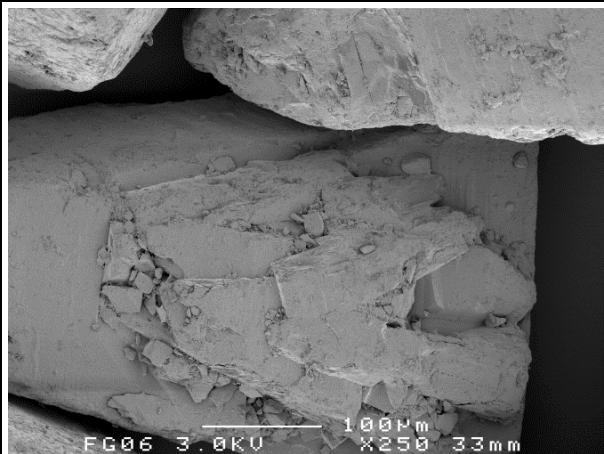


**Figure 3.20b:** 500 rpm, 15 s after dispersion in the classifier (60 L/min)

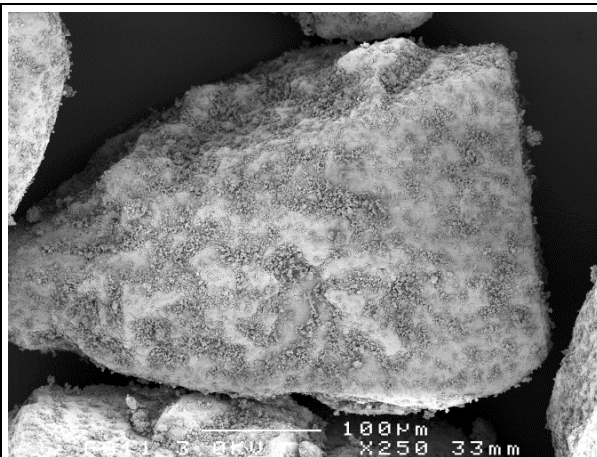


**Figure 3.21a:** 1000 rpm, 300 s

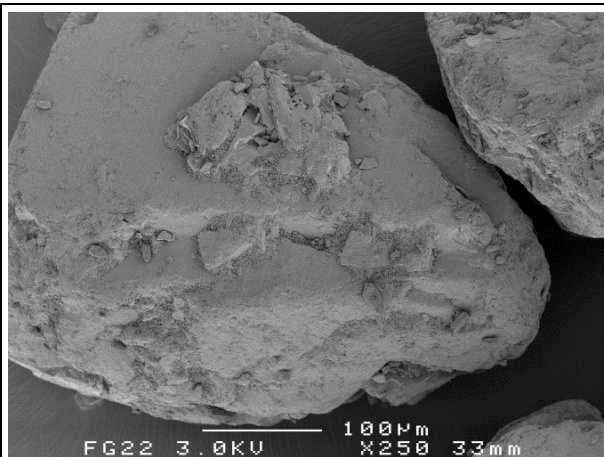


**Figure 3.21b:** 1000 rpm, 300 s after dispersion in the classifier (60 L/min)

## **3.4 Discussion**

### **3.4.1 Blend homogeneity**

Both, high shear mixer (Picomix®) and free-fall mixer (Turbula®) were able to distribute the salbutamol sulfate homogeneously over the carrier particle surface to form adhesive powder mixtures within short periods of time. Due to the higher energy input during mixing for the high shear mixer lower process times could be selected. However, it also became apparent that intensive mixing conditions (for example, 1000 rpm for 300 s) may lead to a decrease in the salbutamol sulfate content and may cause particle size reduction due to mechanical abrasion.

### **3.4.2 Laser diffraction**

The small changes in particle size distribution with continuous increase of mixing speed is indicative of lactose crystal attrition and thus generation of intrinsic lactose fines, however, the slight deviations in  $x_{10}$  values are believed to be of minor relevance for the interpretation of further dispersion measurement results. As mentioned in section 2.5.1, differences in excipient fines content are known to increase the detachment of API fines adhered to the carrier. In contrast, the CR results show rather a decrease in drug detachment with increasing mixing times and speed. Therefore, the slight changes in PSD were considered to be of minor importance for the interpretation of the dispersion test data.

### **3.4.3 Carrier residue**

The results of the carrier residue measurements and impaction analysis with the NGI illustrate that despite almost constant homogeneity of the mixtures, the continuation of the mixing process led to subsequent changes in the

dispersion behavior. Thus, the increased drug residues on the lactose carrier (after dispersion at 40 L/min and 60 L/min) at prolonged mixing times and accelerated rotor speeds may directly be correlated to an enhanced occurrence of “press-on forces”. It comes to a distinct redistribution of salbutamol sulfate particles on the lactose surface towards higher energy binding sites. These “hot spots” can be found mainly in surface irregularities or discontinuities such as cavities, cracks, or fractures on the surface. The impressions of the scanning electron microscope images after dispersion (Figure 3.20b and Figure 3.21b) support this theory. An increased amount of fine particles remains in the above-mentioned irregularities with intensified mixing conditions.

Despite the differences between the two mixing principles used and the associated deviations in energy input during the process, comparable results for the carrier residue measurements at 40 L/min and 60 L/min could be observed. Also, equivalent fine particle fractions (impaction analysis) were obtained for the Picomix®- and Turbula®-blends.

However, not all results can be explained by an increased exposure to “press-on forces”. Remarkably, Turbula®-mixtures at 20 rpm reveal no significant differences in the dispersion behavior (CR, NGI) as a function of the mixing time. Even with a mixing time of 60 minutes, the forces responsible for considerable drug particle redistribution across the carrier surface seem to be insufficient. Thus, such weaker conditions could generally be used to optimize homogeneity of the drug mixture through prolonged processing times without influencing its subsequent dispersion behavior.

It is even more striking that an inconsistent dispersion behavior became apparent for carrier residue measurements at a flow rate of 20 L/min. Both, Picomix®- as well as Turbula®-mixes indicated an increased drug release

with prolonged mixing times under these conditions. The observations are contradictory to the previously formulated theory of API redistribution towards higher energy binding sites promoted by “press-on forces”. Hagedoorn *et al.* (Hagedoorn *et al.*, 2011) observed a similar flow-rate dependent behavior in their experiments for 0.4% (w/w) drug mixtures. They concluded that, in addition to the increase in “press-on forces”, an accumulation or agglomeration of fine drug particles takes place within the carriers’ surface irregularities, which is enhanced by prolonged mixing times. Just like individual particles, the formed agglomerates may further be redistributed across the surface of the carrier particles.

At a flow rate of 20 L/min, predominantly these agglomerates detach, as the leading inertial detachment forces are proportional to the third power of the particle or agglomerate diameter, respectively. However, the strength of adhesion forces between drug and carrier lactose (mainly van der Waals forces) is only proportional to the first or second power of the particle diameter (de Boer *et al.*, 2003). Thus, an increase in particle size or agglomeration of primary particles predominantly leads to an enhanced separation by inertial forces, whereas adhered primary drug particles (whose adhesion may have been strengthened through increased “press-on forces”) do not contribute to the detached fraction to a considerable extent. Also, agglomerates generally show a significantly smaller contact area in relation to their diameter compared to primary particles. This reduction leads to a further decline in agglomerate/carrier-adhesion and, therefore, to enhanced particle/agglomerate detachment. Figure 3.22 illustrates the detachment behavior at different flow rates. For carrier residue measurements at 20 L/min, mainly agglomerates detach from the carrier surfaces and are subsequently dispersed (see section 3.4.4). Since agglomeration of drug particles on the host crystal surface is believed to

### 3.4 DISCUSSION

increase with prolonged mixing, an increase in detached drug fraction can be detected at this flow rate. Certainly, the detachment of agglomerates takes also place when testing at 40 or 60 L/min. However at these elevated flow rates, the generated forces acting on the formulation are considerably larger and are able to detach individually bound particles from the carrier surfaces, which represent the main fraction of drug particles. Thus, the observed carrier residue values at these flow rates are significantly lower than the ones observed at 20 L/min. Further, the adhesive forces of the individually bound particles are believed to be affected by increased “press-on forces”, which is the cause for decreasing CR values with intensified mixing conditions.

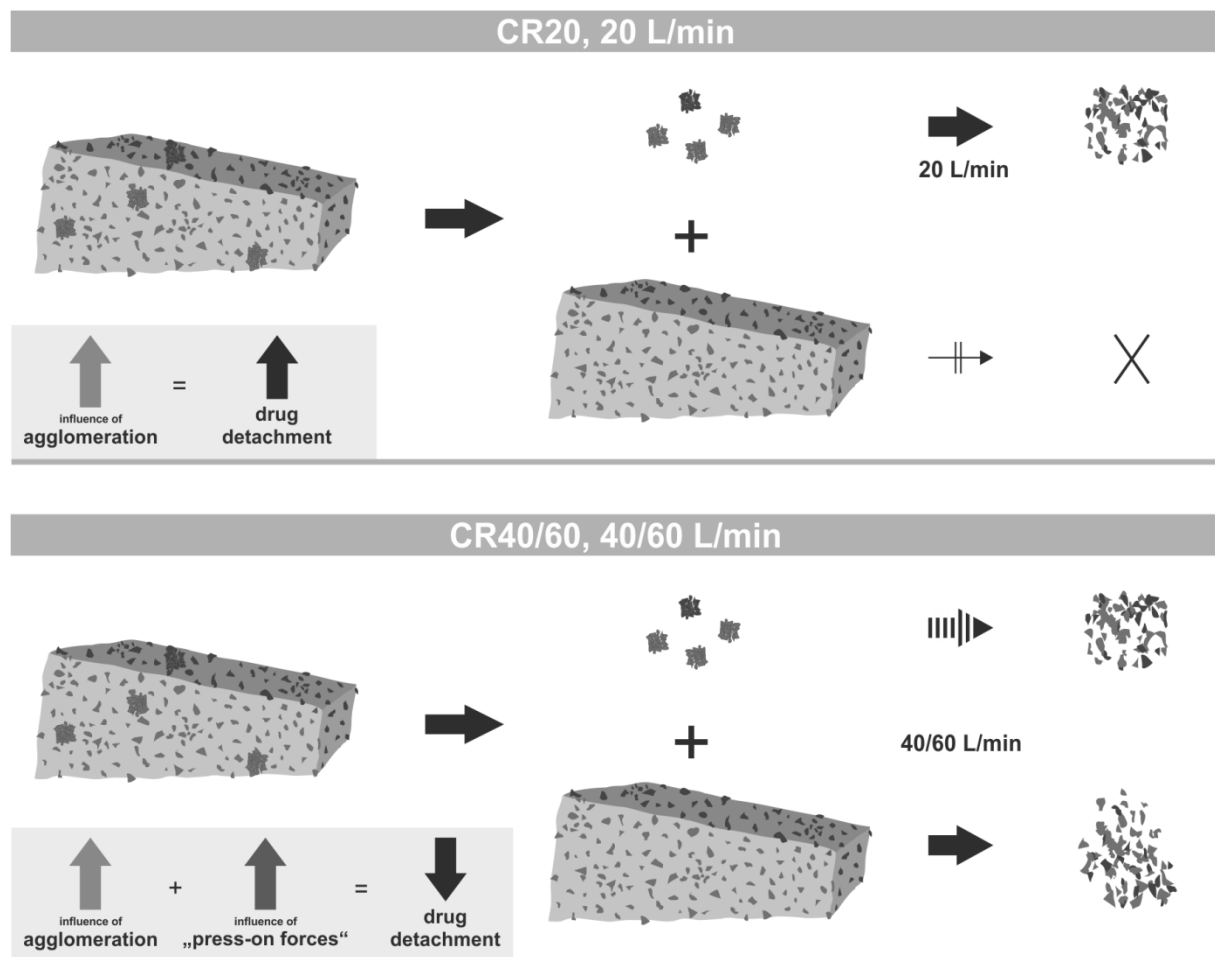


**Figure 3.22:** Driving detachment principles at different flow rates

The scanning electron microscope images of the adhesive powder mixtures with different mixing intensities (Figure 3.20a and Figure 3.21a) support the theory of an increased agglomeration tendency. The more intense mixing conditions led to a visual increase in the adhered agglomerates' size. However, no qualitative statement about the agglomerate composition can be made this way. Thus, incorporation of fine lactose particles (for example, residual intrinsic lactose fines or fines resulting from abrasion) is just as conceivable as the construction of mere salbutamol sulfate particles.

#### **3.4.4 Impaction analysis**

The low values for the fine particle fractions obtained with NGI analysis (section 3.3.2.3) are primarily the results of the simple and basic test inhaler design used for these measurements. Commercially available inhalation devices usually contain dedicated parts to promote particle impaction and/or turbulences within the device and thus increase powder dispersion (Smith and Parry-Billings, 2003). The test inhaler, however, has a very straight forward design to put formulation-related differences in the dispersion behavior better into focus.

This fact should also be taken into account with respect to the flow-rate dependent results of the carrier residue measurements. The results implicate that the magnitude of forces acting on the powder within the test inhalation device and NGI are speculatively be comparable with those in the classifier at the flow rate of 20 L/min. As described in section 3.4.3, predominantly the agglomerated drug fraction detaches from the carrier at these low flow rates. The increase in adhesion forces between salbutamol sulfate and lactose particles (as a result of the increased “press-on forces”) cannot be detected with these test conditions. Consequently, an increase in the fine particle fraction with prolonged mixing time can be observed (Table 3.6). Similar to

the carrier residue studies, the influence of rotational speed is, again, less pronounced.

The NGI results further indicate that the detached agglomerates partially impact in the induction port due to their large inertia. The deposited amount increases with intensified mixing conditions, again, indicating a pronounced agglomerated drug fraction. However, decreasing preseparator fractions and increased lower stage depositions suggest that a part of agglomerates is subsequently broken up to into primary particles during passage through the NGI and contribute to the measured fine particle fraction.

### **3.5 Conclusion**

This study showed that mixing parameters for an inhalation powder blend need to be carefully chosen. Both, mixing speed and mixing time have a significant influence on the dispersion performance of the mixture as indicated by the results from carrier residue measurements and cascade impaction analysis.

Moreover, it can be seen that for the blend obtained with the Picomix® acceptable homogeneity is achieved relatively quickly, whereas the dispersion efficiency still gets affected by the continuation of the mixing process. Depending on the dispersion efficacy of the inhalation device, the influence of mixing intensity or, more important, mixing time can be opposite. Therefore, the importance for an optimization of the mixing process in consideration of the chosen inhalation device becomes obvious.

Factors, such as redistribution of drug fines towards high energy binding sites, press-on forces and the formation of agglomerates are being discussed to explain the observed behavior.

It appears that despite their differences in mixing principle, the Picomix® and Turbula® both generate mixtures that result in a similar fine particle fraction or carrier residue upon dispersion. However, this finding may be dependent on the inhalation device used for these experiments since drug detachment is considered to be mainly the result of inertial separation mechanisms. The impact of further discussed changes in “press-on forces” will likely become relevant for higher turbulence devices and should be the basis for continuing investigations. Also, it may be of interest to study possible changes to physico-chemical properties of the blends induced by the mixing process. For example, amorphous regions may be generated as a result of increased energy input.

## **4. PART 2 – POWDER RHEOLOGY AS TOOL FOR ADVANCED POWDER CHARACTERIZATION**

### **4.1 Introduction**

It was already mentioned in section 3.1 that the exact mechanisms driving particle adhesion and dispersion of carrier based powder mixtures for inhalation are very complex and still remain unclear. The extent of particle interactions is influenced by an almost unmanageable amount of factors and their interactions. For example, particle size and distribution (of carrier, API, and ternary fines material), shape, surface roughness, porosity, electrostatic charge, hygroscopicity, and amorphous contents have been reported to impact interfacial forces between particles (see section 2.5). Eventually, the quantitative composition of constituents affects the dispersion behavior of an adhesive mixture and hence its fine particle dose, as well.

A lot of research has focused on possible consequences for the dispersion behavior when conducting changes to one of the above mentioned parameters. It is believed that being able to measure and control the force of adhesion between particles a formulation with improved de-aggregation characteristics can be generated. One approach to directly measure attractive forces between single particle surfaces is the atomic force microscope (AFM) colloid probe technique (Ducker *et al.*, 1991). Briefly, a particle gets attached to the tip of a micro cantilever (see Figure 4.2), which is used to scan the specimen surface. When they are brought into proximity, the cantilever gets deflected slightly, which can be detected by a photodiode sensor (see Figure 4.1). The vertical displacement of the cantilever is further converted into force according to Hooke's law. With a sub-angstrom vertical sensitivity, the AFM can detect forces of the order of picoNewtons (Price *et al.*, 2002).

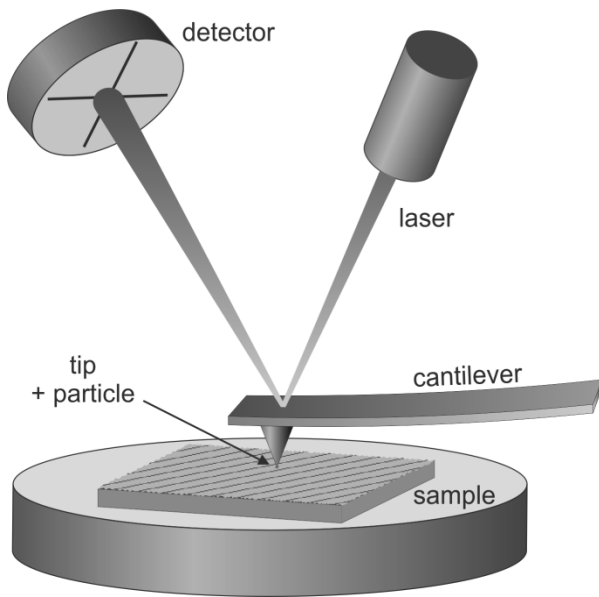


**Figure 4.1:** Schematic AFM colloidal probe set-up

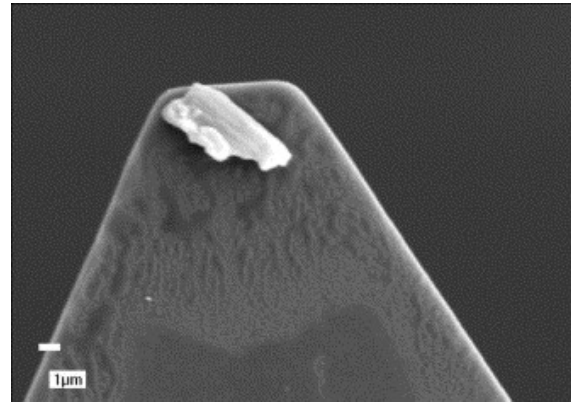


**Figure 4.2:** particle on cantilever (Price *et al.*, 2002)

This technique was further modified by Begat *et al.* (Begat *et al.*, 2004a, 2004b), who calculated the cohesive-adhesive balance (CAB) of 2 substances and were able to correlate some of their AFM measurements to *in-vitro* aerosolization behavior (Young *et al.*, 2006). However, AFM measurements only focus on single particle interactions, or even concentrate on limited surface regions of the substances. Consequently, this type of analysis may be suitable for basic considerations about interfacial interactions, but generally cannot be used to predict the more complex bulk powder behavior.

Many researchers have investigated the influence of known performance modifying factors (shape, size, etc.) on the dispersion properties of an adhesive mixture over the past years. But their effects have mostly been investigated individually, without considering likely interactions between them (de Boer *et al.*, 2012). One factor may be of less relevance when changing the parameters of another one; hence, even an opposite effect may be obtained.

In this thesis, bulk characteristics of adhesive blends were investigated by means of powder rheology. This fairly novel approach in inhalation powder characterization evaluates differences in flow properties of a bulk powder and therefore captures the sum of forces acting on the bulk directly rather than trying to relate single particle measurements to the more complex overall behavior. It was tested, whether changes in powder rheology tests could subsequently be correlated to aerosolization performance and, thus, may help to gain a better mechanistic understanding of processes affecting dispersion properties.

### **4.1.1 Ternary fines addition**

As mentioned in section 2.5.1, the inclusion of fine particle excipient (especially lactose fines) within an adhesive powder mixture was shown to be a suitable method to enhance the fraction of detached drug upon aerosolization (Jones and Price, 2006). However, despite the extensive literature basis dealing with this topic, there are still uncertainties about the influence of differences in particle size and optimal amount of added fines. Part of this is due to the diverse methodologies used in the reported research studies. The differences in employed excipient materials, mixing process, inhalation device, and further test conditions makes comparability between these studies (with the goal of an improved mechanistic understanding) almost impossible. On the other hand, a general increase in FPF with ternary fines inclusion can be found almost consistently throughout literature (Adi *et al.*, 2004; Adi *et al.*, 2006; Islam *et al.*, 2004; Louey *et al.*, 2003; Louey and Stewart, 2002; Lucas *et al.*, 1998b; Zeng *et al.*, 1998; Zeng *et al.*, 2001). Similar to the type of material used as carrier, the majority of work deals with  $\alpha$ -lactose monohydrate to investigate the influence of fines addition. Alternatives, such as glucose, mannitol, sorbitol, and others (Jones *et al.*, 2005; Louey and Stewart, 2002; Tee *et al.*, 2000) were investigated also, but

did not show an overall superiority compared to more widespread used lactose fines.

As mentioned before and discussed in a review by Jones and Price (Jones and Price, 2006), the extensive knowledgebase around ternary inhalation mixtures has not yet lead to a distinct recommendation about optimal ternary component concentration or its ideal particle size. Mainly, two hypotheses about underlying mechanisms are present in the literature. The first one proposes the adhesion of ternary fines to the strongest binding sites on the carrier surface, thus, cause the adhesion of API fines towards lower energy binding sites and increase drug detachment upon aerosolization. The second one hypothesizes the formation of fines' agglomerates that are more easily dispersed during inhalation and, hence, increase the FPF. However, only empirical evidence is present for each of the two theories. Much of this data derives from experiments that relate changes in the mixing order of carrier, drug and ternary fines and their further dispersion properties to possible passivation of active sites. But again, a thorough interpretation of this data is extremely complicated and unable to provide any mechanistic evidence beyond pure speculation (Hartmann and Steckel, 2004).

*“In truth, the evidence in support of both mechanisms is limited, being restricted to the presence or absence of an effect of blending order (...), images showing the presence of mixed multiplets in unaerosolised formulations and calculations based upon the effects of adding different proportions of fines, which have been used in support of both mechanisms.”* (Jones and Price, 2006)

Therefore, this study assesses advanced bulk characterization techniques, i.e. powder rheology analysis, with the goal of an improved mechanistic understanding about the influence of fines addition to an adhesive mixture.

## 4.2 Bulk powder properties

Powders are disperse systems consisting of a solid internal phase and gaseous outer phase (solid in gas). It is a characteristic for the inner phase that particles are in constant, loose contact with each other. Conceptually, this fact separates a powder from an aerosol in which the particles of the inner phase are usually thoroughly dispersed in the outer gas phase. In addition to the solid and gas phase, there is almost always a third, liquid proportion included, which exists either condensed to the solid surfaces or is bound within the particles. Thus, a powder can generally be conceived as a three-phase mixture (Figure 4.3), whose exact composition of solid, liquid and gaseous phase is changing constantly during handling and storage (Figure 4.4).

*„Powders are complex materials. Often perceived as just a collection of particles, they are in fact a complex mixture of solids, liquids and gases.”*  
(Freeman Technology, 2012)

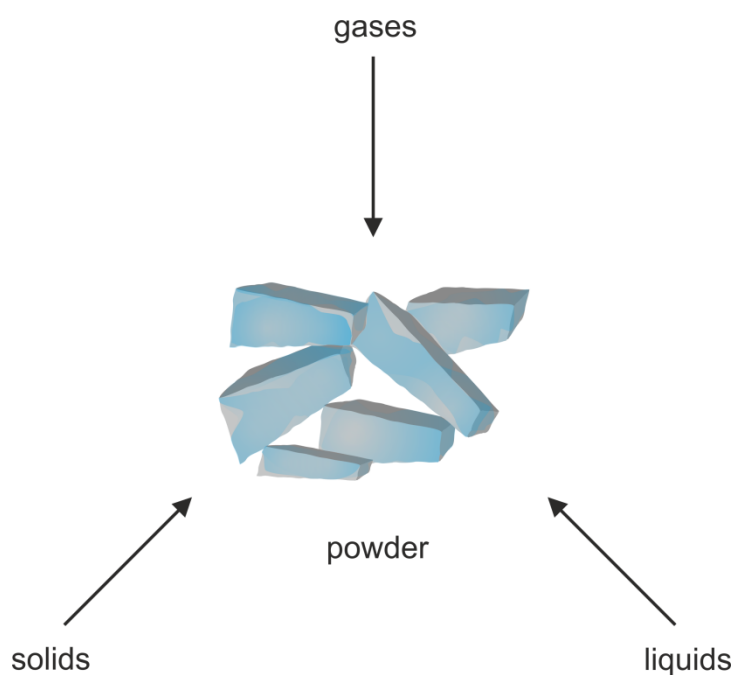


**Figure 4.3:** Powder composition

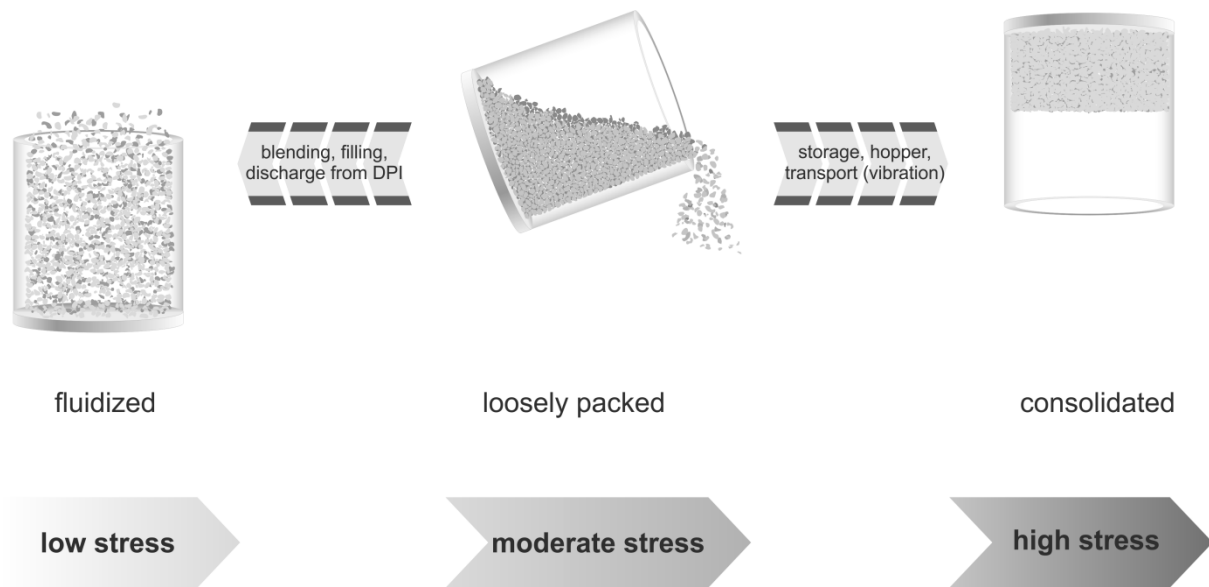


**Figure 4.4:** Possible powder states of one powder (adapted from Freeman (2013))

Consequently, the description of the bulk powder behavior is challenging as it can simultaneously take on different properties of the individual components. For example, it can:

- be deformed elastically and plastically like solids,
- be compressed like gases,
- and flow like fluids.

First indications about the bulk properties of a powder can be derived from single phase characterizations. For example, particle characteristics such as size distribution, morphology, surface characteristics, hygroscopicity, porosity, elasticity, density, surface energy, etc. may give a rough idea about an overall behavior. In addition, the poured bulk density indicates the gas or air content within the sample and sorption isotherm information can be gathered to investigate the adsorbed amount of liquid.

The difficulty of a comprehensive description of a powder, however, is to transfer findings from a single factor analysis to the overall bulk properties. Factors show varying magnitudes of impact on different forces within the

powder (frictional forces, van der Waals forces, mechanical interlocking, liquid bridges, gravitational forces) and also interact with each other. A purely mathematical approach for the description of powder behavior has thus remained unsuccessful so far.

### **4.3 Test methodologies to assess bulk behavior**

#### **4.3.1 Methodologies of the Pharmacopoeia**

The European and United States Pharmacopoeias list only three methodologies to analyze bulk behavior of powders:

- Poured and tapped density
- Angle of repose (Figure 4.5)
- Flow (time) through an orifice

The results of these basic tests are further used to estimate and categorize the powder flow properties. Monographs 2.9.34 of the Ph. Eur. and <1174> of the USP, respectively, describe the calculation of flow parameters (Carr's or Compressibility Index, Hausner Ratio, and angle of repose) that can be derived from the previously attained results according to Equations 4.1 to 4.3.

$$\text{Carr's Index} = 100 \cdot \left( \frac{\rho_{\text{tapped}} - \rho_{\text{bulk}}}{\rho_{\text{tapped}}} \right) \quad (4.1)$$

$$\text{Hausner Ratio} = \left( \frac{\rho_{\text{tapped}}}{\rho_{\text{bulk}}} \right) \quad (4.2)$$

$$\tan(\alpha) = \frac{\text{pile height}}{0.5 \text{ base diameter}} \quad (4.3)$$

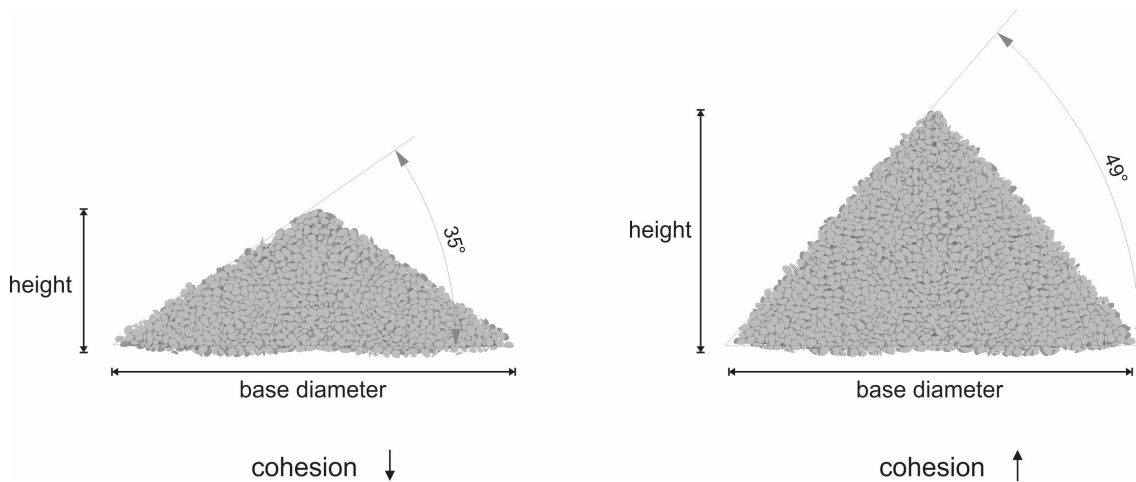


**Figure 4.5:** Angle of repose for powders with different cohesion (auto-adhesion) forces

Both, Carr's Index and Hausner Ratio are values based on the differences in bulk and tapped density, and thus express compressibility. The changes in compressibility get further directly (and oftentimes rashly) related to overall flow properties. The angle of repose measurements are influenced by material properties (see examples in Figure 4.5) at very low compaction conditions. In general, angle of repose is highly dependent on the test procedure and, thus, it is not an intrinsic property of the bulk solid (Schulze, 2008). Only the flow time measurements through an orifice directly measures powder flowability, however, more sophisticated statements concerning flowability and consolidation over time cannot be made. The

results are furthermore influenced by operators' differences in filling procedure as well as the flow regime (mass flow or funnel flow).

The USP also mentions shear cell measurements as a valuable addition in order to gain a comprehensive understanding of the powder flow behavior, however it does not specify its use further. It also states:

*"It bears repeating that no one simple powder flow method will adequately or completely characterize the wide range of flow properties experienced in the pharmaceutical industry. An appropriate strategy may well be the use of multiple standardized test methods to characterize the various aspects of powder flow as needed by the pharmaceutical scientist."* (USP, 2013a)

The ability to flow freely is an essential requirement for many pharmaceutical processes. For example, it relates to hopper discharge and die filling on rotary tablet presses or affects other filling and conveying processes. Diverse manufacturers offer partially automated equipment for the standard pharmacopoeia tests to minimize experimental variations. Still, the sensitivity and significance of the tests oftentimes remain rather poor and are inadequate to thoroughly describe powder flow behavior (Soh *et al.*, 2006). As indicated above and despite its importance, advanced techniques for a thorough powder flow characterization are limited.

#### **4.3.2 Non-pharmacopoeia techniques to investigate powder flow**

In addition to the partially automated test systems, some manufacturers designed advanced powder characterization methodologies to improve the predictive statements of powder flowability analysis with respect to their powder handling processes.

For example, the avalanching behavior (Kaye *et al.*, 1995) of a powder in a revolving cylinder can be investigated with appropriate test equipment (REVOLUTION®, Mercury Scientific Inc., USA or AeroFlow®, TSI GmbH, Germany). A detector (camera) collects the amount of light that passes through the powder containing, transparent cylinder, which can be used to quantify the size and frequency of avalanche appearance. Avalanches can be observed particularly with cohesive material and since avalanching is a chaotic process it is not possible to predict their magnitude. Therefore, a “strange attractor” plot (see Figure 4.6) is generated. The time between two successive avalanches is recorded as  $t_n$  and can already give indications about the avalanche size. Further, the time difference to the next avalanche is recorded as  $t_{n+1}$ . The scatter serves as an index of the cohesivity, which relates to an irregularity of flow. Short and reproducible times between avalanches, i.e. low mean time and scatter, indicate better flow properties (Lindberg *et al.*, 2004).

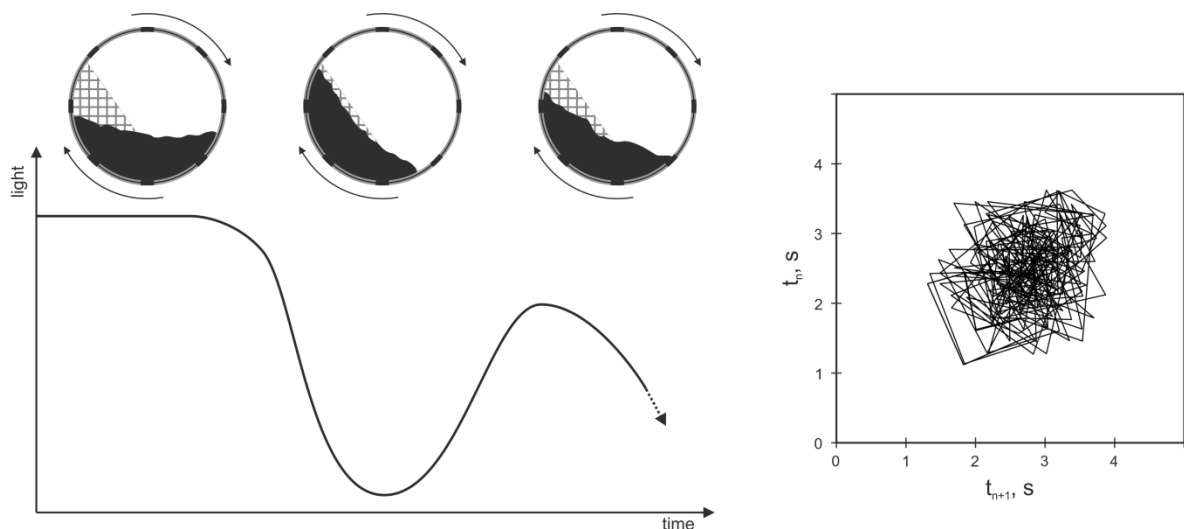


**Figure 4.6:** Schematic avalanching test set-up and strange attractor plot of AeroFlow® tester, modified from Markefka (2004)

Improved detection systems are also able to capture a variety of further powder parameters, such as sample density, avalanche angle, volume increase with increasing rotational speeds, etc. However, their practical implications on the powder behavior within a specific process often remain unclear.

Another approach to get a deeper insight into particle interactions is the use of shear cell equipment as mentioned in USP monograph <1174>. Based on the work of Jenike *et al.* a translational shear cell was developed, which can be used to gather information derived from these shear measurements. Also, Schulze's rotational ring shear cell and the newer Brookfield PFT Powder Flow Tester® are commercially available tools to directly measure shear stresses within a powder. The obtained data is used to calculate the flow function which further serves as an indicator of powder flow behavior. However, results from shear cell measurements are generally derived from compacted powder (measurement of shear stress at defined consolidation stresses). Therefore, interpretations about the shear strength of a powder in its unconsolidated state have proved rather elusive and tests provide only limited information about powder flowability.

Consequently, the described methods can still be considered as niche techniques and are not used on a routine basis.

### **4.3.3 Powder rheology**

“Rheology” is the science that studies the flow behavior of matter. Primarily, rheology measurements are used with liquid or semi-solid systems and record how the test materials' flow behavior changes when applying different strain rates. Theoretical aspects are the relation of the flow/deformation behavior of material and its internal structure. Whereas rheology analysis for

liquid or semi-solid systems has been described extensively in the literature and is now used as a routine characterization technique for these materials, only very limited data is available about the rheology of solids. If a solid responds with plastic flow rather than with elastic or plastic deformation in response to an applied force (for example, powder particles), this technique may as well be used to relate different flow behaviors to its inner structure.

Generally, powder rheology analysis offers a promising characterization approach in any powder processing environment, such as powdered paints and pigments, ceramics, plastics, pharmaceuticals, and fine chemicals handling industries. However, this study focuses on the suitability of powder rheology methodologies for pharmaceutical purposes, i.e. powder characterization with regards to processing, storage, or other handling properties – specifically, this study uses it to obtain further mechanistic understanding of processes within inhalation powder blends.

Principally, there are two powder rheology systems commercially available at the moment. Both work with a twisted blade that is agitated through a cylindrical test vessel filled with powder. The force detected versus the distance traveled by the blade, rotating at a predetermined angle into the given powder sample, depicts the work involved in getting the powder to flow (Navaneethan *et al.*, 2005).

The Powder Flow Analyser add-on for the TA.XTplus Texture Analyser platform (both Stable Micro Systems, Surrey, UK) is a basic tool to start testing quickly and conveniently after installation and calibration. On the other hand, the Freeman FT4 Powder Rheometer® (Freeman Technology, Tewkesbury, UK) is a dedicated equipment that is much more sophisticated and allows to adjust the specific test set-up with additional modifications.

Consequently, the Freeman FT4 Powder Rheometer® was used for the presented studies.

### **4.4 FT4 Powder Rheometer®**

#### **4.4.1 Platform**

The basic set-up of the Freeman FT4 Powder Rheometer® consists of a height adjustable, precision twisted blade, which rotates through a powder sample that is weighed into a borosilicate test vessel. During the measurement, the instrument records the energy needed to induce a certain flow pattern within the sample. Depending on the test methodology, appropriate vessels of different diameter (25 mm or 50 mm) and height are available and can be combined with either a 23.5 mm or 48 mm blade. Subsequently, the sample volume varies between 1 and 260 mL and the sample mass can be measured by a built-in scale if required.

In addition to the general rheological behavior from dynamic measurements, information about the bulk and shear properties can be obtained by adjusting the basic test set-up with dedicated accessories. Thus, the Freeman FT4 Powder Rheometer® can rather be considered as a universal powder tester than as a conventional rheometer.

Powders can exhibit many behavioral characteristics, which drive how they perform during subsequent processing. These characteristics are often independent of one another, so it is important to understand the influence of each of them. Therefore, different methodologies are necessary to fully characterize a sample. To name only a few, behavioral characteristics are: flowability, compressibility, adhesivity, permeability, particle attrition, flooding, and others (Freeman Technology, 2012).

For this thesis, the extension of the test set-up with a separate aeration unit (Aeration Control Unit, ACU) was believed to be of particular interest to investigate the changes in behavior of inhalation powders. The general equipment set-up is displayed in Figure 4.7. The ACU allows feeding a controlled air flow through the sample during the blade movement and the resulting changes in powder characteristics can be recorded. When exposed to air entrainment, inhalation powders have already shown to react differently - the air stream may lead to a constant erosion of the bulk material or move it as a whole when reaching a certain threshold velocity. Depending on the mechanism, subsequent changes to the achieved fine particle fractions were observed (Shur *et al.*, 2008). These results indicate that looking into the powder blend response to air entrainment may allow further conclusions about the aerosolization behavior.



**Figure 4.7:** Freeman FT4 Powder Rheometer® with Aeration Control Unit

#### 4.4.2 Sample preparation

The correct sample preparation is an essential part of any powder bulk measurement in order to obtain reliable and reproducible results. It has already been discussed in section 4.2 that the quantitative composition of a powder (by means of solid, aqueous, and gaseous phase, respectively) is not fixed, but rather variable as a result of dynamic changes depending on powder handling. Thus, differences in sample preparation may particularly influence the bulk density of the powder and, hence, lead to subsequent variations in flow properties. Also, the control of ambient conditions (temperature, humidity) helps to improve repeatability and validity of the obtained results (Freeman *et al.*, 2013).

For these reasons, the FT4 Powder Rheometer® executes additional conditioning cycles prior to each individual test cycle. By reversing the direction of the blade rotation (compared to the test cycles), a loosening of the powder can be observed and a somewhat standardized packing density can be obtained (see Figure 4.8a).

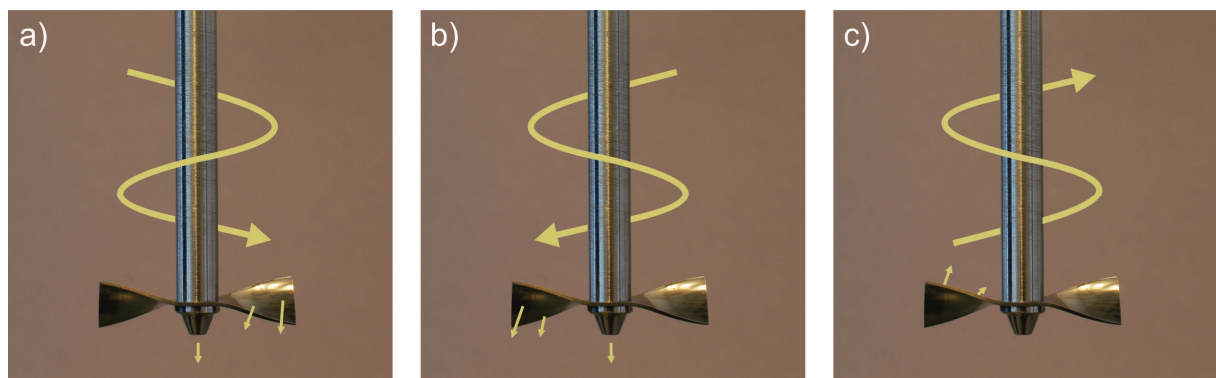


**Figure 4.8a-c:** Blade movement during: **a)** conditioning, **b)** BFE testing, **c)** specific energy testing

### **4.4.3 Bulk properties**

#### **4.4.3.1 Conditioned bulk density (CBD)**

Due to the use of test vessels with fixed volumes and the built-in scale, the rheometer provides a very straight forward approach to calculate the density (g/mL) of the test powder. After conditioning and splitting the test vessel to the defined volume, the conditioned bulk density (CBD) is calculated from the sample mass. Compared to the bulk and tapped density testing listed in the European Pharmacopoeia, CBD determinations show improved reproducibility, as user- and equipment-specific differences, or confounding factors such as previous consolidation or inhomogeneity can be significantly reduced by the powder conditioning process.

#### **4.4.3.2 Compressibility**

Furthermore, the divided powder sample can be compressed by a vented piston and be subjected to a defined normal stress (kPa). Similar to the interpretation of Carr's index and/or Hausner Ratio (see section 4.3.1) an increase in the compressibility indicates a more cohesive powder in a comparative measurement. Even though the FT4 Powder Rheometer® offers an enhanced control over process parameter (i.e. defined applied normal stress) compared to the Pharmacopoeia test methodologies, no sophisticated conclusions about powder flowability can be obtained by this simple test.

#### **4.4.3.3 Permeability**

The standard solid base of the borosilicate test vessel can be replaced by a porous, air-permeable accessory and further be linked to the aeration control unit. During the permeability measurement, the ACU supplies a constant

amount of air through the sample and records the corresponding pressure to establish this flow. Simultaneously, the powder gets consolidated by the vented piston, which applies defined values of normal stress to the top of the column (see Figure 4.9).

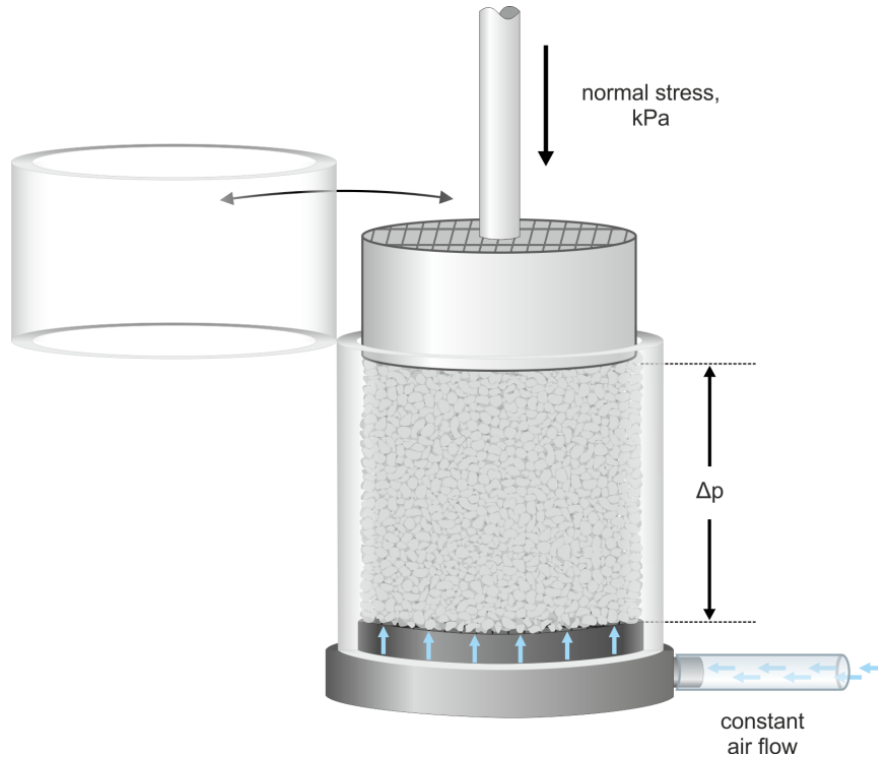


**Figure 4.9:** Schematic set-up of permeability test

Subsequently, the pressure drop across the powder bed ( $\Delta p$ ) gets analyzed as a function of applied normal stress and the sample permeability can be calculated according to Darcy's law (Equation 4.1).

$$Q = \frac{k \cdot A}{\mu} \cdot \frac{\Delta p}{L} \quad (4.1)$$

$Q$  is the applied air volume flow rate ( $\text{cm}^3/\text{s}$ ),  $A$  is the cross sectional area of the powder column ( $\text{cm}^2$ ),  $\Delta p$  is the measured pressure drop across the bed of powder (Pa),  $\mu$  represents the viscosity of air ( $1.74 \cdot 10^{-5} \text{ Pa}\cdot\text{s}$ ) and  $L$  the height of the powder column (cm).

By transforming and simplifying the formula with the introduction of the flux  $q$  (cm/s) (4.2), the permeability value  $k$  (cm<sup>2</sup>) (4.3) can be calculated (Freeman Technology, 2006).

$$q = \frac{Q}{A} \quad (4.2)$$

$$k = \frac{q \cdot \mu \cdot L}{\Delta p} \quad (4.3)$$

The permeability of a sample is dependent on the porosity or density of the sample on the one hand, but then also on characteristics such as particle shape and surface, as well as the amount of fluid adsorbed.

#### **4.4.4 Dynamic flow measurements**

##### **4.4.4.1 Basic flowability energy**

The basic flowability energy (BFE) is measured during the downward traverse of the blade through the test vessel and describes the energy (energy flow) needed to generate a defined flow pattern within the powder sample. The twisted blade rotates counterclockwise (tip speed = 100 mm/s) and, therefore, rather confines particles instead of loosening the bulk as achieved through a clockwise motion (as seen for conditioning) (see Figure 4.8b).

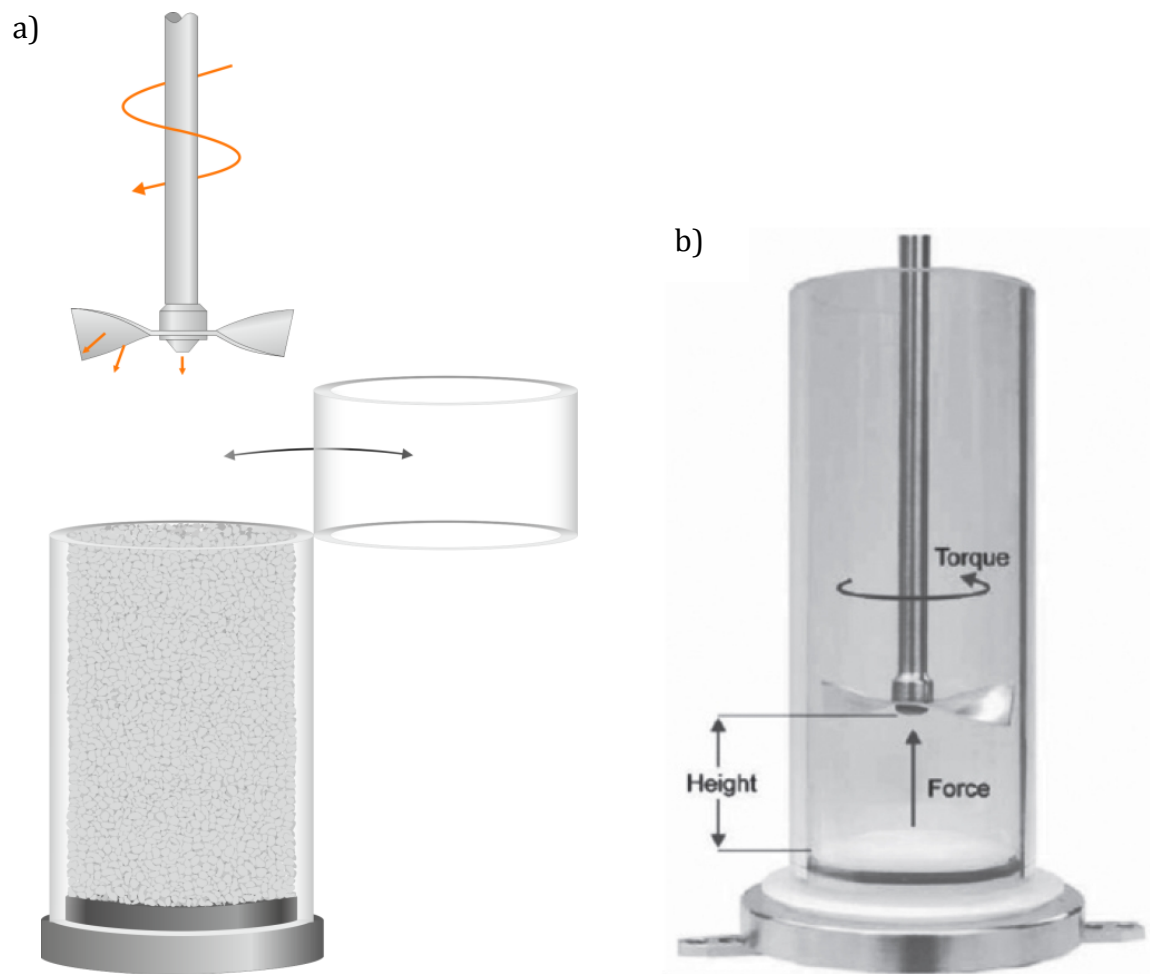


**Figure 4.10a:** Schematic set-up of BFE test

**Figure 4.10b:** Cross-section of set-up (Price and Shur, 2010)

A low value for the BFE gets oftentimes associated with improved powder flowability. This conclusion may be true for many cases - for example, when comparing two samples, one with and one without flow additive. However, the exact opposite may also be found. For instance, comminuted particles generally exhibit worse flow characteristics as result of their increased surface area and enhanced cohesive forces. The influence of gravitational force on each particle decreases and the particles get reassembled in agglomerates, which results in a non-uniform packaging (lowering the bulk density) through incorporation of air voids. There is a decrease in stress

transmission between particles and, subsequently, the total energy decreases (see Figure 4.11a and b).

Again, it turns out that evaluation and prediction of the complex powder behavior cannot be achieved through considerations of a single outcome parameter.

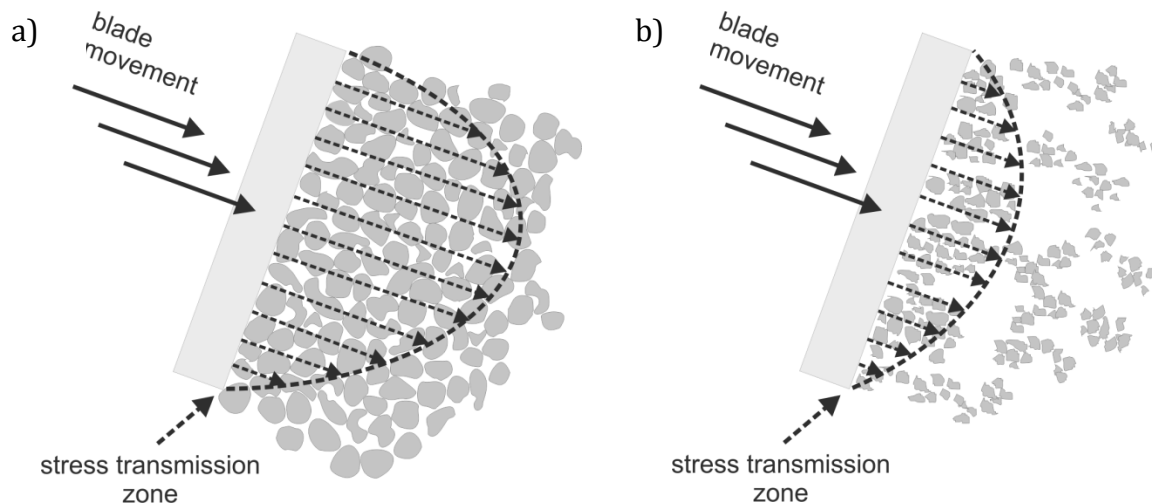


**Figure 4.11a and b:** Stress transmission zones of a) non-cohesive and b) cohesive powders, adapted from Freeman Technology (2008)

#### 4.4.4.2 Stability studies

By conducting multiple consecutive BFE tests, information on the stability of the investigated sample can be obtained. A flow energy de- or increase may be observed with cumulative number of test cycles and is, for example, indicative of segregation tendencies and/or particle destruction through attrition. This way, first conclusions on the powder's mechanical stability can be drawn, which may become relevant in subsequent processing steps (such as segregation in hoppers or other conveying systems).

Moreover, the results of the stability studies are used as a basis for the correct programming of different test sequences. If the powder sample is sensitive to only reversible segregation during the very first test cycles, reproducibility of the final results can be improved by adding further conditioning cycles to the beginning of the respective test program.

To judge the sample stability during the measurement, the stability index (SI) can be calculated according to Equation 4.4.

$$SI = \frac{\text{flow energy (test } n), mJ}{\text{flow energy (test 1), mJ}} \quad (4.4)$$

SI values close to 1.0 indicate a mechanically stable sample over the testing period.

#### 4.4.4.3 Specific energy

Just like the measurement of the total energy during the downward traverse of the blade, the energy can also be analyzed during its upward, clockwise movement (see Figure 4.8c). This parameter is referred to as the specific energy (SE) and is expressed as energy per mass unit (mJ/g).

A similar powder flow as in the downward movement is induced to the sample, however, the blade is now particularly leading to a lifting of the powder, instead of a compression. Less forces act on the particles and the measured energy is mainly influenced by the interparticulate forces. Thus, an increase in the specific energy can generally be related to a greater cohesive strength or to enhanced mechanical interlocking of irregularly shaped particles, respectively.

#### 4.4.4.4 Variation to blade tip speed

The flow properties of a powder (and therefore the blade's total energy) may behave differently depending on the applied forces. In general, the amount of energy needed to establish a certain flow pattern increases when decreasing the rotational speed since less air gets entrained by the blade leading to enhanced stress transmission, i.e. friction between particles (see Figure 4.11). Particularly strong energy gains appear in cohesive powders, free-flowing materials with smooth surfaces, however, are less susceptible to a total energy change with decreasing rotational speed.

For this test, the FT4 Powder Rheometer® reduces the blade tip speed of 100 mm/s gradually to 10 mm/s and records the corresponding total energies. The flow rate index (FRI) can be calculated as a measure for the susceptibility to flow rate changes (see Equation 4.5):

$$FRI = \frac{\text{flow energy at } 10 \frac{\text{mm}}{\text{s}}, \text{ mJ}}{\text{flow energy at } 100 \frac{\text{mm}}{\text{s}}, \text{ mJ}} \quad (4.5)$$

#### 4.4.4.5 Program sequence

A measurement with the FT4 Powder Rheometer® (dynamic flow behavior) is made up of alternating conditioning (C) and test (T) cycles. The program sequence is generally designed (or can be modified) in a way that multiple test cycles are performed consecutively to reduce unnecessary operator intervention. Figure 4.12 shows an example test sequence to simultaneously determine the basic flowability energy (BFE), specific energy (SE), the stability index (SI), and the flow rate index (FRI), respectively.

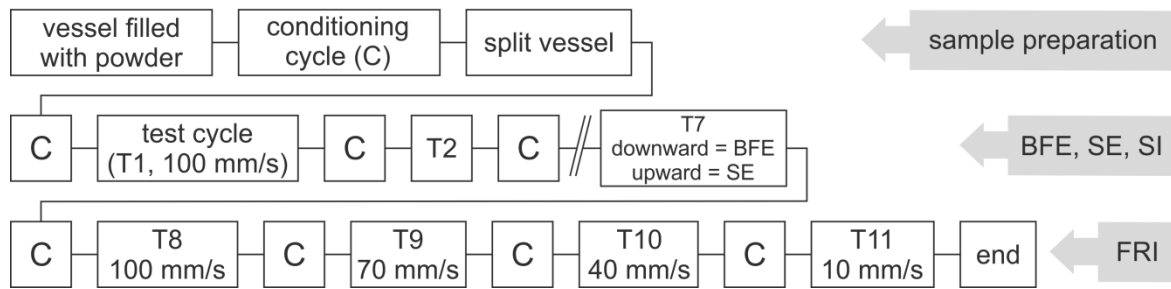


**Figure 4.12:** Program sequence of dynamic FT4 measurement

If required, the test program can be modified by adding additional conditioning and/or test cycles.

#### 4.4.4.6 Aeration measurements

Likewise to the permeability test set-up (Figure 4.9), the standard solid base of the borosilicate test vessel for dynamic flow tests can be replaced by a porous base and be linked to the aeration control unit.

By connecting the aeration control unit to the porous vessel base, the amount of additionally introduced air can be controlled during a test program (see Figure 4.13). Plotting the recorded changes in flow energy (mJ) as a function of introduced air flow, conclusions about the fluidization behavior of the powder can be drawn. With increasing air entrainment, the required total energy of the blade gets lowered (during the downward movement) and finally reaches a plateau at the level of its minimum. For free flowing powders, each particle is now separated by surrounding air and, thus, interparticulate forces are reduced to a minimum. The corresponding energy value is called fluidization energy (or aeration energy, respectively). Further, the required airflow to reach this plateau value, i.e. obtain the fluidized powder state, can be evaluated as the minimum fluidization velocity.



**Figure 4.13:** Schematic set-up of aeration tests

#### 4.4.5 Shear measurements

Even though shear measurements have not been used for the current tests, the possibilities of the FT4 Powder Rheometer® for measuring the shear behavior of powders should be highlighted briefly in the following sections.

#### 4.4.5.1 Shear cell measurements

With the help of the shear head information on various parameters of the powder's shear behavior can be collected, such as unconfined yield strength, major principal stress, flow function, internal angle of friction, or cohesion values. The shear head exerts a defined normal stress on the sample and starts to rotate. During the test cycle, different pre-shear and test phases alternate with varying pressures. Subsequently, a shear plane is generated underneath the inserted blades (see Figure 4.14). Depending on the test set-up, sample volumes of as low as 1 mL are adequate for these tests.

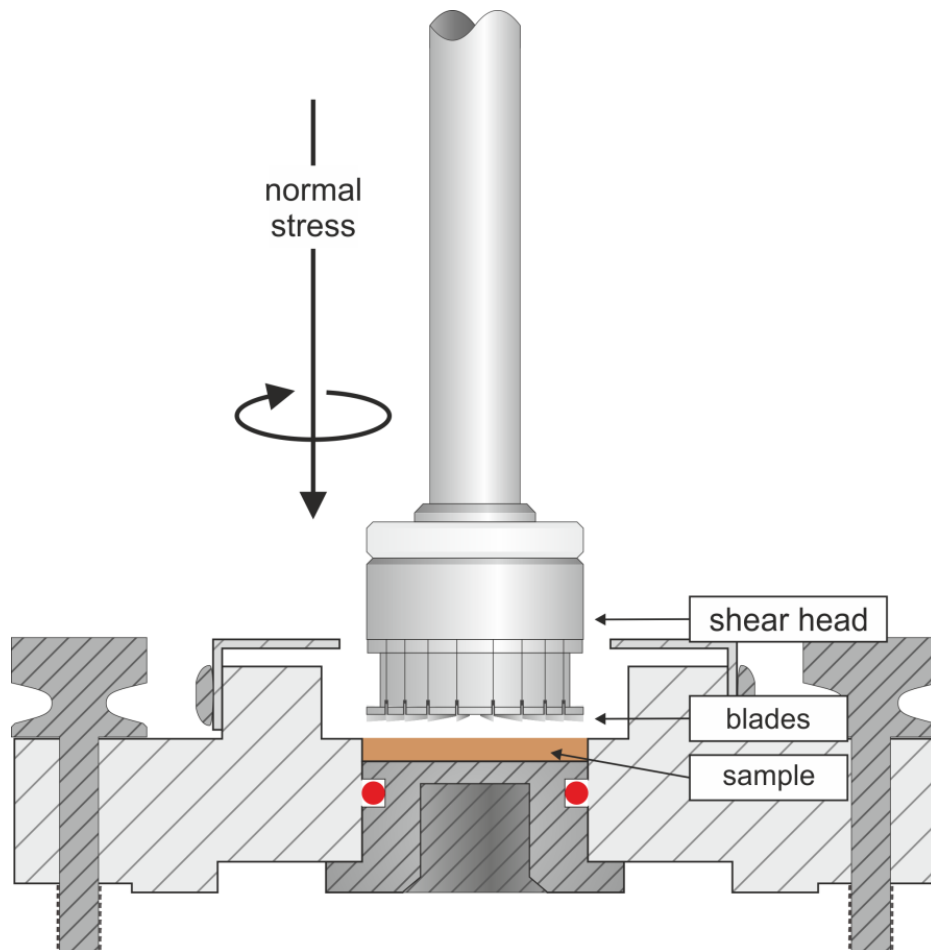


**Figure 4.14:** Schematic set-up for rotational shear cell measurements

It may be referred to the work of Zhou *et al.* (Zhou *et al.*, 2010; Zhou *et al.*, 2011) and Stank (Stank, 2014) for a more detailed description and practical application. In their studies, they used this method to investigate the effects of surface modifications with magnesium stearate on interparticulate forces.

#### **4.4.5.2 Wall friction test**

In addition to measuring particle-particle interactions, the wall friction set-up can be used to investigate interactions between powder and different material surfaces, as well. For this purpose, the shear head is replaced with a piston whose bottom can be equipped with plates of the appropriate material and/or roughness. The piston then exerts a defined pressure on the powder sample and measures the energy required for rotation. The resulting wall friction angle values of these tests provide useful information on the material selection of powder processing or conveying equipment (Freeman *et al.*, 2009).

### **4.5 Preliminary considerations and tests**

Only little knowledge about powder rheology testing of inhalation powder blends is present in the scientific databases. Therefore, some preliminary tests were run with model substances as general feasibility studies.

#### **4.5.1 Test reproducibility**

One essential requirement to obtain reliable results is the achievement of repeatable characteristic values when testing one material multiple times. Thus, a reproducibility and variable flow rate test sequence was run with plain  $\alpha$ -lactose-monohydrate carrier, i.e. Respitose® SV003 powder. After conditioning, the test program commences with 10 individual test and

conditioning cycles to record BFE and SE values and terminates with the FRI test sequence (see sections 4.4.4.1. to 4.4.4.5). This test was then repeated three times and subsequently analyzed. Intra- and inter-reproducibility results are displayed in Figure 4.15.

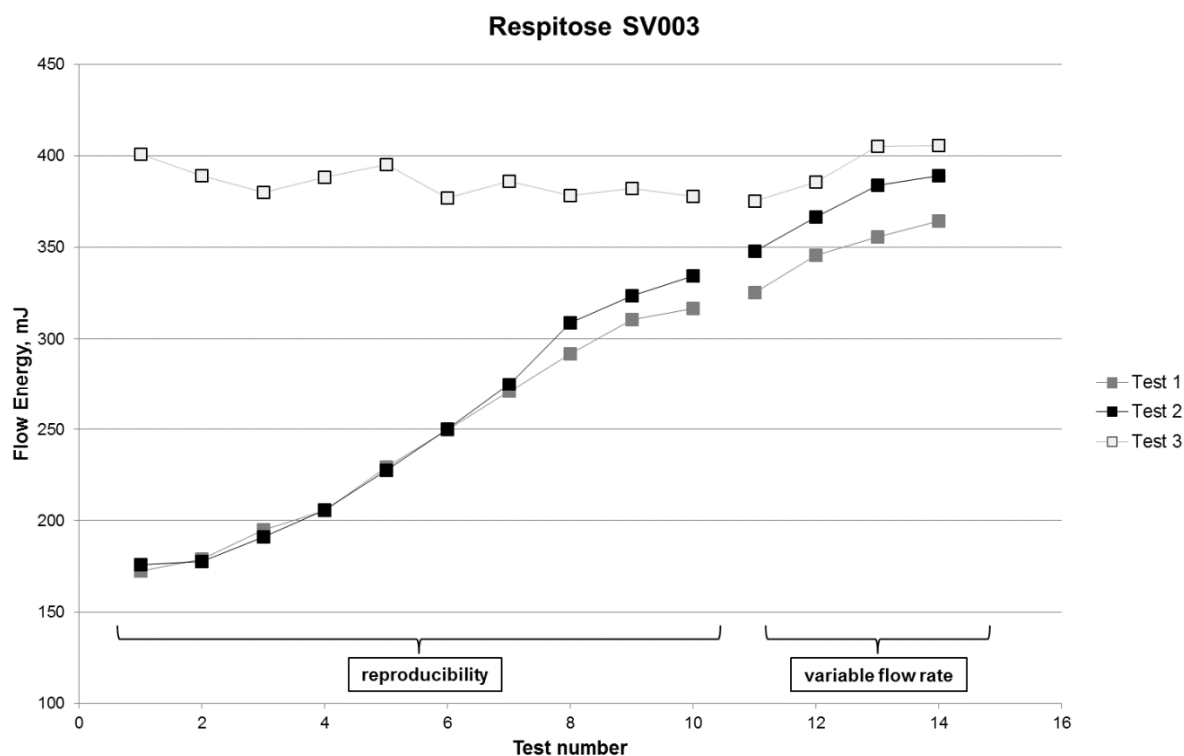


**Figure 4.15:** Standard reproducibility and variable flow rate (REP+VFR) test sequence for Respitose® SV003, n = 3

Starting with test 1, a continuing increase in flow energy can be observed with ongoing testing indicating instability of the powder sample. After the test, the vessel was rinsed with water and thoroughly dried with pressurized air. The powder sample was transferred to a separate storage container and tumbled gently before installed again for the following test 2. Again, non-consistent energy values were recorded, however, the conformity to the values of test 1 suggest no irreversible instability of the powder; the instability could be the result of segregation. This instability was further acknowledged by calculated stability indices (SI) of 1.84 and 1.90,

respectively. Surprisingly, test 3 showed reasonably stable energy values (SI = 1.08) which lay above the highest energy values of tests 1 and 2. To check whether increasing energy values also plateau off at this higher energy level, the first REP+VFR test sequence was modified to contain additional test cycles for the reproducibility section (Figure 4.16). Flow rate indices (FRI) for all tests exhibited similar values and were not further investigated.

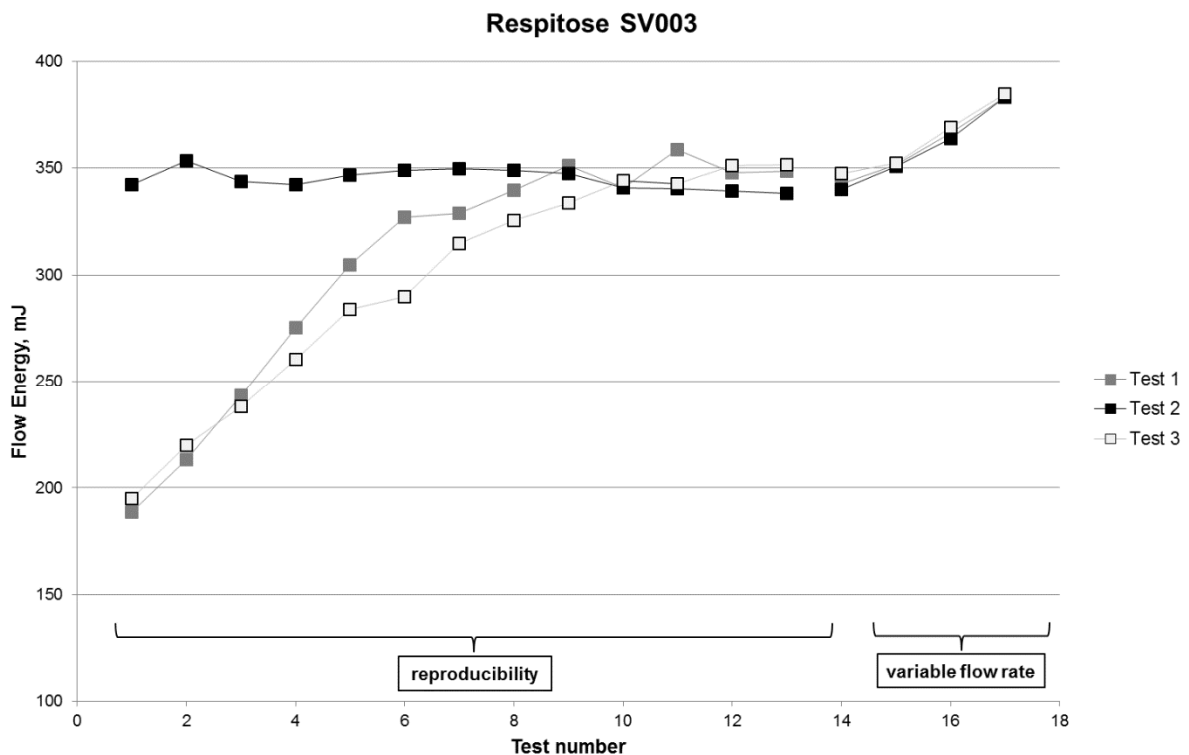


**Figure 4.16:** Modified reproducibility and variable flow rate (REP+VFR) test sequence for Respitose® SV003, n = 3

Again, two of the three runs exhibit the increase in flow energy values. As expected this increase levels off after the first test points. However this time, not the last but test 2 shows reproducible energy values throughout the entire test sequence (SI = 0.99). Since similar powder samples can show stable flow energy values for one test and increasing values for another one, the previously hypothesized theory of reversible segregation during testing had to be discarded.

A closer look at the preparation of the samples and the test vessel was taken. Finally, differences in cleaning procedure of the borosilicate test vessel in between the runs were determined to be the cause for the inconsistent results. When the vessels had been rinsed with water and were dried with pressurized air, the increase in energy values clearly became apparent during the following test sequence. However, for some tests, the vessel was only cleaned with a dry cloth until it appeared visually clean. The test sequences following this dry cleaning process are represented by the reproducible test results. Apparently, the flow behavior of the Respitose® SV003 is affected by the surface properties of the inner test vessel walls. Hence, it is concluded that these surfaces get subsequently coated with fine particles, which remain invisible for the naked eye. Consequently, only dry cleaned test vessels were used for the further investigation. In case a test series was started with a new or wet-cleaned vessel, the results of the first runs were monitored and discarded until results had become stable.

This finding highlights the importance of a careful sample and test equipment preparation and is, on the other hand, a good indication for the high sensitivity of this methodology.

### **4.5.2 Differences between lactose qualities**

Three different lactose qualities (see Table 4.1) were tested with the standard REP+VFR test program to check for general rheology differences between the blends.

**Table 4.1:** PSD of lactose samples (laser diffraction, dry dispersion, 3 bar, lenses R4/R2, n = 3)

material	quality	$x_{10} \pm SD, \mu\text{m}$	$x_{50} \pm SD, \mu\text{m}$	$x_{90} \pm SD, \mu\text{m}$
Lactohale® LH200	milled	10.36 $\pm$ 0.16	70.65 $\pm$ 0.73	160.58 $\pm$ 0.20
jet-milled Respitose® SV003	micronized	0.93 $\pm$ 0.18	5.92 $\pm$ 0.69	25.62 $\pm$ 2.41
Lactohale® LH300	micronized	0.90 $\pm$ 0.00	3.25 $\pm$ 0.09	7.46 $\pm$ 0.18

The graphs in Figure 4.17 and the according values listed in Table 4.2 show the differences between the samples. The basic flowability energy (BFE) of the milled lactose quality (Lactohale® LH200) clearly deviates from the two micronized batches and emphasizes the differences in particle size distributions and conditioned bulk densities (CBD). More interestingly, the two micronized materials exhibit similar BFE values; however, their specific energy values (SE) show different characteristics. It appears that the differences in PSD are not reflected by the basic flowability energy; on the other hand, the deviating SE value and CBD suggest different bulk powder behavior as a consequence of differences in particle shape or agglomeration tendency.

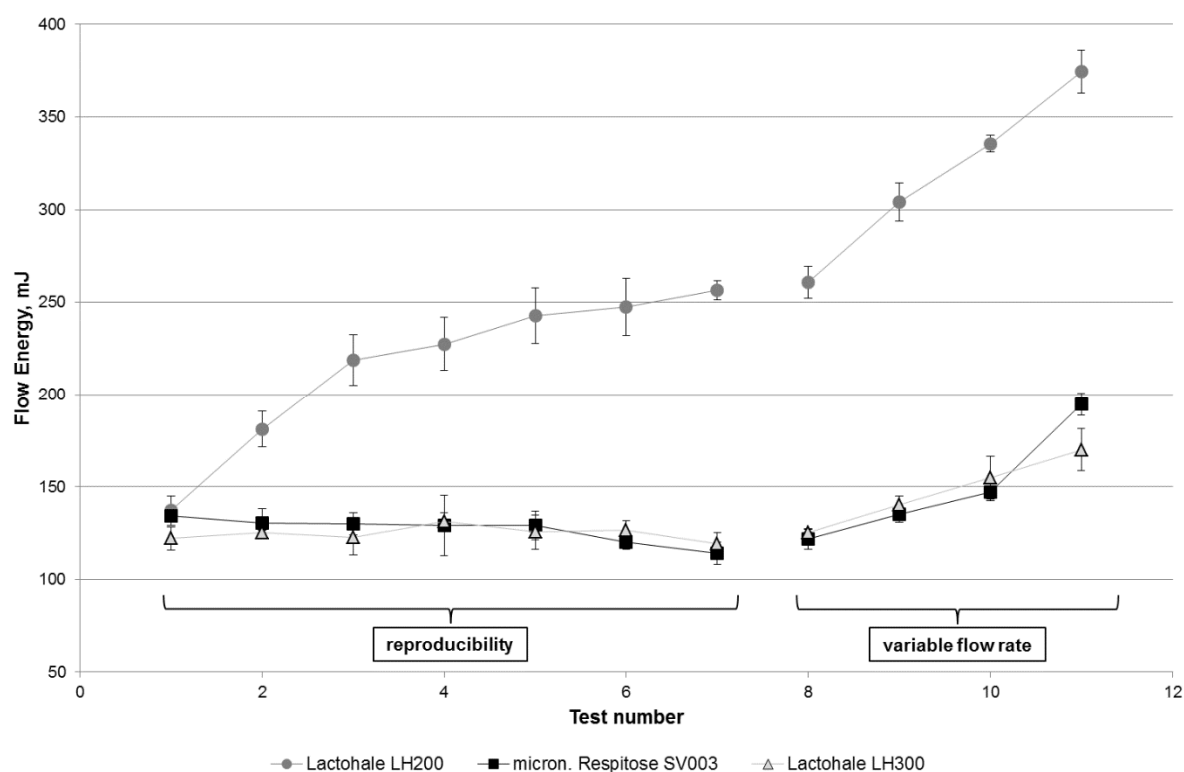


**Figure 4.17:** REP+VFR testing of different lactose qualities, n = 3

**Table 4.2:** Values of REP+VFR testing for different lactose qualities

blend	BFE, mJ	SE, mJ/g	CBD, g/mL
Lactohale® LH200	257 ± 5.08	6.67 ± 0.34	0.63 ± 0.00
jet-milled Respirose® SV003	114 ± 6.00	6.15 ± 1.02	0.33 ± 0.01
Lactohale® LH300	119 ± 5.69	7.88 ± 0.42	0.28 ± 0.01

## 4.6 Materials and Methods

### 4.6.1 Sample preparation

The blends were produced with a T2C Turbula® blender (W.A. Bachofen AG, Basel, Switzerland) at 42 rpm in cylindrical 250 mL polypropylene vessels (height: 75.5 mm, diameter: 65 mm).

The starting materials were sieved through a 355  $\mu\text{m}$  mesh in order to destroy larger agglomerates prior to weighing and bringing together the separate powders.

The addition of starting materials to the mixing vessel was carried out in alternate layers: lactose carrier – lactose fines – lactose carrier [– micronized API – lactose carrier] – lactose fines – lactose carrier. The fill volume of the vessel ranged from approximately 30% - 50% (v/v).

During the mixing process the powder blends were repeatedly given through a 355  $\mu\text{m}$  mesh after 15 and 30 minutes, respectively, to destroy agglomerates of fine material that might have been formed during the beginning of the mixing process. The overall mixing time was 45 minutes for each powder blend.

#### **4.6.1.1 Binary (drug-free) mixtures**

For the binary powder blends Respitose<sup>®</sup> SV003 (DMV-Fonterra, Vehgel, The Netherlands) was used as a carrier and increasing amounts of a micronized lactose, Lactohale<sup>®</sup> LH 300 (Friesland Foods Domo, Zwolle, The Netherlands), acted as the second component. The particle size distribution of the raw materials is shown in Table 4.3.

Different amounts of LH 300 fines were added to the lactose carrier in order to obtain mixtures with a stepwise (2.5%) increase in fines content, covering a range from 0% - 20.0% (w/w) in the final mixtures of 60.0 g.

#### **4.6.1.2 Ternary mixtures**

Ternary adhesive mixtures contained additionally 0.8 - 1% (w/w) micronized budesonide (Shanghai Hengtian Pharmaceutical Co., Ltd.,

Shanghai, China). The preparation of the ternary blends was performed according to the preparation of the binary lactose mixtures.

Table 4.3 lists the used materials and corresponding particle size distributions obtained with laser diffraction measurements. After mixing, homogeneity (2.1.2.1.) and the exact content of budesonide in the blends were determined via HPLC.

**Table 4.3:** PSD of mixture components (laser diffraction, dry dispersion, 3 bar, lenses R4/R2, n = 3)

material	quality	$x_{10} \pm SD,$ $\mu\text{m}$	$x_{50} \pm SD,$ $\mu\text{m}$	$x_{90} \pm SD,$ $\mu\text{m}$	lactose- only	ternary
Respitose®	sieved	20.61	56.76	93.04	✓	✓
SV003		$\pm 4.91$	$\pm 0.74$	$\pm 1.44$		
Lactohale®	micronized	0.90	3.25	7.46	✓	✓
LH300		$\pm 0.00$	$\pm 0.09$	$\pm 0.18$		
Budesonide	micronized	0.41 $\pm 0.02$	1.35 $\pm 0.01$	3.70 $\pm 0.04$		✓

#### 4.6.2 Content Uniformity

Nine samples, 15 mg each, from the ternary blend containing 2.5% LH300 – three samples from the top, three from the middle and three from the bottom of the mixing vessel – were analyzed via HPLC. The ternary mixture containing 20.0% LH300 was analyzed accordingly. From the remaining blends three samples were taken and used for content determination.

Sufficient homogeneity was assumed for the mixtures if the coefficient of variation (CV) remained below 5%.

### 4.6.3 Dispersion measurements

The dispersion behavior was investigated by means of laser diffraction for the drug-free blends, and cascade impaction (i.e. NGI) analysis for the budesonide samples, respectively. Again, the model device mentioned in section 3.2.4 was used to administer the powder to the test equipment for 3 seconds at 80 L/min (4 kPa pressure drop).

In order to determine the dispersed fraction  $< 5 \mu\text{m}$  of the binary mixtures, the laser diffraction sensor was connected with an INHALER<sup>®</sup> module, which enabled the possibility to directly administer a formulation through the inhalation device at a controlled air flow. Subsequently, the dispersed particle collective  $< 5 \mu\text{m}$  (volumetric particle size) was calculated based on the cumulative distribution (Figure 4.18a and b).

As laser diffraction is not capable to distinguish between particles of different material, NGI analysis was performed for the ternary mixtures to determine the drug's fine particle fraction. Collected lactose fines did not interfere with the HPLC analysis of the budesonide content.

## 4.6 MATERIALS AND METHODS

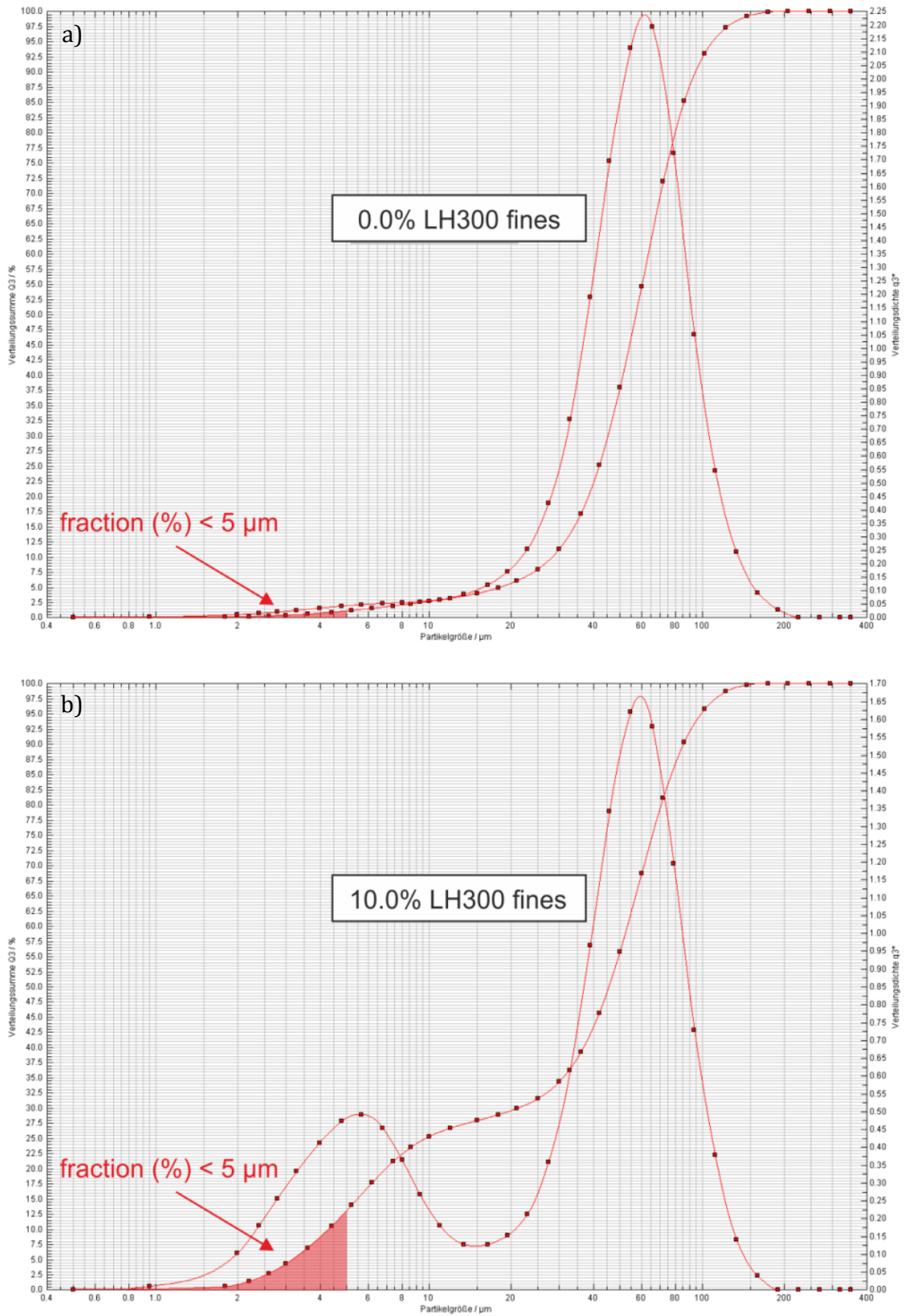


**Figure 4.18:** Particle size distribution (PSD) of lactose-only mixtures measured with the INHALER<sup>®</sup> module

#### **4.6.4 Powder rheology analysis**

##### **4.6.4.1 Dynamic flowability testing of non-aerated powders**

The reproducibility (REP) test program (7 consecutive conditioning and test cycles) was used to study the sample stability during the test sequence and determine the split mass, which is needed for the subsequent aeration testing. A 25 mm x 25 mL borosilicate split vessel was used for the analysis.

##### **4.6.4.2 Permeability**

The permeability test set-up consisted of a 25 mm x 10 mL bore borosilicate split vessel, a porous aeration base connected to an aeration control unit, a 24 mm vented piston and a 23.5 mm blade for conditioning. The ACU kept the air flow through the porous base constant at 2 mm/s while the normal stress applied by the vented piston increased in 8 steps up to 15 kPa normal stress. Each test was repeated three times, for every repeat a new powder sample from the original blend was used.

##### **4.6.4.3 Aeration testing**

The aeration test set-up included a porous aeration base connected to the ACU, a 25 mm x 35 mL bore borosilicate non-split vessel and the 23.5 mm blade. Prior to the aeration tests, multiple basic flowability energy (BFE) measurements without air throughput had been carried out to ensure that the powder samples remained stable for the duration of the aeration test sequence. The aeration tests were then performed in triplicate.

## 4.7 Results and Discussion

### 4.7.1 Aerosolization behavior

Laser diffraction results for the binary lactose powder mixtures show, as expected, a significant increase in the fraction of particles  $< 5 \mu\text{m}$  with increasing amounts of LH300 fines within the mixtures. However, above a LH300 content of 7.5% the curve approaches a plateau at around 15% (Figure 4.19).

A possible explanation for this behavior is the formation of stable agglomerates with further addition of lactose fines. Whereas, at the beginning, lactose fines are able to bind to the lactose carrier surface in monolayers and are easily detached during dispersion, further addition of fines may lead to the saturation of the carrier surface. Thus, an excess of fines results in the formation of agglomerates, which remain stable to a certain extent upon dispersion.

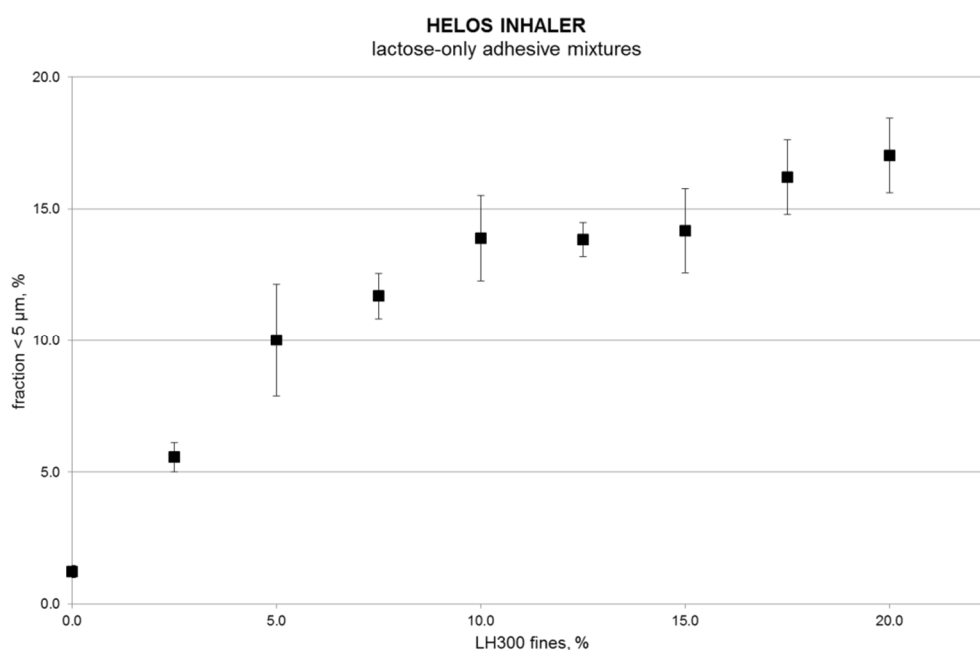


**Figure 4.19:** Dispersion behavior of powder blends as measured with laser diffraction, Fraction  $< 5 \mu\text{m}$  versus LH300 content,  $n= 3$ , mean  $\pm$  SD

Up to 7.5% LH300 fines within the ternary blends, an increase in budesonide FPF can be observed accordingly. The addition of LH300 fines leads to a clear increase in resulting FPF, but only up to a certain threshold. After reaching this threshold, the budesonide FPF drops again – a content of 20.0% LH300 results in an even lower FPF compared to the value of the starting mixture of untreated Respitose® SV003 and budesonide without additional fines (Figure 4.20).

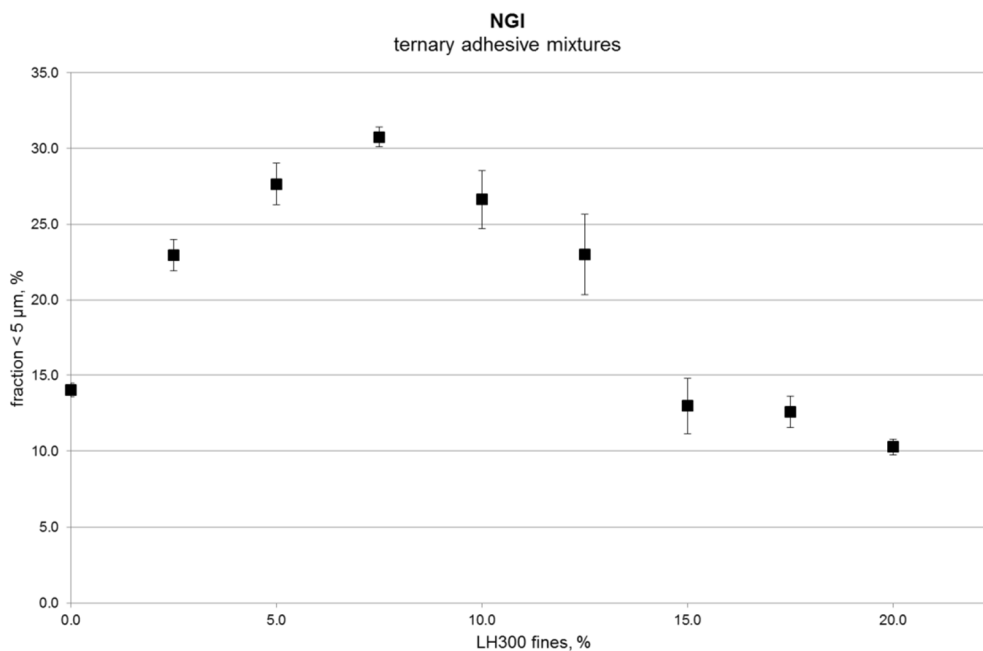


**Figure 4.20:** NGI data, FPF versus LH300 content,  $n = 3$ , mean  $\pm$  SD

Again, this behavior could be explained with the formation of stable agglomerates. During the mixing process, budesonide fines start adhering to the carrier surface and get detached upon dispersion. With the addition of lactose fines budesonide fines compete for binding sites on the carrier surface, resulting in a distribution towards lower energy binding sites (Figure 4.21). This shift towards lower energy spots leads to a higher dispersion efficiency and thus to the increase in FPF indicated by NGI measurements.

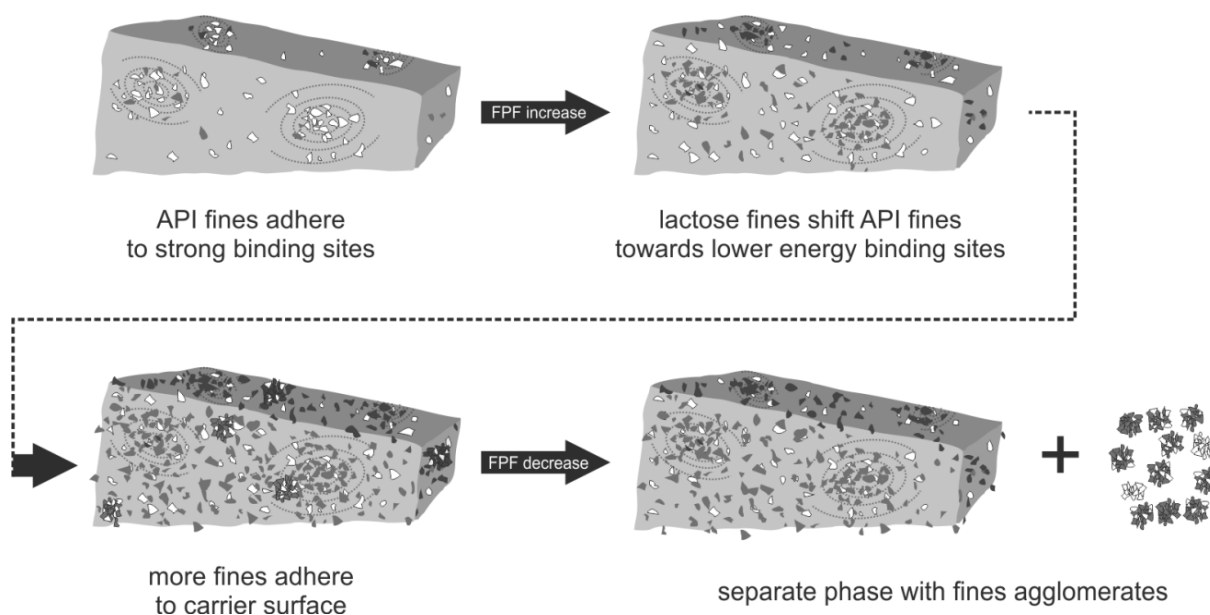


**Figure 4.21:** Possible mechanisms upon ternary fines addition

A fines content of 7.5% (+ the amount of intrinsic fines of the Respitose® SV003) seems to be the most beneficial for this particular set-up. The addition of more LH300 fines leads to a further displacement of budesonide fines, supposedly forming either drug agglomerates or drug/lactose fines agglomerates, which are more dispersion insensitive. Since with higher amounts of LH300 fines more budesonide gets displaced from the carrier surface and gets incorporated in the described agglomerates, the resulting FPF drops significantly. This behavior can also be derived when taking a closer look at the deposition patterns of the mixtures (Figure 4.22). The initial decrease in budesonide deposition in the preseparator suggests a more thorough detachment from the carrier crystal surfaces. However, the following deposition increase indicates that API fines are getting incorporated in fines' aggregates and subsequently impact in the preseparator due to their larger size.

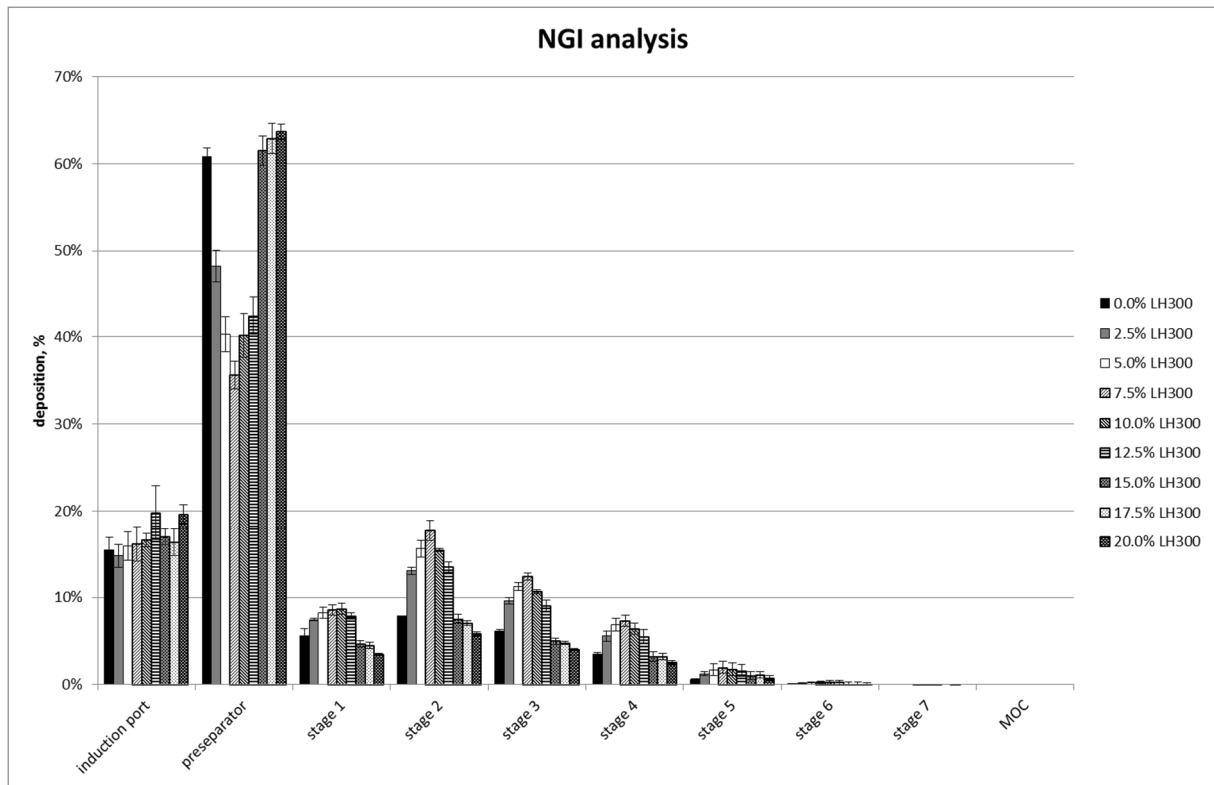


**Figure 4.22:** NGI deposition patterns of ternary mixtures,  $n = 3$ , mean  $\pm$  SD

This hypothesis can be supported by studies from Young *et al.* (Young *et al.*, 2007) and Louey *et al.* (Louey *et al.*, 2003). Both groups proposed a linear increase in FPF with increasing amounts of excipient fines up to a certain threshold value (10% and 13.9%, respectively). Further addition of fines resulted in a clear decrease in fine particle fraction. Young *et al.* speculated that above this threshold value, drug/lactose fines agglomerates fail to adhere to the larger lactose monohydrate carrier particles and become segregated. The authors further assumed that this biphasic system is likely to result in deviation from an expected agglomerate-carrier relationship and therefore can be seen as a cause for the decrease in FPF.

### 4.7.2 FT4 Powder Rheometer® measurements

#### 4.7.2.1 Dynamic flow behavior with non-aerated powder

Flow energies for the non-aerated samples presented in Figure 4.23 show a good reproducibility for the measured values, which is further confirmed by stability indices (SI) close to 1.0 (Table 4.4).

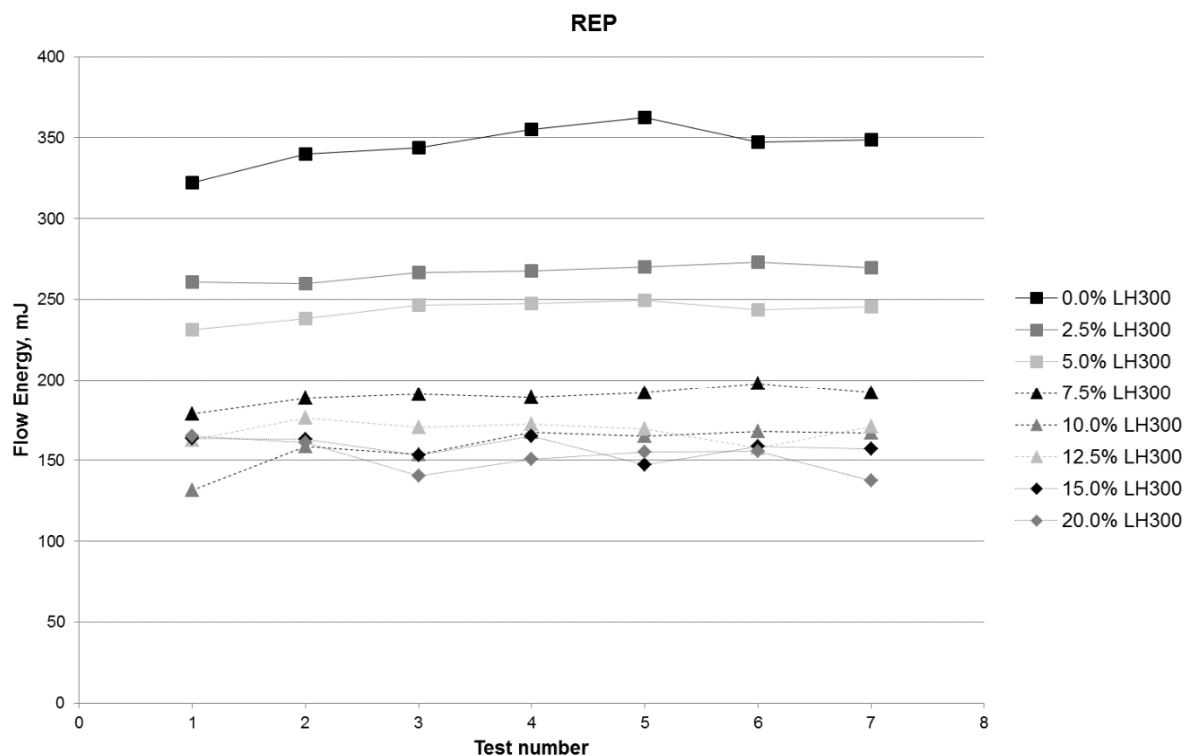


**Figure 4.23:** Reproducibility testing for non-aerated ternary mixtures

BFE values are decreasing with more LH300 fines added to the mixtures; this is in accordance with the observed decrease in bulk densities (CBD). Interestingly, the specific energy (SE) increases with the successive increase in lactose fines. This is an indicator for the generation of agglomerates, since more energy is needed by the blade to cut through these aggregates compared to the mere agitation of individual particles.

**Table 4.4:** Reproducibility test results of non-aerated ternary powder blends

budesonide blend	BE, mJ	SI	SE, mJ/g	CBD, g/mL
+ 0.0% LH300	348.99	1.08	3.57	0.67
+ 2.5% LH300	269.49	1.03	4.75	0.65
+ 5.0% LH300	245.57	1.06	4.27	0.62
+ 7.5% LH300	191.79	1.07	5.21	0.60
+ 10.0% LH300	166.79	1.27	5.72	0.58
+ 12.5% LH300	171.06	1.05	5.06	0.59
+ 15.0% LH300	157.30	0.96	5.68	0.57
+ 20.0% LH300	137.68	0.83	6.08	0.58

Reproducibility testing was also performed with the lactose-only blends to ensure sufficient stability of the sample during aeration measurements. The results revealed similar trends as observed for the ternary budesonide mixtures and are, therefore, not discussed in further detail.

#### 4.7.2.2 Permeability

Permeability results and the corresponding values for the pressure drop across the powder bed of the binary (Figure 4.24a and b) and ternary blends (Figure 4.25a and b) indicate a correlation to the overall fines content. As expected, the more fines within the mixtures, the smaller the permeability value at a given applied normal stress. The fine particles fill up residual spaces between the larger carrier particles and, therefore, upon compression lead to an increase in resistance to air throughput. Whereas the formation of fines agglomerates was discussed as an explanation for the behavior seen in dispersion performance the applied normal stress in the permeability test set-up leads to a destruction of agglomerates and prevents influences caused by these particle formations.

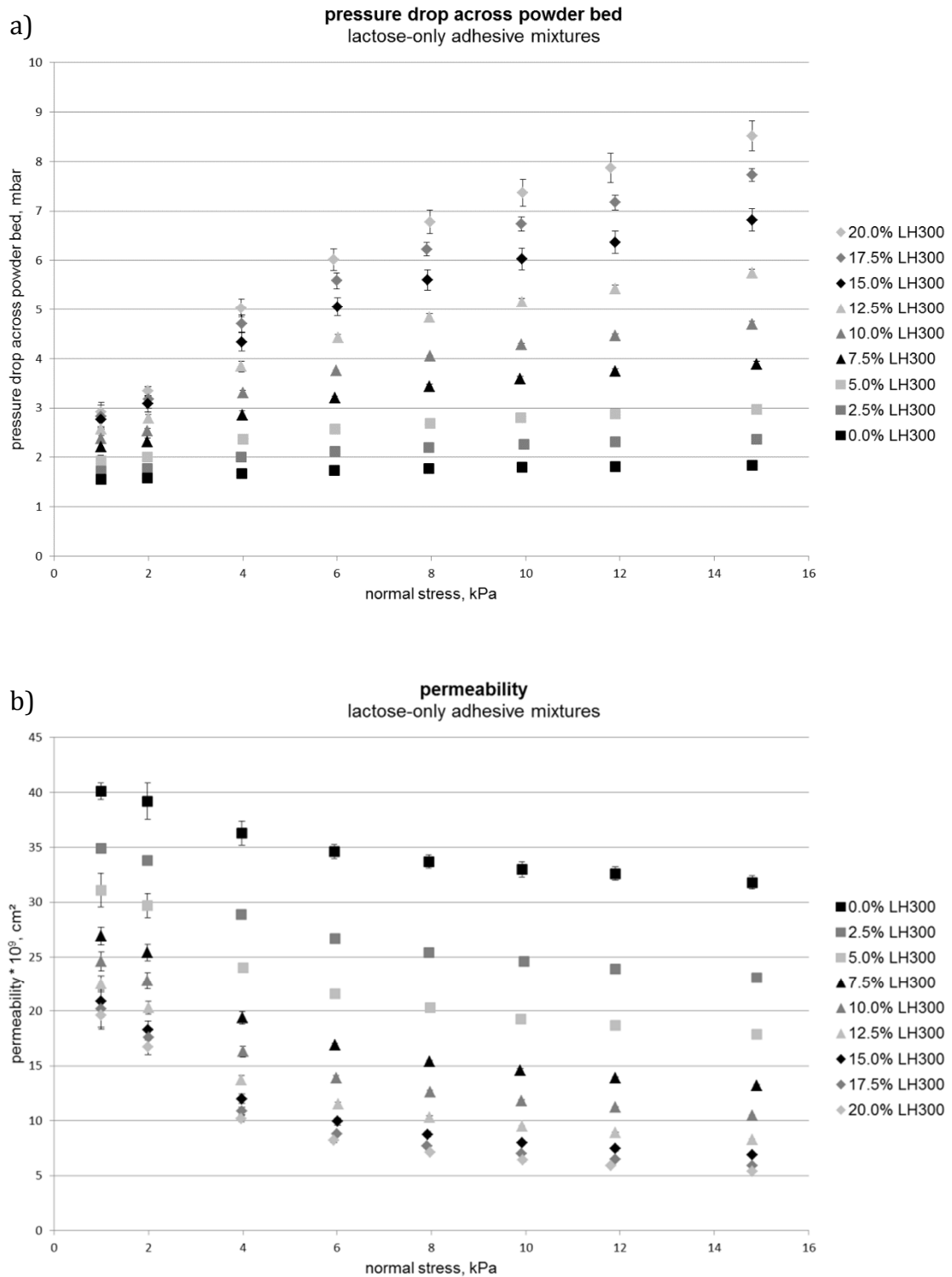
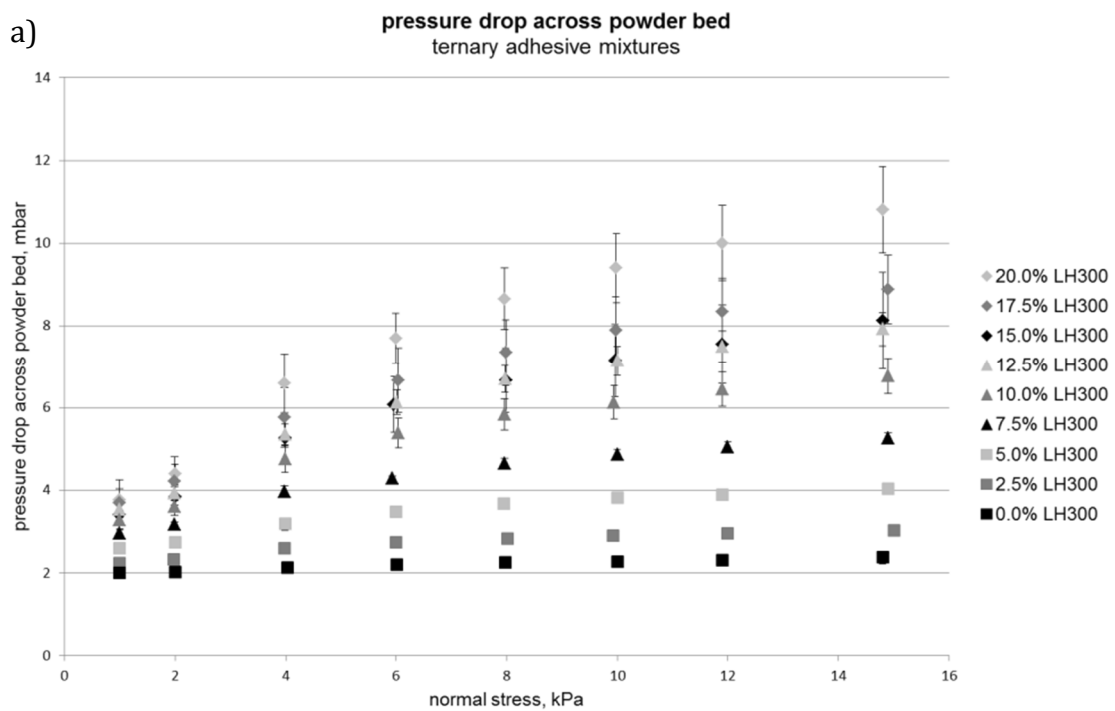


**Figure 4.24: a)** Pressure drop across powder bed **b)** permeability of lactose-only blends

For the binary blends, a linear correlation ( $R^2=0.9924$ , 15 kPa) between the pressure drop across the powder bed ( $\Delta P$ ) and the amount of added fines can be detected. In contrast, permeability values seem to drop exponentially with

the increase in fines since its calculation accounts for the higher compressibility of blends with larger contents of fines.

Taking a look at the analysis of linear regression of the pressure drop across the powder bed and added LH300 fines of the ternary mixtures, the coefficient of determination drops to 0.9829. The decrease in  $R^2$  value is attributed to the higher variability of the measurements with the ternary blends.



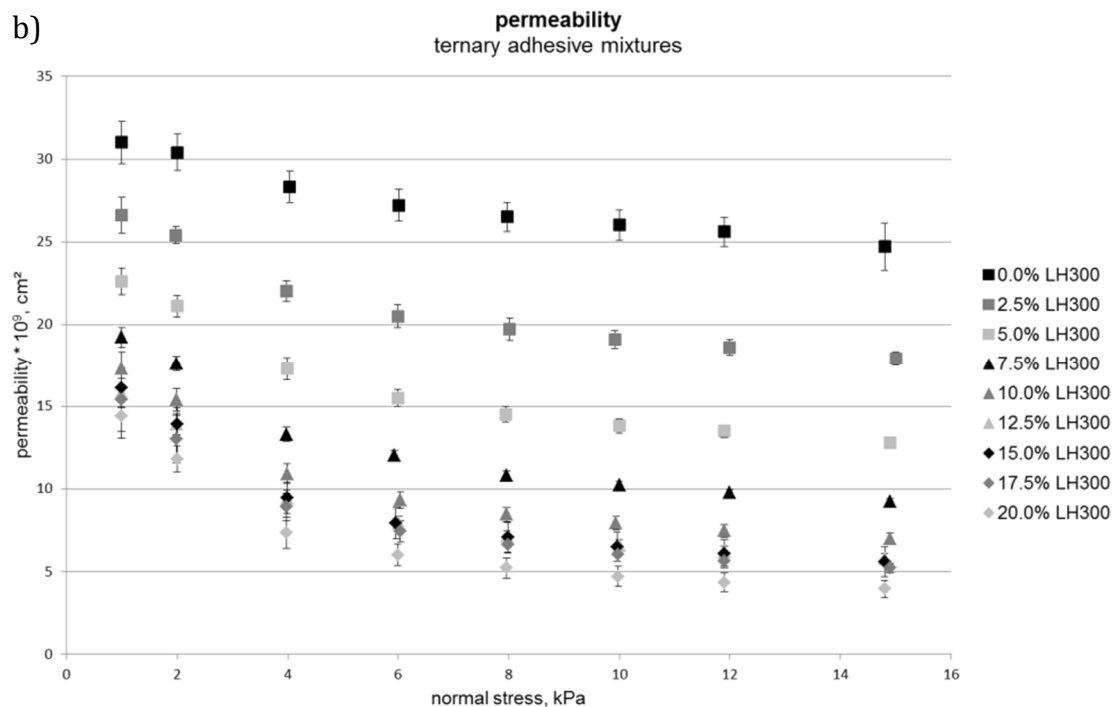


**Figure 4.25: a)** Pressure drop across powder bed **b)** permeability of ternary budesonide adhesive mixtures

Whereas the prediction of fines within the mixture based on the linear regression of the pressure drop across the powder bed works well for each separate system (lactose-only and ternary, respectively), no generalized equation for the prediction of overall fines via permeability measurements can be obtained. This is not surprising, since differences in lactose and budesonide fines morphology likely lead to different characteristics of the overall blends, i.e. different reactions to air throughput.

#### 4.7.2.3 Dynamic Aeration Tests

To understand the characteristics of the aeration test curves (Figure 4.26) the main influencing factors on the measured energy values of the blade should be pointed out. The larger the sample mass – respectively, the denser the powder bulk – the larger the expected energy values for the blade movement. Since the twisted blade needs to displace a larger mass, the resulting total

energy increases accordingly. This behavior can be observed for the energy values at 0 mm/s air throughput.

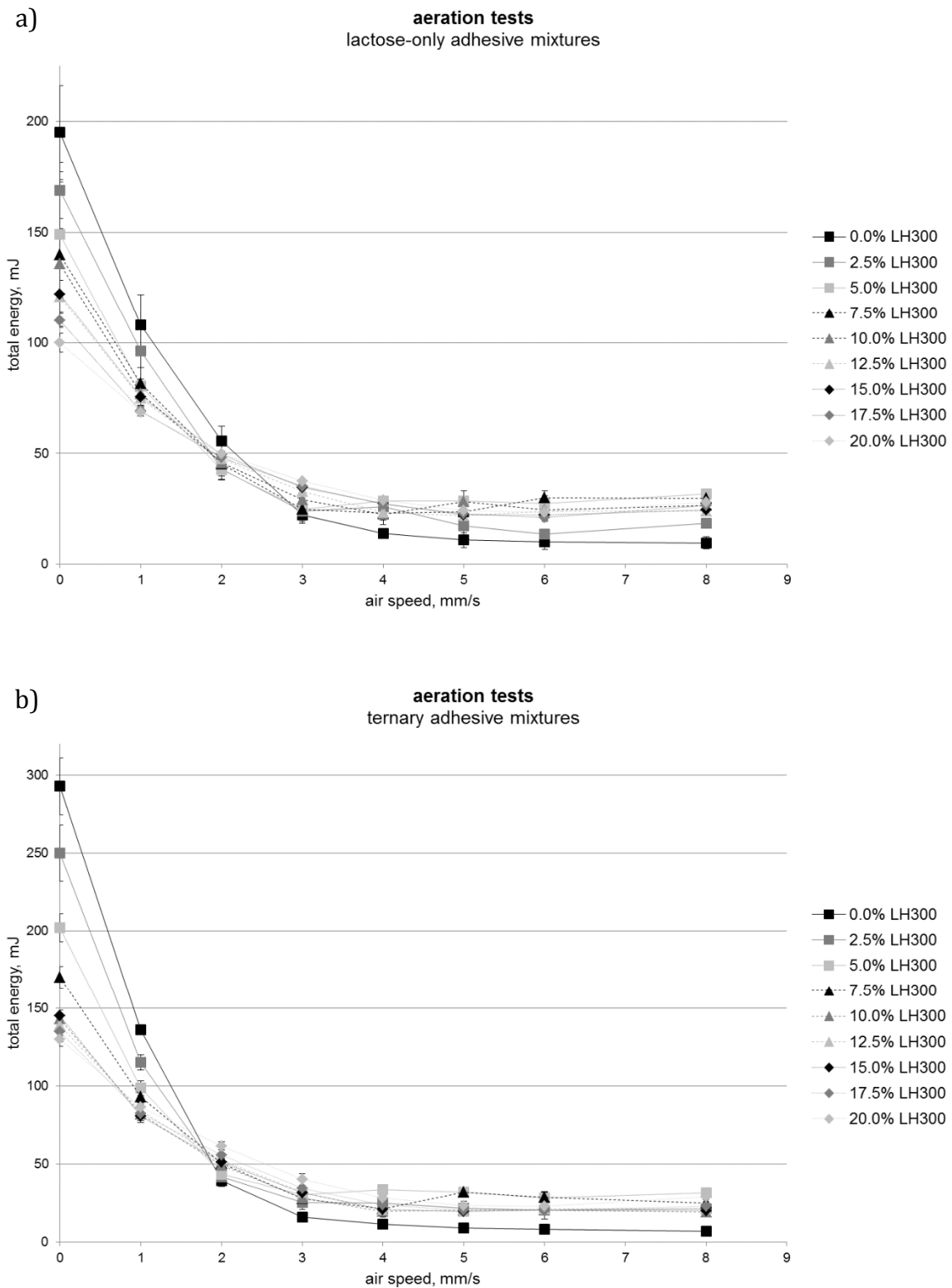


**Figure 4.26:** Changes in flow energy upon successive air entrainment for **a)** lactose-only blends, and **b)** ternary budesonide adhesive mixtures

## 4.7 RESULTS AND DISCUSSION

This trend inverses when taking a look at the minimum fluidization energies (Figure 4.27a). At this point the powder is fully fluidized and therefore the influence of the mass is negligible. Ideally, each powder particle is entrained separately by the airflow. In addition, attracting interparticulate forces decrease as well. However, for the powder blends containing larger amounts of fines, the fines get entrained as stable agglomerates rather than as single particles. This results in an increase in total energy measured by the blade, since larger amounts of energy are needed to cut through these agglomerates (see Figure 4.27a-c).

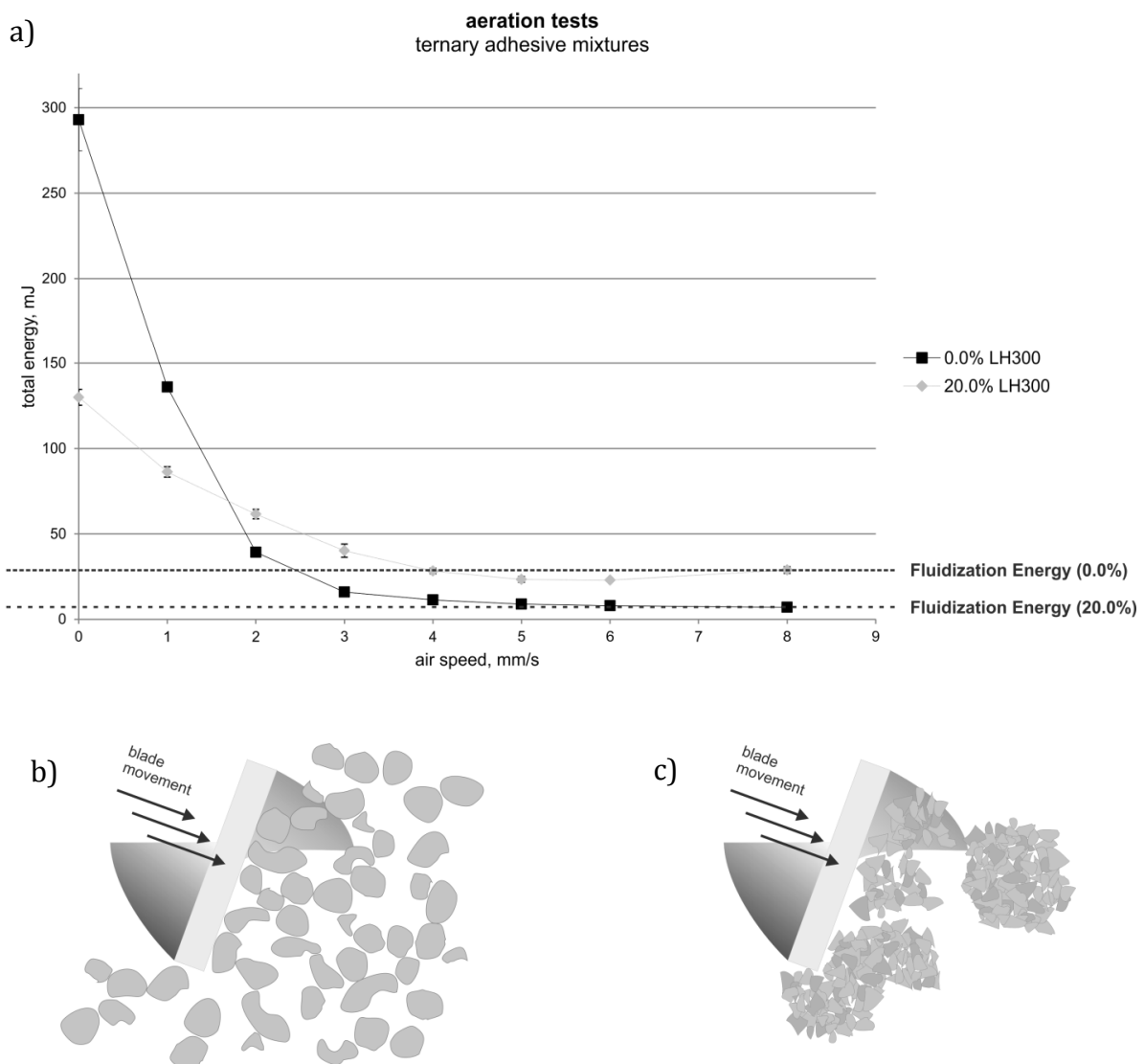


**Figure 4.27a - c:** a) Differences in minimum fluidization energies and b) schema for low fluidization energy and c) schema for high fluidization energy

### 4.7.3 Comparison of permeability, aeration, and impaction analysis results

While the comparison of permeability (i.e. pressure drop across the powder bed) values to the total amount of fines added to a mixture results in a decent correlation, no significance of the permeability towards the amount of released fines < 5  $\mu\text{m}$  upon dispersion can be obtained (Figure 4.28).

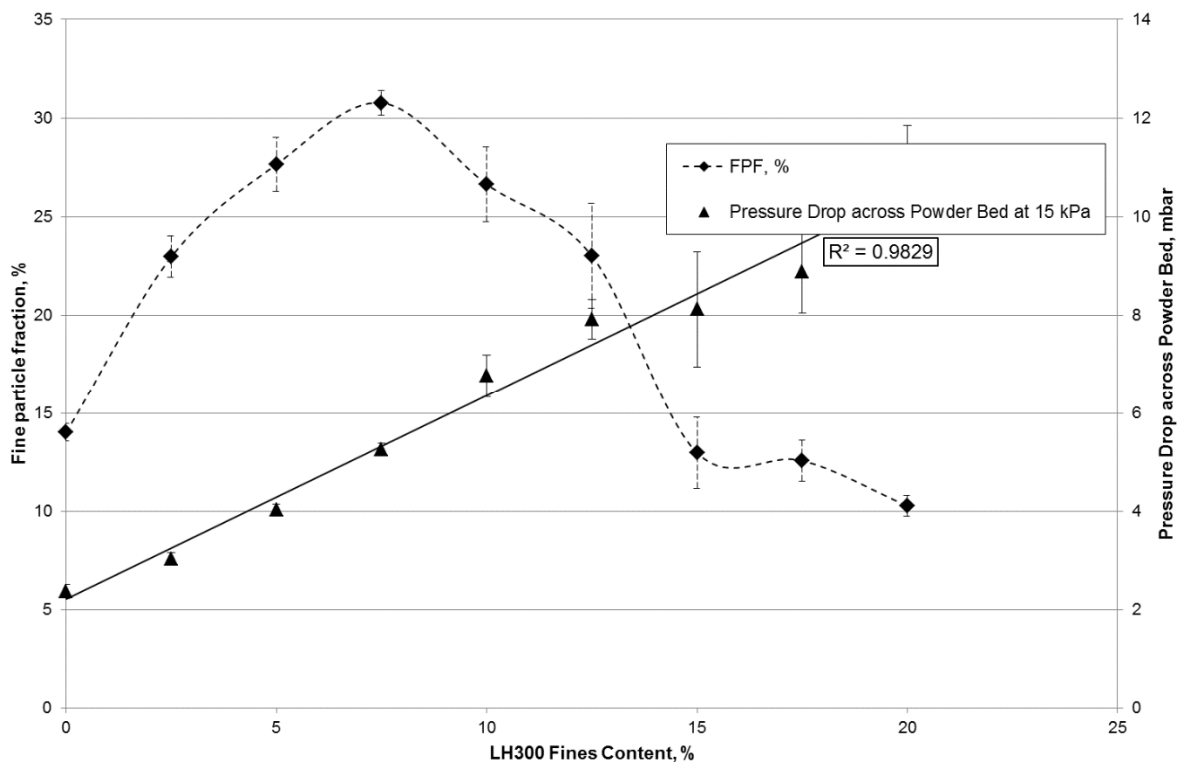


**Figure 4.28:** FPF and Pressure Drop across Powder Bed as a function of ternary fines content

This seems to be contrary to the findings of Le *et al.* (Le *et al.*, 2010), who proposed a linear relationship between the drug fine particle fraction of lactose mixtures containing fluticasone propionate or terbutaline sulphate and the air permeability measured with an adapted Blaine apparatus. But a more detailed look at the findings in their investigation reveals the differences to the current study: the authors varied the amounts of ternary fines in their mixtures only within ranges that remain below 7.5% overall

fines. Having this in mind, the findings indeed match the results obtained for the ternary budesonide mixtures, since the increase in FPF stays linear up to a LH300 addition of 7.5%. Again, a further increase in fines within the mixtures leads to the loss of linear correlation.

Also, the data presented by Price (Price, 2009) suggests a linear correlation of fluidization energy (measured with a Freeman FT4 Powder Rheometer<sup>®</sup>, too) and budesonide fine particle dose up to an excipient fines content of 20.0%. His group did not detect a drop in FPD above an excipient fines content of 7.5% as seen in this study. Since the main parameters of the adhesive powder blends used by Price and the ones used for this work are alike, the differences in results have to be linked to the impact of the different devices used for dispersion. Price's group has used the Cyclohaler<sup>®</sup> for their tests, in which the formulation is effected by more turbulent air flow at a higher air flow rate compared to the model device used in this work.

The experimental data of the current work matches well the already stated theory of a stable agglomerate formation with higher amounts of excipient fines. Drug/excipient fines in amounts up to approximately 7.5% adhere mostly to the lactose carrier surface, which results in an increase in particle fraction  $< 5 \mu\text{m}$  upon dispersion as supported by the laser diffraction and impactor data. A detailed look at the flow energies at the different air velocities underlines this relationship, and especially flow energies recorded at 6 mm/s air throughput match the trend observed in FPF well. Figure 4.29 shows there is an interesting change in fluidization energy at fines contents larger 7.5%. Below this level there is a linear relationship between FPF and aerated energy at this particular air velocity. Above, there is a distinct change in behavior; a reduction in available FPF, which is also observed as a change in the aeration behavior.

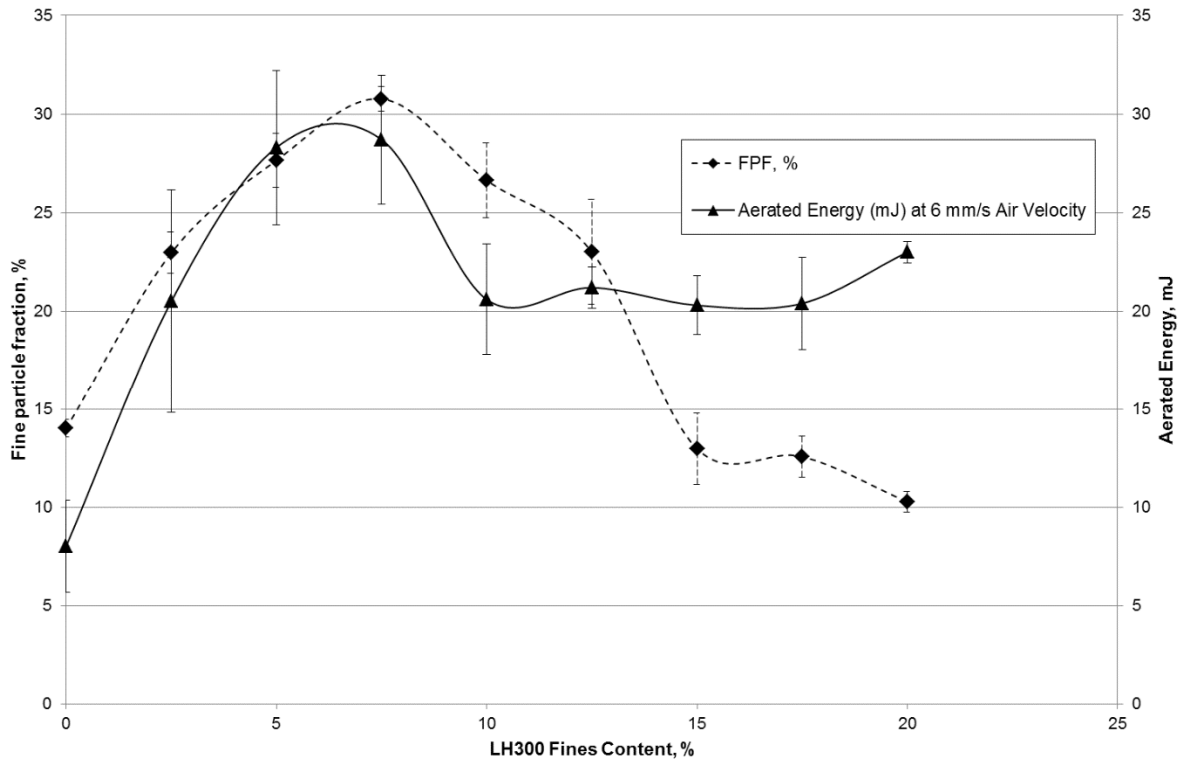


**Figure 4.29:** FPF and Fluidization Energy as a function of fines content

Correlation between aerated energy and FPF is strongest for an air velocity of 6 mm/s. At this particular air speed, forces acting on the particles reveal to be comparable to the ones generated during dispersion in the low turbulence test inhaler.

Finally, a combination of results obtained with both test methodologies leads to the conclusion that lactose fines compete for binding sites on the carrier surface, thus resulting in a shift of budesonide particles towards lower energy spots. Additionally, lactose fines may also bind to the carrier material surface as small agglomerates. Above 7.5% LH300 addition, fines aggregates increase in size and detach from the carrier surface to build a separate phase. This generation of a biphasic system is apparent in both graphs showing the FPF and Aerated Energy (Figure 4.29). The fines' agglomerate (drug/lactose or lactose/lactose) phase cannot be dispersed by the low turbulent airflow in the test inhaler which consequently leads to enhanced aggregate

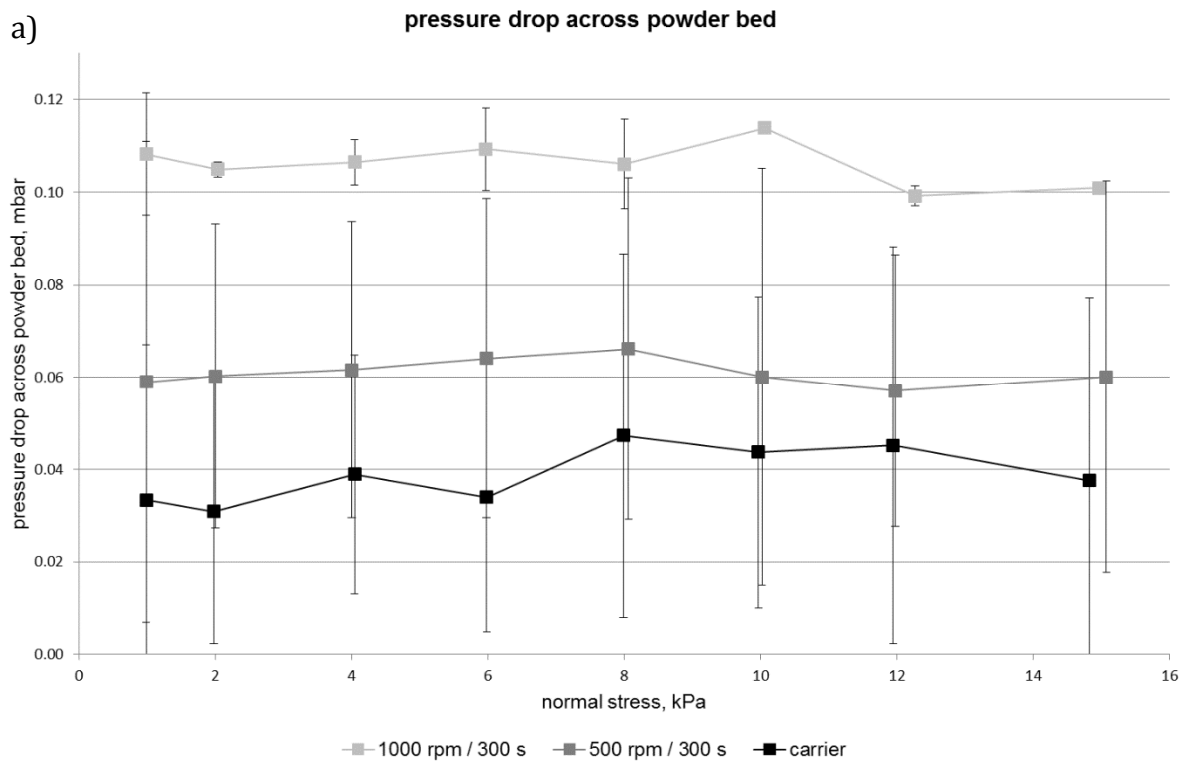
deposition in the NGI preseparator and the observed drop in FPF values. The decrease in aerated energy can be described in a similar way. The flow energy increases due to the lactose fines' addition since more energy is needed to divide bound particles from the carrier material. Also, strongly attached fines lead to a more heterogeneous, non-uniform carrier surface, which also increases the measured flow energies. Further addition of LH300 now leads to the incorporation of particles (or agglomerates) that were previously attached to the carrier surface into the agglomerate-phase. These aggregates consist of more strongly bound particles and behave like single units in the corresponding aerated powder rheology test and exhibit a lower dispersability in the impaction analysis.

Also, the results from Price *et al.* indicate that the impact of these mechanisms is dependent on the inhalation device used. High turbulence inhalers execute more forces on the formulation and are thus capable of further breaking up fines agglomerates. Consequently, a decrease in FPF may not be detected.

#### **4.8 Limitations of FT4 Powder Rheometer® analysis**

Powder rheology analysis can lead to a more profound knowledge about powder bulk properties. However, the significance of the obtained results is usually dependent on the choice of appropriate test methodology. For example, when planning to investigate possible differences of loose agglomerate sizes, test methodologies that use compaction during the measurement may be inappropriate, since aggregates get destroyed under compression. Therefore, the test methodology should be selected with regards to the powder environment in which it will generally be handled.

In addition, certain particle sizes can be inappropriate for specific test set-ups. For instance, the permeability and aeration behavior of the mixtures produced in section 3 were also tested. The results are presented in Figure 4.30 a – c and indicate a poor reproducibility. For the permeability test, pressure drop values found are very low leading to increased variations in test results. This is a direct consequence of the large carrier material used for these blends. Thus, variations to the (already excellent) permeability cannot be used as a reliable differentiator between the blends.



## 4.8 LIMITATIONS OF FT4 POWDER RHEOMETER® ANALYSIS

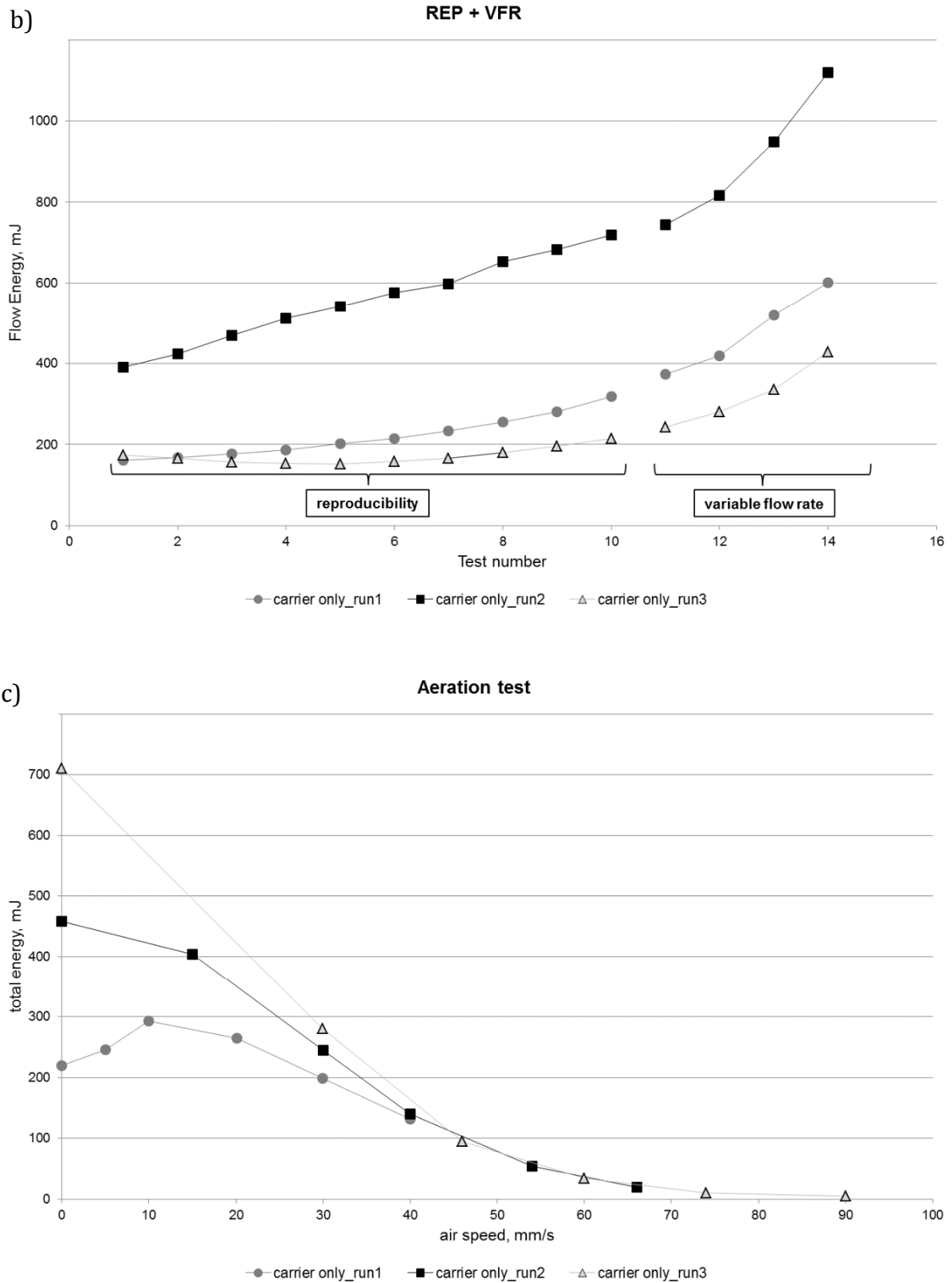


**Figure 4.30:** a) Permeability of salbutamol sulfate/Pharmatose® 80M (250-312  $\mu\text{m}$ ) mixtures; b) REP + VFR (BFE) and c) Aeration test graphs for plain carrier material

The results of the dynamic powder flow measurements (Figure 4.30b) already show non reproducible results for tests with pure carrier material. The high variations in flow energy indicate possible particle crushing or interlocking with the ongoing test sequence. It seems like large carrier particles pinch in the gap (Figure 4.31) between the rotating blade and the vessel walls, hence the recorded energy values needed by the blade to induce powder flow are not reliable and reproducible.

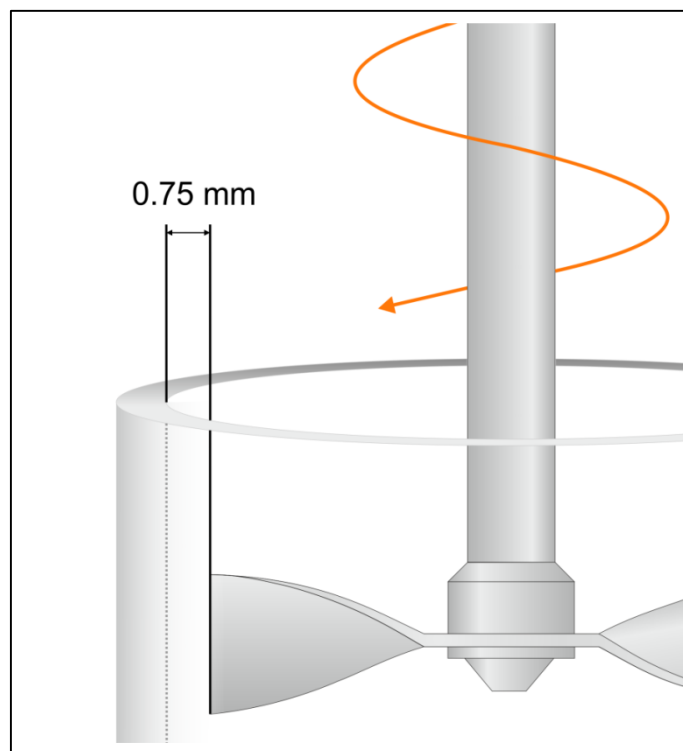


**Figure 4.31:** Gap between blade and vessel walls of 25 mm set-ups

A way to approach this issue can be the change in test set-up. A switch to the 50 mm diameter test vessels and 48 mm blade increases the gap between blade and vessel walls slightly to 1 mm on either side. However, a substantially larger sample volume (160 mL) would be necessary for the measurements and may limit its use for early development studies. A combination of 50 mm diameter vessel and 23.5 mm blade would also provide an alternative; however, this set-up would still require large amounts of powder samples for the measurements.

Despite the inconsistency in basic flowability energy (flow energy at 0 mm/s air throughput), aeration test results also indicate that comparably large air speeds are necessary to fluidize the powder. Further, flow energy decreases to a baseline value, hence, no fluidization energy can be obtained. This behavior is consistent to the low values measured during permeability testing and demonstrates a powder that is largely insensitive to changes in aeration.

However, these “negative” results are still a valuable addition for the thorough characterization of the materials, even though differences in aeration behavior were too small to be detected with this type of equipment.

### **4.9 Conclusion**

Powder rheology measurements have proved to be a valuable addition for the characterization of powder blends. The range of results obtained from different test methodologies highlights the complexity of thorough powder characterization.

With the aeration test set-up it was possible to simulate the forces acting on an inhalation powder blend upon dispersion in a model device. However, only in combination with results obtained from non-aerated dynamic flow measurements and bulk permeability testing a deeper mechanistic understanding about underlying particle interactions could be achieved.

Again, this emphasizes that powder behavior cannot be described by a single measurement value and points out the strengths of the FT4 Powder Rheometer®. Its versatility allows to investigate the powders response under different environmental stress conditions, which may all become relevant at some point during subsequent processing or handling. Therefore, the main

challenge when assessing powder behavior is arguably the correct interpretation of extensive data from various test methodologies.

In this study, it could be demonstrated that budesonide fines adhered to a lactose crystal surface get displaced by ternary lactose fines towards sites from which they are more easily detached. However, successive lactose fines addition ends up in the generation of fine particle agglomerates after reaching a threshold concentration of about 7.5%, which have shown to be less sensitive to dispersion. Arguably, these aggregates consist of ternary lactose fines and micronized budesonide, thus leading to an overall decrease in drug aerosolization performance. This theory supports previously reported speculations about the generation of a biphasic system (carrier and aggregate phase, respectively) with continuing fines addition.

Powder rheology analysis was shown to be an appropriate tool for the investigation of the impact of ternary fines addition to an adhesive powder blend. General relationships could be deduced from the measurement results and have helped to gain an improved knowledge about the underlying mechanisms. Further studies should aim towards the analysis of other factors that have shown to impact aerosolization performance, such as changes in storage humidity, particle size, shape, or morphology, to name only a few. Considering the individual test variability, the FT4 Powder Rheometer® should be challenged with regards to the measurement sensitivity.

It is emphasized that powder characterization is a complex challenge. Powder properties may show to be extremely variable depending on the operator handling and distinct test method used. Many operators are seeking for a simple and straight-forward approach to describe powder properties. However, this understanding is too short-sighted and will automatically fail to reflect the versatile powder appearances. Hence, specific testing should be

performed with regards to the environment of the powder during its intended use. Also, different aspects of a powder may become relevant during processing. For example, flowability of a sample may be important in order to achieve a correct volumetric dosing, whereas the powder's sensitivity to consolidation is of interest when investigating the behavior in a hopper or under storage. It needs to be understood that many of these powder parameters are often independent and unrelated. Two powders may reveal similar flowability, but differ in permeability, or, they show similar compressibility, but exhibit significant differences in flow.

## 5. PART 3 – MIXING INFLUENCE ON DISSOLUTION BEHAVIOR

### 5.1 Introduction

Dissolution testing is a widely used methodology to assess characteristics of solid or semi-solid dosage forms. Standardized test requirements are listed in the Pharmacopoeias and are essential when developing new drug products as the results may be correlated to *in-vivo* pharmacokinetic data. Additionally, the obtained data is used for quality control and assist with the determination of bioequivalence (Dressman *et al.*, 1998).

For inhalation products, larger drug/formulation particles are likely affected by mucociliary clearance mechanisms in the upper region of the lungs, whereas in the lower, non-ciliated lung regions smaller deposited particles will dissolve in the lung fluids and subsequently be absorbed through the alveolar membranes. The dissolution rate of small drug particles is oftentimes expected to be very high due to their large surface area. However, the dissolution rate may become critical when administering low soluble APIs to the little amounts of lung fluid since undissolved particles may be taken up by alveolar macrophages and cleared by further mechanisms (Davies and Feddah, 2003).

While there are standardized dissolution test methods and equipment available for solid dosage forms which are used on a routine basis, collection and dissolution testing of aerosol particles are considerably more sophisticated. The dissolution behavior of inhalation products has gained increased attention in the past years, since researchers are attempting to develop sustained release formulations (Learoyd *et al.*, 2008), or, are seeking

for methodologies to investigate and ensure bioequivalence of inhalation medication (Riley *et al.*, 2012).

In the following experiments, a dissolution test set-up developed by Forbes *et al.* (Forbes *et al.*, 2010) was used to investigate the impact of different mixing conditions on the inhalation performance on the one hand, and the further changes in dissolution time on the other hand. Also, the samples were tested by means of powder rheology analysis to help recognizing possible, mixing induced changes to the formulations. The dissolution tests were performed in cooperation with Parma University while the study set-up, preparation of powder blends, impaction analysis, and powder rheology measurements were conducted at Kiel University.

## **5.2 Materials and Methods**

### **5.2.1 Blend preparation**

Four mixtures were produced with a Picomix<sup>®</sup> module (Picoline<sup>®</sup>, Hosokawa Alpine, Augsburg, Germany). The equipment used for the preparation of these blends is of similar dimensions as the stand-alone Picomix<sup>®</sup> used in the powder blending study (3.2.2.1), however the equipment is now a dedicated module for the Picoline<sup>®</sup> series (see Figure 5.1 and Figure 5.2).

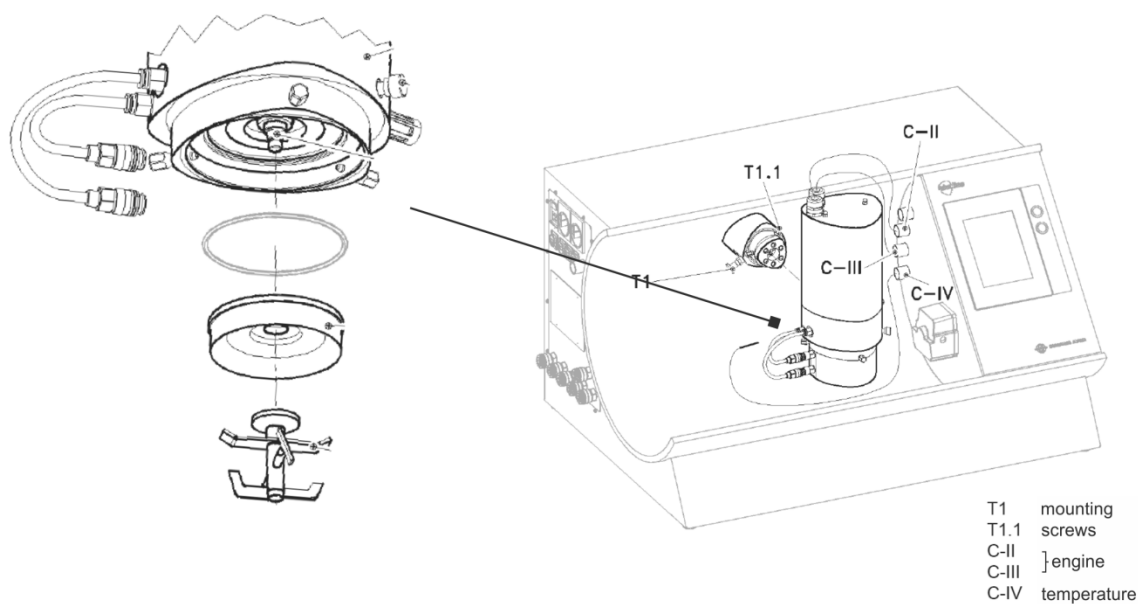


**Figure 5.1:** Schematic of Picoline® with Picomix® module (HOSOKAWA MICRON B.V.)

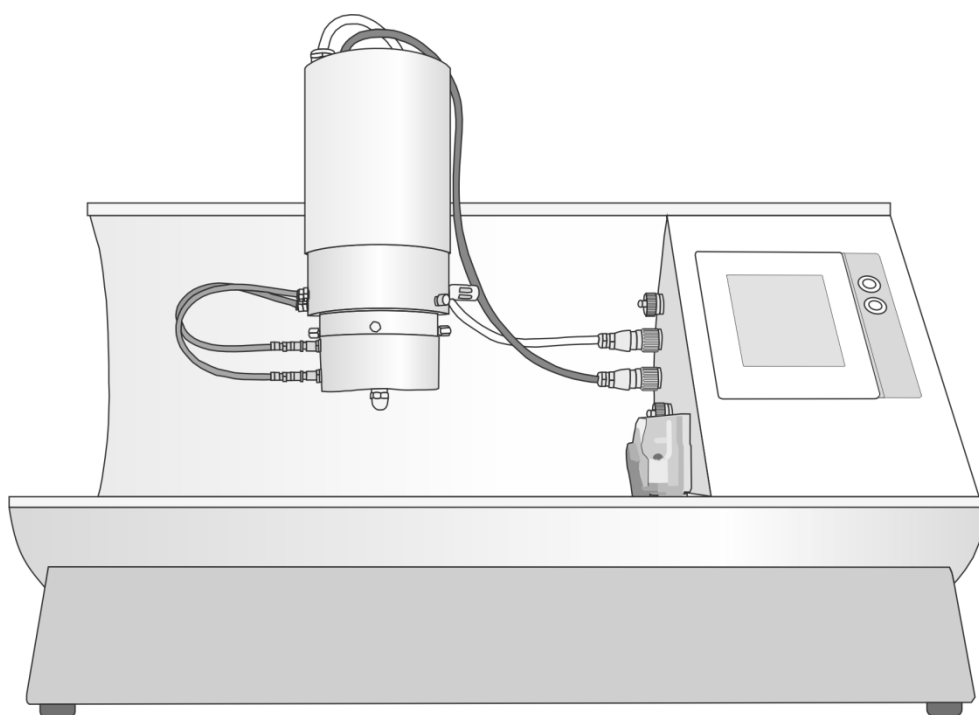


**Figure 5.2:** Picoline® with Picomix® module

Respitose® SV003 (DMV-Fonterra, Veghel, The Netherlands) was mixed with micronized salmeterol xinafoate (Midas Pharma, Ingelheim, Germany) (Table 5.1) with a high shear mixer, i.e. Picoline® + Picomix® module. The salmeterol xinafoate was screened through a 180  $\mu\text{m}$  mesh and subsequently the

excipients were weighed and added to the 180 mL stainless steel mixing container of the Picomix® in alternating layers.

**Table 5.1:** PSD of mixture components (laser diffraction, dry dispersion, 3 bar, R4, n = 3)

material	quality	$x_{10} \pm SD, \mu\text{m}$	$x_{50} \pm SD, \mu\text{m}$	$x_{90} \pm SD, \mu\text{m}$
Respitose® SV003	sieved	$31.29 \pm 0.06$	$58.64 \pm 0.03$	$89.48 \pm 0.04$
Salmeterol xinafoate	micronized	$0.87 \pm 0.00$	$1.99 \pm 0.01$	$4.31 \pm 0.04$

The mixtures were composed to target an API content of 0.58% (m/m), which was adapted to match the commercially available Serevent® Diskus® product. The mass of a single mixture added up to 40.0 g, which corresponded to a filling volume of approximately 30 – 35% (v/v) in the Picomix® stainless steel vessel. In order to obtain a sufficient powder mass for further FT4 Powder Rheometer® analysis, blends were produced in duplicate and the two separate batches were combined by means of Turbula® mixing for 5 consecutive minutes to end up with a total mass of 80.0 g.

Mixing times and mixing speeds were varied to represent different energy inputs during mixing for each of the four produced blends according to Table 5.2.

**Table 5.2:** Picomix® process parameters

	blend 1000/45	blend 2000/60	blend 3000/75	blend 4000/90
speed, rpm	1000	2000	3000	4000
time, s	45	60	75	90
revolutions	45000	120000	225000	360000

### 5.2.2 Content Uniformity

15 samples of 12.5 mg  $\pm$  0.4 mg (1 dose of Serevent® Diskus®: 12.5 mg) were randomly picked from the powder bed, dissolved in a mixture of methanol : dd H<sub>2</sub>O (75 : 25) and the content was analyzed by HPLC.

### 5.2.3 NGI analysis

Cascade impaction analysis was again performed with a Next Generation Pharmaceutical Impactor in combination with the low turbulent, model inhalation device (see section 3.2.4.3). Each blend was tested in triplicate and 10 doses (12.5 mg each) were delivered to the impactor per run. The testing was performed at 80 L/min (4 kPa) and under controlled ambient conditions (21 °C and 45% rh). The impaction stages were washed with a methanol : dd H<sub>2</sub>O (75 : 25) mixture and analyzed with HPLC.

### 5.2.4 Dynamic powder rheology analysis

The standard reproducibility and variable flow rate (REP+VFR) test program of the FT4 Powder Rheometer® was run (see section 4.4.4). 25 mL samples of each blend were filled into a 25 mm x 25 mL split borosilicate test vessel and were conditioned and measured with a 23.5 mm blade. The standard stability (reproducibility) test sequence consists of seven alternating conditioning and test cycles with a tip speed of 100 mm/s and is followed by the variable flow rate sequence comprising of four conditioning and test cycles with reducing blade tip speeds (100 mm/s to 10 mm/s).

In addition, aeration testing was performed with the 25 mm x 35 mL non-split vessel and aeration base. The sample mass was adjusted to equal a volume of 25 mL. The test sequence was programmed to increase the air velocity in 8 steps up to 8 mm/s.

All powder rheometer measurements were performed in duplicate using the same blend.

### 5.2.5 Dissolution behavior

Dissolution behavior of the salmeterol xinafoate (SX) formulations was performed using Franz cells (Buttini *et al.*, 2014; Forbes *et al.*, 2010; Grainger *et al.*, 2012; Lewis *et al.*, 2013). The blends were tested before and after aerosolization. 50 mg ( $\pm$  2.5 mg) of blend before aerosolization were deposited and spread with a spatula on a filter in the donor compartment of the Franz cell. To collect the fraction below 5  $\mu$ m after dispersion, a Fast Screening Impactor (FSI) (Copley Scientific, Nottingham, UK) was used. 10 capsules containing 10 mg each were aerosolized at a pressure drop of 4 kPa using an RS01 inhalation device (Plastiapae, Lecco, Italy) and the central portion of the collecting filter was cut and placed between donor and receptor compartment of the Franz cell.

The Franz cell receiver fluid, 21 mL of phosphate buffered saline (PBS buffer) with a pH of 7.4 at 37 °C, was continually agitated with a small magnetic stirrer. Sample volumes of 1 mL were drawn at defined time points and the dissolved content was determined with HPLC.

## 5.3 Results and Discussion

### 5.3.1 Content uniformity

The coefficient of variation (CV) of all formulations was below 4%, which indicates a sufficient efficiency of the mixing process (Table 5.3).

**Table 5.3:** Salmeterol xinafoate contents of blends

	blend 1000/45	blend 2000/60	blend 3000/75	blend 4000/90
content	0.5699%	0.5651%	0.5392%	0.4372%
SD	0.0100%	0.0213%	0.0054%	0.0039%
CV	1.76%	3.77%	1.00%	0.90%
drug loss	1.83%	2.65%	7.08%	24.66%

However, Table 5.3 also reveals a significant decrease in API content of the blends with increasing mixing speeds and times. This matches with observations of the mixing vessel directly after processing. For the most intense mixing conditions, a white layer on the vessel walls (in this case supposedly salmeterol xinafoate) clearly became apparent. This decrease in API content with increasing mixing intensity was already mentioned for salbutamol sulfate blends produced in section 3.2.2 and needs to be considered when defining appropriate mixing process parameters.

### 5.3.2 Laser diffraction analysis

Laser diffraction results indicate possible particle comminution for blend 4000/90 as the  $x_{10}$  value for this blend decreased compared to the values of the three other mixtures (Table 5.4).

**Table 5.4:** PSD of blends (laser diffraction, dry dispersion, 5 bar, R4, n = 3)

blend	$x_{10} \pm SD, \mu\text{m}$	$x_{50} \pm SD, \mu\text{m}$	$x_{90} \pm SD, \mu\text{m}$
blend 1000/45	18.56 $\pm$ 0.26	54.83 $\pm$ 0.22	85.45 $\pm$ 0.48
blend 2000/60	22.54 $\pm$ 0.60	55.12 $\pm$ 0.16	85.37 $\pm$ 0.14
blend 3000/75	21.52 $\pm$ 0.39	54.95 $\pm$ 0.25	85.41 $\pm$ 0.35
blend 4000/90	15.39 $\pm$ 0.31	53.29 $\pm$ 0.12	84.65 $\pm$ 0.16

### 5.3.3 Cascade impactation analysis

The NGI deposition patterns of the four blends are presented in Figure 5.3. With increasing mixing intensities lower preseparator depositions were detected. Accordingly, the salmeterol xinafoate mass on the lower impactor stages increased. This behavior is also reflected by the calculated fine particle fraction values listed in Table 5.5. The lowest API fraction smaller 5  $\mu\text{m}$  can be observed for blend 1000/45 and slightly increases for blends 2000/60 and 3000/75, respectively. However, FPF for blend 4000/90 almost doubles compared to the lower energy blends.

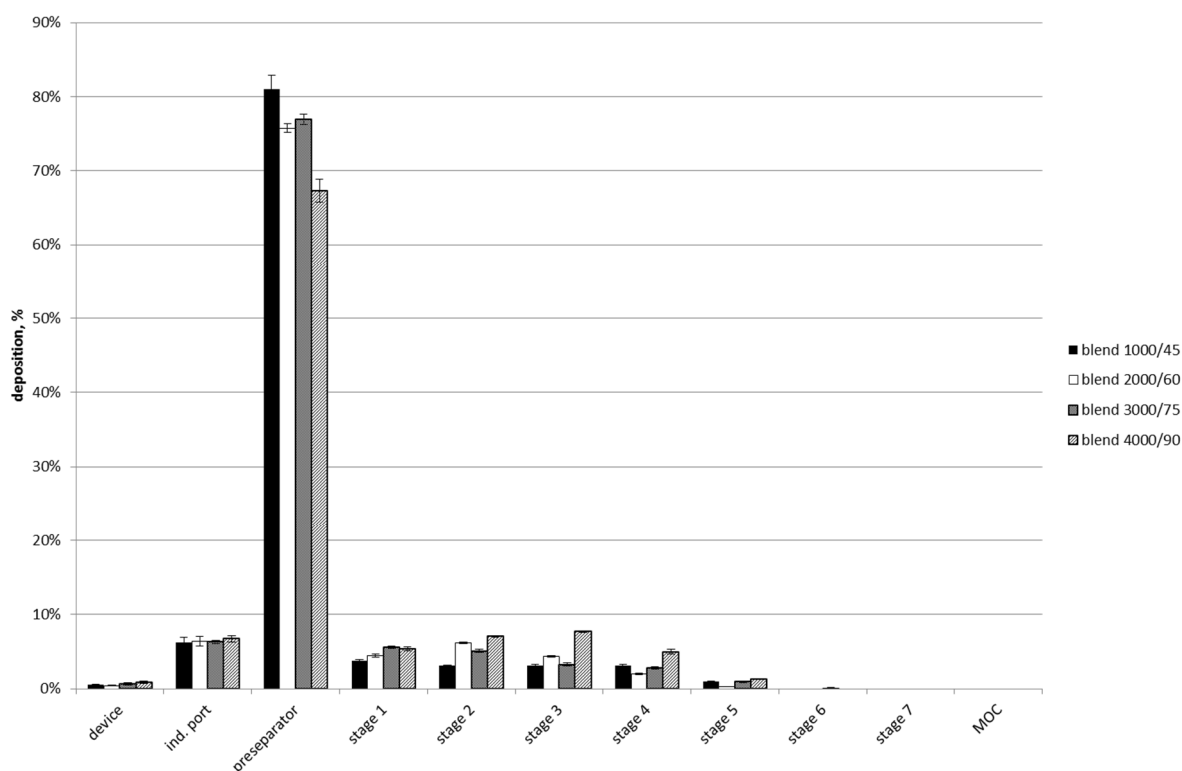


**Figure 5.3:** NGI deposition patterns of Picomix<sup>®</sup>-blend 1000/45 to 4000/90

**Table 5.5:** Mean values + standard deviations of fine particle fraction calculations, n = 3

blend	fine particle fraction, %	SD, %
blend 1000/45	8.65	± 0.33
blend 2000/60	9.64	± 0.10
blend 3000/75	9.37	± 0.57
blend 4000/90	17.31	± 0.61

The significant increase in FPF shows similarities to the behavior of the salbutamol sulfate mixtures tested in section 3.3.2.3. Likewise, the dispersed API fraction increases with enhanced mixing intensity. Consequently, the trend in results may again be linked to increased particle aggregation with prolonged mixing times and faster mixing speeds. Secondly, laser diffraction measurements of the four blends revealed particle comminution for blend 4000/90. Hence, abraded lactose fines were generated and act as additional performance modifying component as described in the previous section 4. The micronized salmeterol xinafoate particles may get redistributed over the lactose carrier surface and shifted to lower energy spots. The reduction in adhesive forces promotes further detachment upon aerosolization. Also, SEM images indicate a generation of free agglomerates (see Figure 5.4b), either composed of API only or API/lactose fines, respectively.

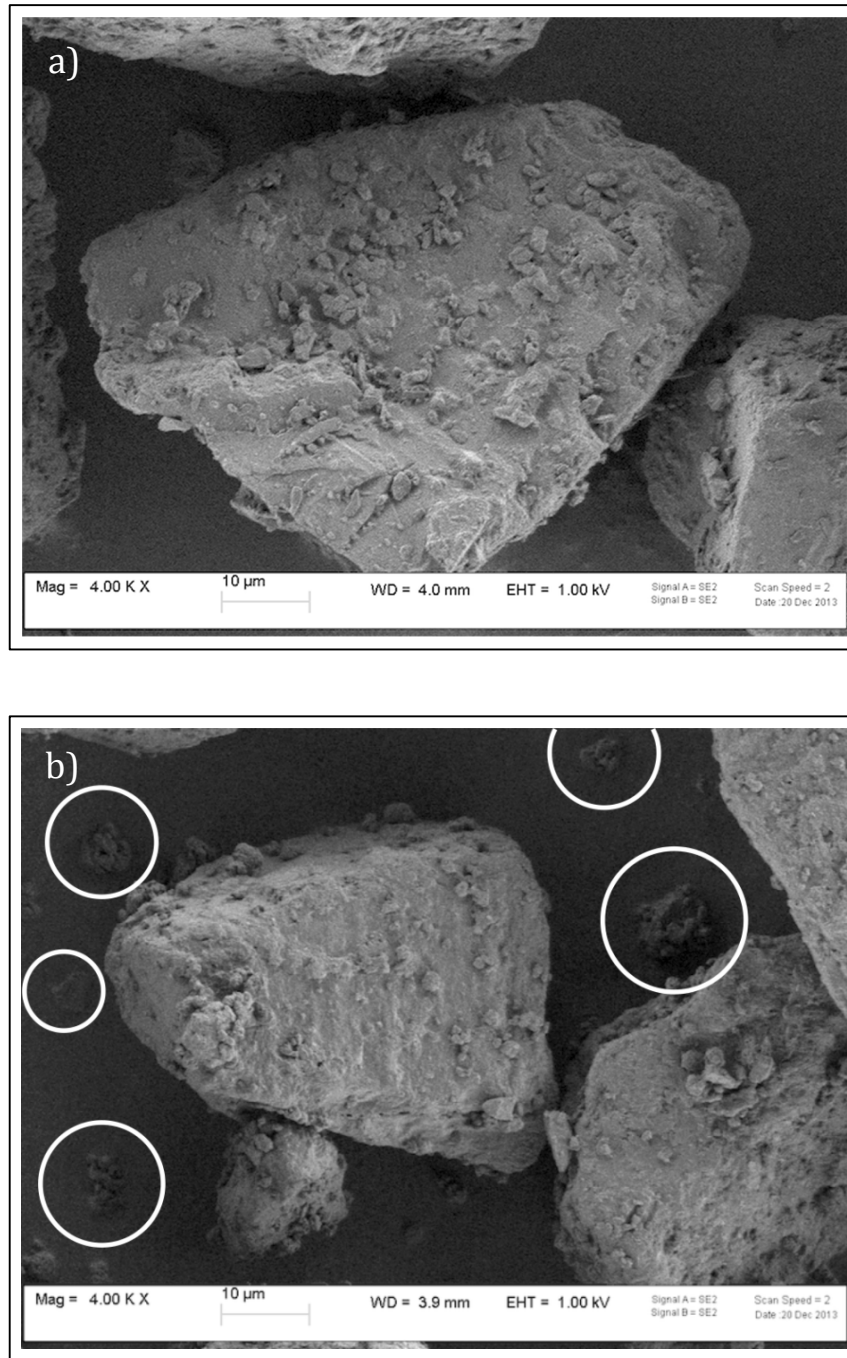


**Figure 5.4:** SEM images of **a)** blend 1000/45 and **b)** blend 4000/90

### 5.3.4 Powder rheology

The consistent energy values for test numbers 1 – 7, i.e. stability indices (SI) close to 1.00 (see Table 5.6) show a good stability of the samples during the test sequence. No attrition or segregation effects occur.

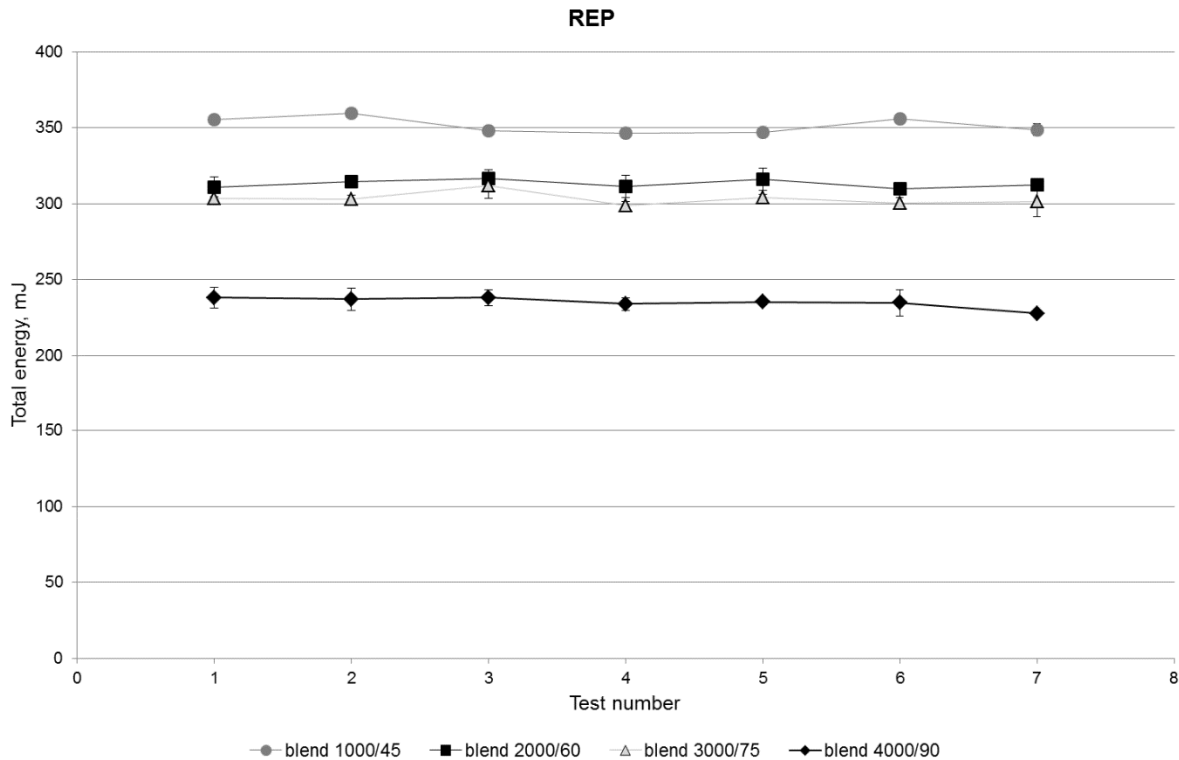


**Figure 5.5:** Stability test for blend 1000/45 to blend 4000/90

Bulk density (conditioned bulk density, CBD) increases slightly from 0.68 g/mL for blend 1000/45 to 0.73 g/mL for blend 4000/90 with increasing mixing times. This is an indication for rounding of the particles during the process which leads to a more firmly packed powder bed. The rounding is further confirmed by the decreasing values of the specific energy (SE), which suggest low mechanical interlocking and support the mentioned theory of particle rounding. The hypothesized lactose carrier edge abrasion goes in line with the fines generation discussed before.

**Table 5.6:** Stability test results for blend 1000/45 to blend 4000/90

blend	BFE, mJ	SE, mJ/g	CBD, g/mL	SI
blend 1000/45	349 ± 4.03	3.96 ± 0.03	0.68 ± 0.00	0.98 ± 0.01
blend 2000/60	312 ± 2.63	3.29 ± 0.07	0.69 ± 0.00	1.00 ± 0.01
blend 3000/75	301 ± 9.98	3.16 ± 0.18	0.72 ± 0.00	0.99 ± 0.02
blend 4000/90	228 ± 0.53	2.96 ± 0.07	0.73 ± 0.01	0.96 ± 0.03

When plotting all separate BFE values against the total number of revolutions, there is an interesting correlation ( $R^2 = 0.94$ ) between the two parameters. Again, this demonstrates how powder rheology can be used to monitor bulk powder behavior.

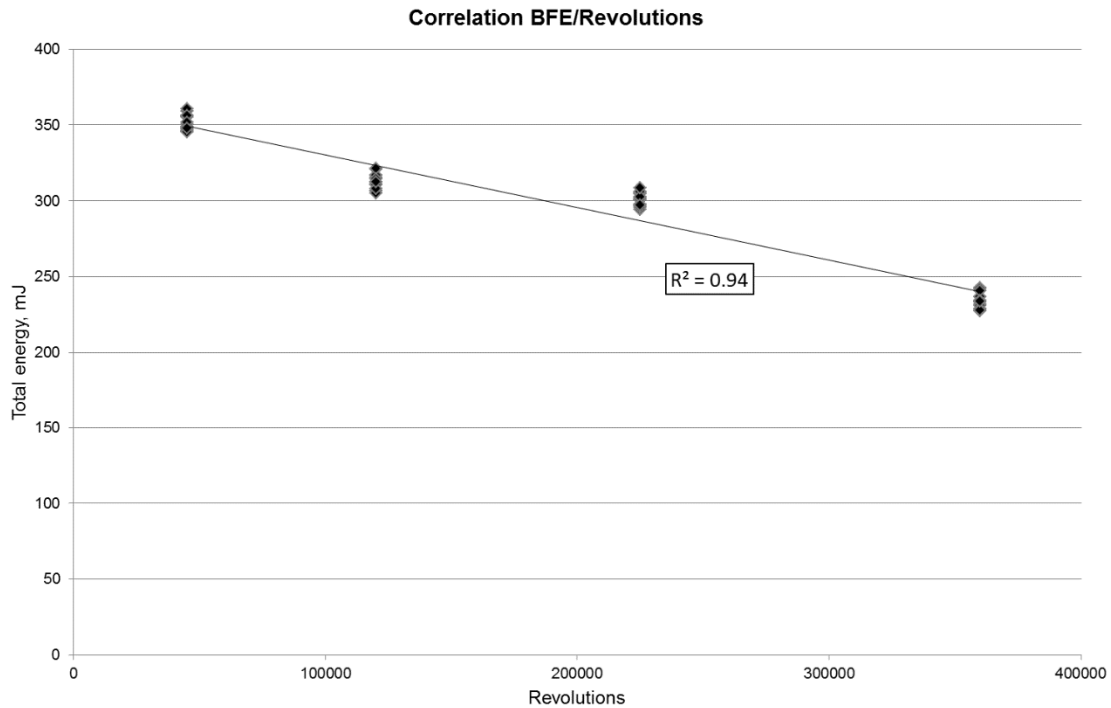


**Figure 5.6:** Correlation Flow Energy, mJ – total number of revolutions

No obvious differences in terms of aeration energy were apparent for the blends (see plateaus in Figure 5.7). However, it was described in section 4.7.3 that an air flow velocity of 6 mm/s through the vessel is suitable to imitate the conditions within the model test inhaler during dispersion. Hence, the flow values at 6 mm/s were investigated in more detail and are listed in Table 5.7.

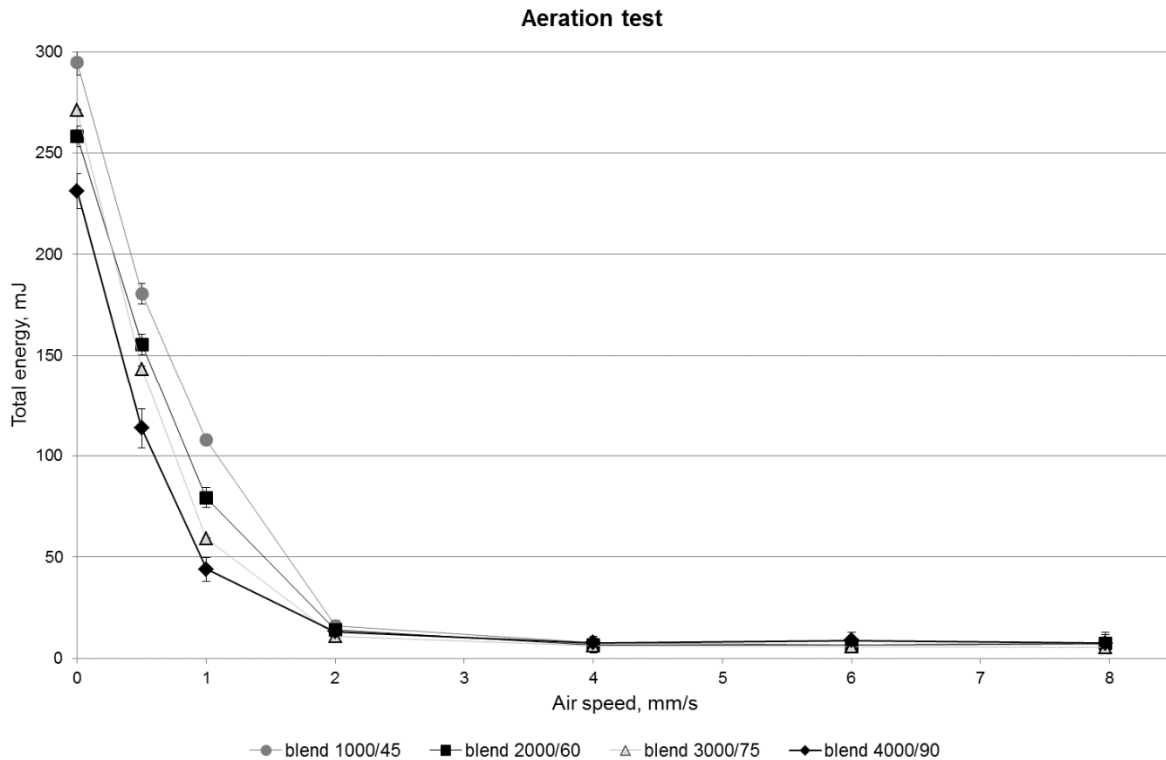


**Figure 5.7:** Aeration test graphs for blend 1000/45 to blend 4000/90

**Table 5.7:** Aeration test results for blend 1000/45 to blend 4000/90

blend	Flow Energy at 6 mm/s	Aeration sensitivity, s/mm
blend 1000/45	6.63 ± 0.251	0.77 ± 0.01
blend 2000/60	6.43 ± 3.39	0.80 ± 0.16
blend 3000/75	5.71 ± 2.5	0.94 ± 0.01
blend 4000/90	8.74 ± 3.99	1.02 ± 0.05

The flow energies do not show significant differences as denoted by the large standard deviations. The low energy values illustrate the lack in large differences in fluidization behavior; however, a trend towards higher flow energy values for blend 4000/90 can be derived from the results. Again, these findings match the hypothesized carrier particle rounding, i.e. lactose fines and agglomerate formation theory and is further supported by the increase in normalized sensitivity to air entrainment from  $0.77 \pm 0.01$  s/mm to  $1.02 \pm 0.05$  s/mm. These values represent the steepest part of the slope in the aeration graphs and are calculated on the basis of normalized total energy

values (total energy at 0 mm/s = 1). Therefore, a higher normalized aeration sensitivity value can be linked to a more pronounced response to the beginning of air entrainment.

### **5.3.5 Dissolution**

Dissolution testing results of the non-dispersed mixtures show that about 80% of drug was dissolved after 30 min for the blends prepared at 4000 rpm and 90 s (Figure 5.8). The dissolution rate was slower when the drug was blended at lower rates and times. Similar to the cascade impaction results, differences between the lower energy input blends appeared to be insignificant. Supposedly, the enhanced dissolution rate for the high energy input mixtures can be linked to the generation of salmeterol xinafoate/lactose fines agglomerates as seen in SEM images (Figure 5.4). As a consequence of the small aggregate formation, total surface area in the mixture and accessible surface area of the micronized API particles increases and, hence, dissolution rate accelerates, too.

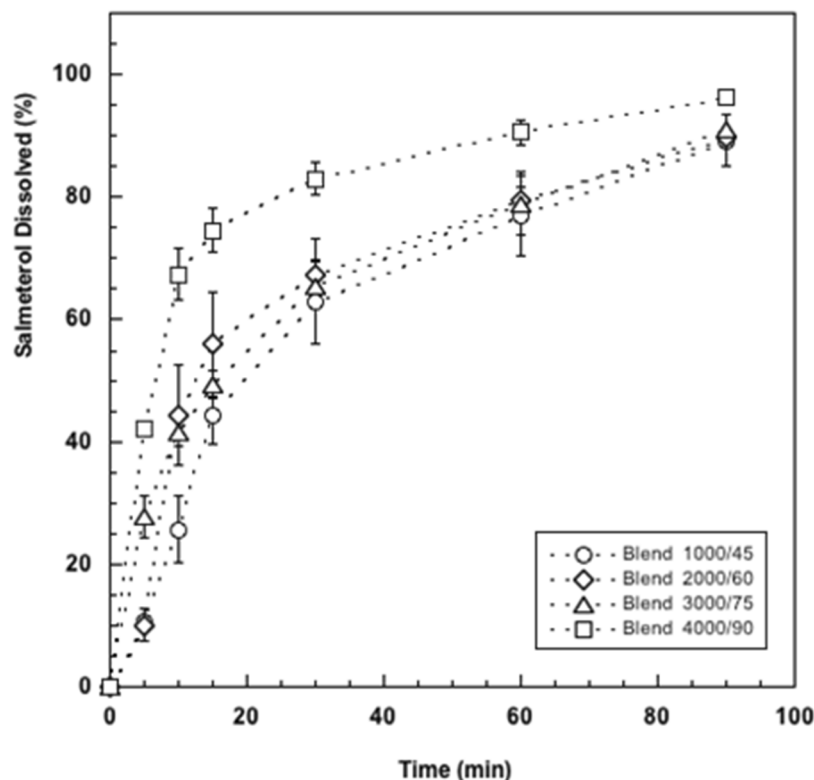


**Figure 5.8:** *In-vitro* dissolution of the powder blends before aerosolization

Opposite to the findings before aerosolization, SX microparticles collected after dispersion (size < 5  $\mu\text{m}$ ) dissolved very quickly (95% in 20 min) independently of the blending energy (Figure 5.9). It needs to be considered that aerosolization of the blends was not performed with the standard model device, but rather with the more turbulence generating RS01 inhalation device at an air flow rate of 100 L/min. Consequently, aerosolization was more efficient and possible fines' agglomerates were separated into single particles. In this case, the drug particles in the fraction below 5  $\mu\text{m}$  were individually exposed to dissolution fluid for all three blends.

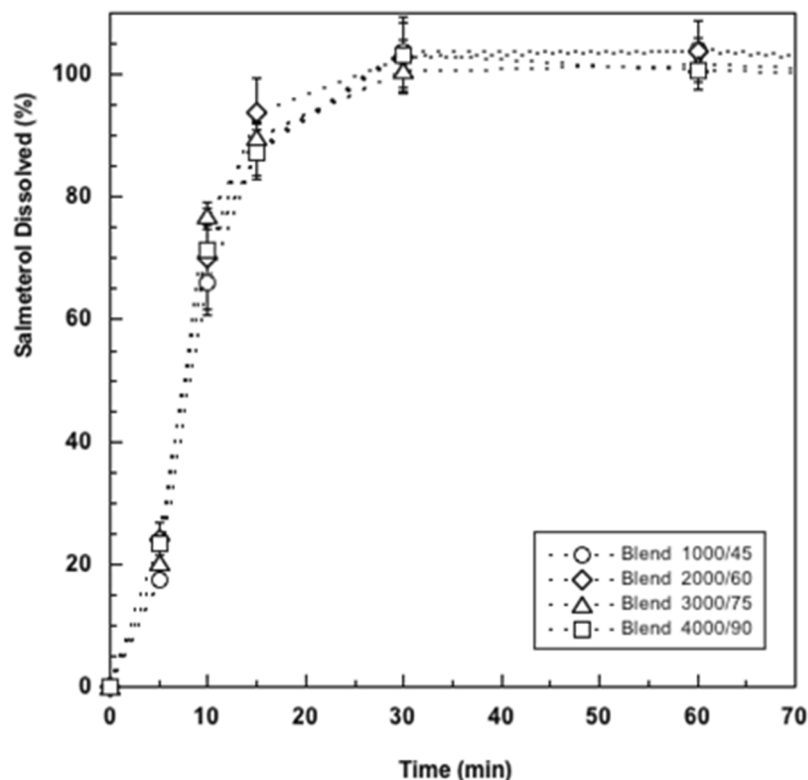


**Figure 5.9:** *In-vitro* dissolution of the powder blends after aerosolization with an RS01 inhalation device

## 5.4 Conclusion

The differences in dissolution behavior of the formulations again highlight the influence of the mixing process on the final drug formulation. As supported by powder rheology measurements, more intense mixing conditions can lead to particle comminution, which results in changes to the formulation composition, i.e. generation of fines, and subsequently to relevant changes in aerosolization behavior. Clearly, mixing intensity also has an influence on de- or re-agglomeration of fine particles, which may affect both, dispersion performance and dissolution rate. In this basic test set-up, no differences in dissolution of the fine particle fraction after aerosolization could be detected. However, the effect of changes to the mixing protocol may

be of greater relevance when considering formulations including less soluble drugs or when using low turbulence inhalation devices. Salmeterol xinafoate is also available as a combination product additionally containing the corticosteroid fluticasone propionate (Seretide<sup>®</sup> Diskus<sup>®</sup>, AirFluSal<sup>®</sup> Forspiro<sup>®</sup>, Rolenium<sup>®</sup> Elpenhaler<sup>®</sup>). Hence, the impact of mixing intensity on the dispersion and dissolution behavior of each of the combined drugs may be influenced to different extents. This leads to the conclusion that extensive research is still necessary to test for further consequences resulting from changes in formulation preparation.

## **6. OVERALL CONCLUSION AND FUTURE PERSPECTIVES**

The presented work highlights the complexity of a thorough powder characterization and its relevance for dry powder inhalation formulations. It could be shown that the combination and extension of routine impaction analysis with carrier residue measurements and powder rheology assessments helped to gain an increased understanding about the impact of changes in formulation composition or processing parameters.

The first part of this work clearly revealed the effects of the mixing process on the subsequent inhalation performance. With the help of carrier residue measurements in combination with NGI analysis, the flow-rate dependent changes on the aerosolization performance could be demonstrated.

Secondly, it was shown that powder rheology analysis is suitable to study effects of changes in formulation composition of inhalation powder blends. It appeared that the dynamic flow behavior of the aerated bulk could be directly related to the inhalation performance in a model device. Even though more sophisticated measurements will be necessary to undermine this relationship, the results of powder rheology measurements were shown to be valuable for a more thorough understanding about changes in particle interactions when adding ternary fines to a formulation. It was presented that powder flow cannot be described by a single number/test value as oftentimes perceived in the pharmacopeia monographs, but rather needs to be interpreted with the help of variable test methodologies. For example, while the mixing process induced decrease in BFE for the salmeterol xinafoate/Respitose® SV003 blends went in line with a decrease in SE, an opposed increase in SE with decreasing BFE values became apparent for the ternary mixtures prepared with Respitose® SV003, salbutamol sulfate, and Lactohale® LH300.

Also, the data obtained from the carrier residue and powder rheology assessment illustrate that in addition to considerations about powder formulation and mixing parameters, the inhalation device used to administer the mixtures needs to be considered when evaluating the overall aerosolization performance. Comparison to data presented in previously published scientific literature, i.e. obtained with altering inhalation devices for impaction analysis, demonstrates how one powder formulation may exhibit opposite performance (FPF) depending of the inhalation device used. Hence, CR and powder rheology measurements can be utilized to explain opposite findings through an improved mechanistic understanding about particle interactions within the formulation.

In the third part, powder rheology measurements could be used to investigate mixing process-induced changes to the adhesive salmeterol xinafoate mixtures. While differences in powder rheology, NGI analysis, and dissolution of undispersed blends suggest significant variation between the blends, no effect could be observed on the dissolution rate of the dispersed drug after aerosolization. However, these findings may again be influenced by the inhalation device used for dispersion (being different for cascade impaction and dissolution testing). Further consequences for the dissolution behavior on less soluble drugs may be expected and will be subject of continuing research.

## 7. SUMMARY

The local delivery of drugs to the lungs has proved to be a suitable option for the treatment of respiratory diseases manifesting with airway obstruction and is used by most patients on a routine basis. Further, the lungs have been recognized as a potential target for systemic drug uptake; hence, the market for inhalation products is likely to grow substantially in the next years. Besides pressurized metered dose inhalers, soft mist inhalers, and active nebulizers, dry powder inhalers are believed to be beneficial in terms of drug stability and administration efficiency.

In order for the drug to reach the lower regions of the lungs, particles need to exhibit an aerodynamic size below 5  $\mu\text{m}$ . While the drug can be processed by various techniques to achieve sizes in the desired range, micronized powders are strongly cohesive, therefore tend to aggregate, and show poor flowability. Thus, the cohesive material is commonly formulated with a lactose carrier material of larger size to form adhesive mixtures. Upon inhalation, the adhered particles are meant to detach from the carrier surface and subsequently follow the inspiratory air flow as individual entities.

Despite intensive research over the past 15 years there is still only little mechanistic understanding about particle interactions and their magnitude of force in adhesive powder mixtures. The complex relationships between factors affecting the powder dispersion properties are manifold and variations in the individual study designs complicate their coherent use in order to obtain a systematic understanding.

Therefore, this thesis focuses on advanced powder characterization techniques to gain an improved mechanistic understanding about particle interaction in adhesive powder mixtures. In the first part of this thesis, drug

detachment experiments with a classifier based test inhaler developed at the Department of Pharmaceutical Technology and Biopharmacy, University of Groningen, The Netherlands, were performed highlighting the importance of mixing process control on the aerosolization performance. By combining different results from drug detachment and cascade impaction analysis, it could further be hypothesized about particle interactions and their impact on the subsequent *in-vitro* inhalation performance. It was shown that the execution of different mixing intensities on the blends lead to changes in the potential lung fractions when the powder is inhaled. More importantly, the observed trend was flow-rate dependent, revealing a decreased drug detachment with increasing mixing intensities at high flow rates, whereas at low flow-rates the trend shifted towards an increased detached fraction. These results indicate the importance of taking the inhalation device design into consideration when evaluating dispersion measurements since the formulation is likely to be exposed to different magnitudes of stress.

Secondly, adhesive powder mixtures were analyzed by means of powder rheology. After first general feasibility studies it was evaluated whether results obtained by this fairly novel approach could be used to correlate differences in bulk behavior to the aerosolization performance of the inhalation blends. It could be demonstrated that the addition of ternary lactose fines to the mixtures led to an increase in obtained fine particle fraction; however, after reaching a maximum value successive addition of fines resulted in a clear decrease again. While permeability and flowability testing methodologies with a powder rheometer were suitable to expose the differences in according powder behavior aspects, no direct correlation between these parameters and the aerosolization performance could be found. However, the rheometer's ability to measure changes in flow energy upon successive air entrainment revealed an interesting relationship, i.e.

correlation, between flow energy at 6 mm/s air throughput and obtained fine particle fraction with a model inhalation device. All the obtained data was then, again, used to hypothesize about mechanisms responsible for the observed dispersion behavior. It could be concluded that drug fines are shifted towards lower energy binding sites on the carrier surface upon ternary fines addition. Yet, larger amounts of lactose fines lead to the formation of fines aggregates, which are more dispersion insensitive and, hence, result in a decrease fine particle fraction.

The final section of this thesis deals with the impact of mixing conditions on the dissolution behavior of adhesive blends. As demonstrated in the first part, changes to the mixing protocol and type of mixer used had a significant influence on the formulations' fine particle fraction. Since many of the drugs used for respiratory treatments (for example, corticosteroids) exhibit poor water solubility, an adapted dissolution test set-up was used to demonstrate the possible impact of variations of the mixing conditions on the dissolution behavior. The tests only revealed changes in dissolution rate for the non-aerosolized blends; however, together with results obtained with powder rheology analysis, mechanistic understanding about underlying processes could be achieved and serve as a basis for further investigations.

In summary, the employed techniques in this thesis proved to be a valuable addition to the routinely used impaction test analysis in order to achieve a thorough understanding about particle interactions within adhesive powder mixtures. The methodologies may be used to characterize, understand and advance the inhalation performance of future dry powder inhaler products.

## 8. SUMMARY (GERMAN)

Die lokale Applikation von Arzneistoffen in der Lunge ist heutzutage ein fester Bestandteil der Behandlung von obstruktiven Lungenerkrankungen, und verschiedene Inhalatoren werden von vielen Patienten als Routinemedikation eingesetzt. Neben druckgasbetriebenen Dosieraerosolen, Soft Mist Inhalern und aktiven Verneblern bieten besonders Trockenpulverinhalatoren einen Vorteil in Bezug auf Arzneistoffstabilität und erfolgreich applizierter Dosis.

Damit Arzneistoffpartikel überhaupt bis in die unteren Lungengänge vordringen können, müssen sie einen aerodynamischen Durchmesser kleiner 5  $\mu\text{m}$  aufweisen. Diese Größe lässt sich durch verschiedene Verfahren realisieren, allerdings bedingt die Partikelzerkleinerung einen signifikanten Anstieg der Kohäsionskräfte; entsprechende Pulver neigen zur Agglomeratbildung und zeigen eine schlechte Fließfähigkeit. Aus diesem Grund werden die kohäsiven Arzneistoffpartikel üblicherweise zusammen mit groben Laktose-Trägerpartikeln zu adhäsiven Pulvermischungen formuliert. Während der Inhalation durch einen Trockenpulverinhalator wird ein Teil des adhärierten Wirkstoffes von der Trägeroberfläche abgelöst und kann dem Luftstrom in die Lunge folgen.

Trotz jahrelanger Forschung herrscht immer noch ein lückenhaftes mechanistisches Verständnis über die Partikelinteraktionen und das Ausmaß verschiedener auftretender Kräfte in solchen adhäsiven Mischungen. Das komplexe Zusammenspiel von Faktoren, die einen Einfluss auf das Dispersionsverhalten zeigen, ist sehr vielfältig. Unterschiedliche Versuchsaufbauten und -bedingungen in den bisher beschriebenen wissenschaftlichen Arbeiten erschweren und behindern eine

zusammenhängende Auswertung mit dem Ziel eines systematischen Verständnisses.

Aus diesem Grund widmet sich diese Arbeit fortgeschrittenen Pulvercharakterisierungsmethoden, die zu einem verbesserten mechanistischen Verständnis von Partikelinteraktionen in adhäsiven Pulvermischungen führen sollen. Im ersten Teil der Arbeit werden Versuche mit einem Testinhalator beschrieben, der am Institut für Pharmazeutische Technologie und Biopharmazie der Universität Groningen, Niederlande, entwickelt wurde. Der Testinhalator ist in der Lage, Pulverpartikel im Luftstrom nach ihrer Größe zu klassieren und erlaubt im Anschluss an die Messung die Analyse der auf dem Träger verbliebenen Arzneistoffmenge. Es wurden Pulver vermessen, die mit verschieden großer Mischintensität hergestellt wurden, um den Einfluss unterschiedlicher Prozessbedingungen bei der Herstellung adhäsiver Pulvermischungen hervorzuheben. Im Zusammenspiel mit Erkenntnissen aus weiteren Impaktionsanalysen konnten Theorien zu mechanistischen Zusammenhängen aufgezeigt und etabliert werden, in denen das entsprechende *in-vitro* Dispersionsverhalten wiedergespiegelt werden konnte. Steigende Mischintensitäten bei den Modellformulierungen hatten einen signifikanten Einfluss auf die erhaltene Feinpartikelfraktion. Besonders hervorzuheben ist dabei, dass der beobachtete Trend flussratenabhängig auftrat. So bewirkten intensivere Mischprozessbedingungen eine Abnahme des abgelösten Arzneistoffanteils vom Träger bei hohen Flussraten; dieser Trend kehrte sich jedoch um und führte zu einer Zunahme der abgelösten Fraktion bei niedriger Flussrate. Die erhaltenen Ergebnisse verdeutlichen, dass neben den vielen Formulierungsaspekten auch das Inhalationsgerät mit in die umfassende Beurteilung des Dispersionsverhaltens einbezogen werden muss. Je nach

Gerätetyp wirken unterschiedlich starke Kräfte auf die Formulierung und können abweichende Ergebnisse zur Folge haben.

Der zweite Teil der Arbeit beschäftigt sich mit der pulverrheologischen Beurteilung von adhäsiven Mischungen. Nach anfänglicher, genereller Überprüfung der Eignung dieser Methode wurde im Weiteren untersucht, inwiefern sich Ergebnisse, die mit diesem vergleichbar neuen Charakterisierungsansatz generiert wurden, zu Aerosolisierungseffizienz korrelieren lassen. Es konnte gezeigt werden, dass der Zusatz eines ternären Laktosefeinanteils zu einem signifikanten Anstieg der Feinpartikelfraktion führte. Allerdings bewirkte ein weiteres, sukzessives Zuführen nach dem Erreichen eines primären Maximums zu einer deutlichen Verschlechterung der FPF. Mit Hilfe von Permeabilitäts- und dynamischen Fließfähigkeitsmessungen mit einem Pulverrheometer konnten deutliche Unterschiede im entsprechenden Pulververhalten aufgezeigt werden, jedoch keine direkte Korrelation zur Aerosolisierungseffizienz. Dies konnte schließlich durch Fließfähigkeitsmessungen realisiert werden, die das Verhalten des Pulvers während der Durchströmung mit verschiedenen Luftmengen erfassen. So zeigte sich ein interessanter Zusammenhang zwischen Fließfähigkeit bei 6 mm/s Luftdurchsatz und der Feinpartikelfraktion, die mit einem Testinhalator erhalten wurde. Die Ergebnisse der verschiedenen Testverfahren wurden weiterhin verwendet, um eine Theorie über die für das entsprechende Dispersionsverhalten relevanten Mechanismen der Partikelinteraktionen zu erstellen. Es konnte geschlussfolgert werden, dass die Zugabe eines ternären Laktosefeinanteils zu einer Verdrängung von Arzneistoffpartikeln von Stellen mit erhöhten Adhäsionskräften auf der Trägeroberfläche führt und somit anfänglich in einer erhöhten Arzneistoffablösung resultiert. Bei weiterer Zugabe jedoch bildet sich eine zweite, separate Phase aus Feinanteil-Agglomeraten mit

erhöhter mechanischer Stabilität, die somit eine verminderte Dispersion zeigen und für den Abfall in FPF verantwortlich sind.

Im finalen Teil der Arbeit wurde der Fokus auf den Einfluss von Unterschieden im Mischprozess auf das Dissolutionsverhalten der Partikel gelegt. Wie bereits im ersten Abschnitt der Arbeit aufgezeigt, ist ein Zusammenhang zwischen Mischintensität und Feinpartikelfraktion vorhanden. Da viele zur Inhalation eingesetzte Arzneistoffe (z.B. Corticosteroide) eine schlechte Wasserlöslichkeit zeigen, sind auch Auswirkungen auf das Dissolutionsverhalten des dispergierten Wirkstoffanteils zu vermuten. Dieses wurde mit Hilfe einer Franz-Zell-Apparatur untersucht und zusammen mit Ergebnissen aus pulverrheologischen Betrachtungen und Impaktionsanalysen beurteilt. Zwar ließen sich mit dem verwendeten Testaufbau nur Unterschiede in der Freisetzungsgeschwindigkeit der undispergierten Mischungen feststellen; mit Hilfe weiterer Ergebnissen aus der Impaktionsanalyse und den pulverrheologischen Betrachtungen ließen sich jedoch weitere, durch den Mischprozess bedingte Unterschiede zwischen den Formulierungen herausstellen. Diese beinhalten eine Bildung von Arzneistoff/Laktose-Feinpartikelagglomeraten, die jedoch während der Aerosolisierung für die Bestimmung des Dissolutionsverhaltens dispergiert wurden und somit nicht zu Unterschieden in den anschließenden Messungen führten.

Zusammenfassend lässt sich schlussfolgern, dass mit Hilfe der verwendeten Pulvercharakterisierungsmethoden und der routinemäßig eingesetzten Impaktionsanalyse ein erweitertes mechanistisches Verständnis für Partikelinteraktionen innerhalb einer adhäsiven Pulvermischung erhalten werden konnte. Der Einsatz der aufgeführten Methoden könnte demnach einen Mehrwert für die zukünftige Entwicklung neuer und effizienter Trockenpulverinhalatoren darstellen.

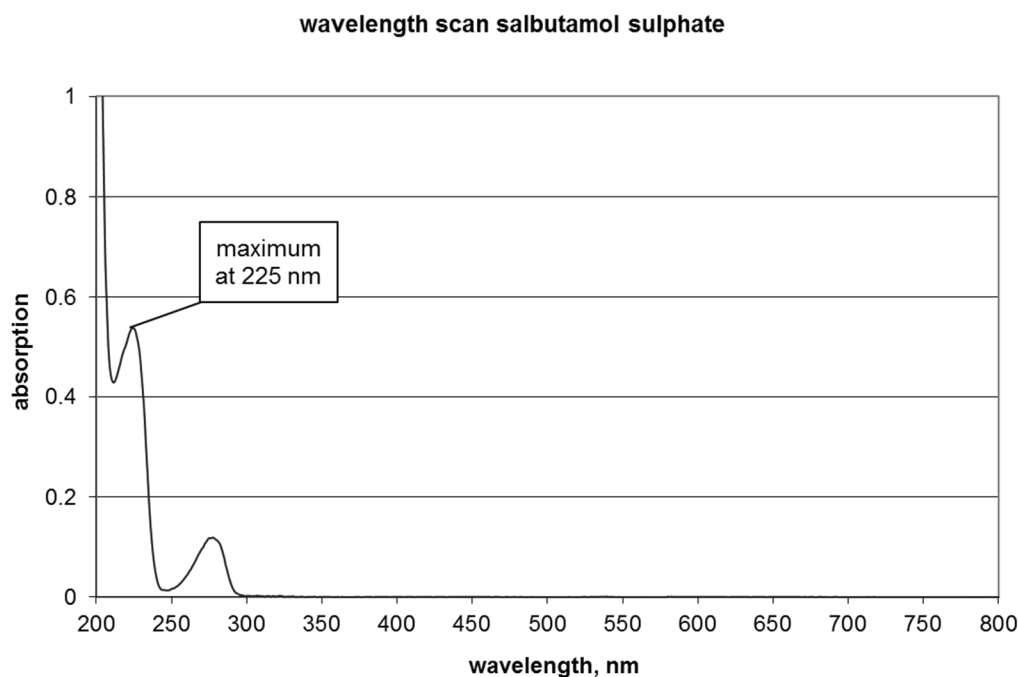
## 9. APPENDIX

### 9.1 Methods

#### 9.1.1 Quantification of salbutamol sulfate content – UV/VIS

The quantification of dd H<sub>2</sub>O-dissolved salbutamol sulfate contents was obtained from UV/VIS spectroscopic analysis at a wavelength of 225 nm. Depending on the concentration in the samples, a 1 cm flow-through cuvette (2.5 – 75 µg/mL) or 5 cm flow-through cuvette (0.5 – 15 µg/mL) was used, respectively.

Calculation of the sample contents was based on a linear regression of a six-point dilution series with external standard.



### 9.1.2 Quantification of API content – HPLC

A Waters HPLC system (Waters Corp., Milford, USA) was used for the quantification of the sample contents. The obtained data was evaluated with Empower® Pro 2 software (Waters Corp., Milford, USA).

#### 9.1.2.1 Salbutamol sulfate

Stationary phase:	LiChroCART® 125-4 LiChrospher® 100 RP-18 (5 µm) with pre-column
Mobile phase:	78% buffer (2.87 g/L sodium heptansulfonate + 2.5 g/L KH <sub>2</sub> PO <sub>4</sub> (0.2 mmol); pH adjusted to 3.65 with o-phosphoric acid 85 %)  22% acetonitrile
Flow rate:	0.8 mL/min
Detection wavelength:	225 nm
Injection volume:	100 µl
Calibrated range:	0.1 – 100 µg/mL

Samples were dissolved in 100% dd H<sub>2</sub>O

#### 9.1.2.2 Budesonide

Stationary phase:	LiChroCART® 125-4 LiChrospher® 100 RP-18 (5 µm) with pre-column
Mobile phase:	75% methanol 25% dd H <sub>2</sub> O
Flow rate:	1 mL/min
Detection wavelength:	248 nm

Injection volume: 100  $\mu$ l  
Calibrated range: 0.5 – 50  $\mu$ g/mL

Samples were dissolved in the mobile phase.

### 9.1.2.3 Salmeterol xinafoate

Stationary phase: LiChroCART® 125-4  
LiChrospher® 100 RP-8 (5  $\mu$ m)  
with pre-column

Column oven: 40 °C

Mobile phase: 60% (40% dd H<sub>2</sub>O + 0.1% Tetrabutyl-  
ammoniumhydrogensulfate; pH adjusted to  
3.30 with ammonium acetate) + 30%  
acetonitrile)

40% dd H<sub>2</sub>O

Flow rate: 1 mL/min

Detection wavelength: 228 nm

Injection volume: 100  $\mu$ l

Calibrated range: 0.5 – 75  $\mu$ g/mL

Samples were dissolved in a 75% methanol / 25% dd H<sub>2</sub>O mixture.

In case of undissolved lactose remains in the samples, the supernatant was used for further analysis. Calculation of the sample contents was based on a linear regression of a dilution series with external standard.

## 9.2 Materials

Acetonitrile (HPLC)	SIGMA-ALDRICH, Inc., St. Louis, USA
Ammonium acetate	Merck KGaA, Darmstadt, Germany
Brij 35	ICI Specialty Chemicals, Essen, Germany
Budesonide	Shanghai Hengtian Pharmaceuticals Co., Ltd., Shanghai, China
dd H <sub>2</sub> O	freshly produced with the in-house Finn Aqua 75, San-Asalo – Sohlberg Corp., Helsinki, Finland
Ethanol, 96%	Merck KGaA, Darmstadt, Germany
Glycerol	Merck KGaA, Darmstadt, Germany
Lactohale® LH200 batch: 623653	Friesland Foods Domo, Zwolle, The Netherlands
Lactohale® LH300 batch: 625065	Friesland Foods Domo, Zwolle, The Netherlands
Methanol (HPLC)	J.T. Baker, Deventer, The Netherlands
Pharmatose 80M	DMV-Fonterra Excipients, Goch, Germany
o-Phosphoric acid 85 %	Merck KGaA, Darmstadt, Germany
Potassium dihydrogen phosphate	FAGRON, Barsbüttel, Germany
Respitose® SV003 batch: 10522807 batch: 10680001	DMV-Fonterra, Vehgel, The Netherlands
Salbutamol sulfate batch: SS10204002	supplied by DFE Pharma, Goch, Germany

Salmeterol xinafoate      Midas Pharma, Ingelheim, Germany  
batch: 2004013144

Sodium                      SIGMA-ALDRICH, Inc., St. Louis, USA  
heptansulfonate

Tetrabutylammonium      SIGMA-ALDRICH, Inc., St. Louis, USA  
hydrogensulfate

### 9.3 List of abbreviations

AE, FE	aeration energy, fluidization energy, mJ
API	active pharmaceutical ingredient
BFE	basic flowability energy, mJ
CBD	conditioned bulk density, g/mL
CR	carrier residue
CV	coefficient of variation
dd H <sub>2</sub> O	double distilled water
DPI	dry powder inhaler
EMA	European Medicines Agency
PSD	particle size distribution
FDA	US Food and Drug Administration
FPD	fine particle does
FPF	fine particle fraction
FRI	flow rate index
GINA	global initiative for asthma
GOLD	Global Initiative for Chronic Obstructive Lung Disease
GSD	geometric standard deviation
HPLC	high performance liquid chromatography
MMAD	mass median aerodynamic diameter
NGI	Next Generation (Pharmaceutical) Impactor
Ph. Eur.	<i>Pharmacopoea Europaea</i> , European Pharmacopeia

pMDI	pressurized metered dose inhaler
rpm	rounds per minute
RSD	relative standard deviation
SD	standard deviation
SE	specific energy, mJ/g
SI	stability index
USP	United States Pharmacopeia
x <sub>10</sub>	10%-quantile of a particle size distribution
x <sub>50</sub>	50%-quantile of a particle size distribution
x <sub>90</sub>	90%-quantile of a particle size distribution

## 10. REFERENCES

- Adi, H., Larson, I., Chiou, H., Young, P., Traini, D., Stewart, P., 2006. Agglomerate Strength and Dispersion of Salmeterol Xinafoate from Powder Mixtures for Inhalation. *Pharm Res* 23 (11), 2556–2565.
- Adi, H., Larson, I., Stewart, P., 2004. Influence of particle size of the fine lactose in the dispersion of salmeterol xinafoate from lactose mixtures for inhalation. *Respiratory Drug Delivery IX*.
- Anderson, P.J., 2005. History of Aerosol Therapy: Liquid Nebulization to MDIs to DPIs. *Respiratory Care* 50 (9), 1139–1150.
- Anderson, S.D., Rozea, P.J., Dolton, R., Lindsay, D.A., 1975. Inhaled and Oral Bronchodilator Therapy in Exercise Induced Asthma. *Aust Nz J Med* 5 (6), 544–550.
- Baverstock, M., Woodhall, N., Maarman, V., 2010. P94 Do healthcare professionals have sufficient knowledge of inhaler techniques in order to educate their patients effectively in their use? *Thorax* 65 (Suppl 4), A117.
- Begat, P., Morton, D.A.V., Staniforth, J.N., Price, R., 2004a. The Cohesive-Adhesive Balances in Dry Powder Inhaler Formulations I: Direct Quantification by Atomic Force Microscopy. *Pharmaceutical Research* 21 (9), 1591–1597.
- Begat, P., Morton, D.A.V., Staniforth, J.N., Price, R., 2004b. The Cohesive-Adhesive Balances in Dry Powder Inhaler Formulations II: Influence on Fine Particle Delivery Characteristics. *Pharmaceutical Research* 21 (10), 1826–1833.
- Bell, J.H., 1979. Composition for treating airway disease. Accessed 25 March 2014, 10 pp.
- Bell, J.H., Hartley, P.S., Cox, J.S.G., 1971. Dry powder aerosols I: A new powder inhalation device. *J Pharm Sci* 60 (10), 1559–1564.
- Bossé, Y., Riesenfeld, E.P., Paré, P.D., Irvin, C.G., 2010. It's Not All Smooth Muscle: Non-Smooth-Muscle Elements in Control of Resistance to Airflow. *Annu. Rev. Physiol.* 72 (1), 437–462.
- Brand, P., Hederer, B., Austen, G., Dewberry, H., Meyer, T., 2008. Higher lung deposition with Respimat Soft Mist inhaler than HFA-MDI in COPD

- patients with poor technique. *Int J Chron Obstruct Pulmon Dis* 3 (4), 763–770.
- Buttini, F., Miozzi, M., Balducci, A.G., Royall, P.G., Brambilla, G., Colombo, P., Bettini, R., Forbes, B., 2014. Differences in physical chemistry and dissolution rate of solid particle aerosols from solution pressurised inhalers. *Int J Pharm.*
- Carvalho, T.C., Peters, J.I., Williams III, R.O., 2011. Influence of particle size on regional lung deposition – What evidence is there? *Int J Pharm* 406 (1-2), 1–10.
- Chan, H.-K., Chew, N.Y., 2003. Novel alternative methods for the delivery of drugs for the treatment of asthma. *Adv. Drug Delivery Rev.* 55 (7), 793–805.
- Chow, A.H.L., Tong, H.H.Y., Chattopadhyay, P., Shekunov, B.Y., 2007. Particle Engineering for Pulmonary Drug Delivery. *Pharmaceut Res* 24 (3), 411–437.
- Das, S., Larson, I., Young, P., Stewart, P., 2009. Influence of storage relative humidity on the dispersion of salmeterol xinafoate powders for inhalation. *J. Pharm. Sci.* 98 (3), 1015–1027.
- Davies, N.M., Feddah, M.R., 2003. A novel method for assessing dissolution of aerosol inhaler products. *International Journal of Pharmaceutics* 255 (1-2), 175–187.
- de Boer, A.H., Chan, H.-K., Price, R., 2012. A critical view on lactose-based drug formulation and device studies for dry powder inhalation: Which are relevant and what interactions to expect?: Lactose as a carrier for inhalation products. *Advanced Drug Delivery Reviews* 64 (3), 257–274.
- de Boer, A.H., Gjaltema, D., Hagedoorn, P., Frijlink, H.W., 2002a. Characterization of inhalation aerosols: a critical evaluation of cascade impactor analysis and laser diffraction technique. *International Journal of Pharmaceutics* 249 (1-2), 219–231.
- de Boer, A.H., Gjaltema, D., Hagedoorn, P., Schaller, M., Witt, W., Frijlink, H., 2002b. Design and application of a new modular adapter for laser diffraction characterization of inhalation aerosols. *International Journal of Pharmaceutics* 249 (1-2), 233–245.
- de Boer, A.H., Hagedoorn, P., Gjaltema, D., Goede, J., Frijlink, H.W., 2003. Air classifier technology (ACT) in dry powder inhalation: Part 1.

- Introduction of a novel force distribution concept (FDC) explaining the performance of a basic air classifier on adhesive mixtures. *Int J Pharm* 260 (2), 187–200.
- Dickhoff, B.H.J., de Boer, A.H., Lambregts, D., Frijlink, H.W., 2003. The effect of carrier surface and bulk properties on drug particle detachment from crystalline lactose carrier particles during inhalation, as function of carrier payload and mixing time. *European Journal of Pharmaceutics and Biopharmaceutics* 56 (2), 291–302.
- Dressman, J.B., Amidon, G.L., Reppas, C., Shah, V.P., 1998. Dissolution Testing as a Prognostic Tool for Oral Drug Absorption: Immediate Release Dosage Forms. *Pharmaceutical Research* 15 (1), 11–22.
- Ducker, W.A., Senden, T.J., Pashley, R.M., 1991. Direct measurement of colloidal forces using an atomic force microscope. *Nature* 353 (6341), 239–241.
- Egermann, H., 1991. Mischen von Feststoffen, in: Nürnberg, E., Surmann, P. (Eds.), *Hagers Handbuch der pharmazeutischen Praxis. Mischen*, vol. 2, 5 ed. Springer, Berlin Heidelberg, pp. 565–582.
- Forbes, B., Colombo, P., Brambilla, G., Saunders, M., Jones, S.A., Buttini, F., 2010. Important Considerations Regarding the Bioequivalence of Particles Emitted from Beclometasone Dipropionate Solution Metered Dose Inhalers. *Respiratory Drug Delivery* 2010.
- Freedman, T., 1956. Medihaler therapy for bronchial asthma; a new type of aerosol therapy. *Postgrad Med* 20 (6), 667–673.
- Freeman, T., 2013. Understanding the Material Science of Powders as Primary Materials. Freeman Technology, 24 June 2013, Hong Kong.
- Freeman, T., Armstrong, B., Brockbank, K., Clayton, J., 2013. The Influence of Ambient Moisture on Powder Flow Characteristics. Partec 2013.
- Freeman, T., Fu, X., Armstrong, B., Seyfang, K., 2009. An Investigation into the Wall Friction Angle of a Range of Low Friction Materials Used in the Manufacture of Pharmaceutical Processing Equipment. AAPS Annual Meeting and Exposition, 8 November 2009, Los Angeles.
- Freeman Technology, 2006. instruction documents: W7017 Permeability.
- Freeman Technology, 2008. instruction documents: W7030 The Basic Flowability Energy.

- Freeman Technology, 2012. FT4 Powder Rheometer Brochure: Measuring and understanding the flow properties of powders with the FT4 Powder Rheometer.
- Friebel, C., 2010. Rationale Entwicklung eines Inhalationssystems, Kiel.
- Global Initiative for Asthma (GINA), 2013. From the Global Strategy for Asthma Management and Prevention. <http://www.ginasthma.org/>.
- Global Initiative for Chronic Obstructive Lung Disease (GOLD), 2013. Global Strategy for Diagnosis, Management, and Prevention of COPD. <http://www.goldcopd.org/>.
- Grainger, C.I., Saunders, M., Buttini, F., Telford, R., Merolla, L.L., Martin, G.P., Jones, S.A., Forbes, B., 2012. Critical Characteristics for Corticosteroid Solution Metered Dose Inhaler Bioequivalence. *Mol. Pharmaceutics* 9 (3), 563–569.
- Grasmeijer, F., Hagedoorn, P., Frijlink, H.W., de Boer, A.H., 2012. Characterisation of high dose aerosols from dry powder inhalers. *International Journal of Pharmaceutics* 437 (1–2), 242–249.
- Grasmeijer, F., Hagedoorn, P., Frijlink, H.W., de Boer, A.H., 2013. Drug Content Effects on the Dispersion Performance of Adhesive Mixtures for Inhalation. *PLoS ONE* 8 (8), e71339 EP -.
- Guchardi, R., Frei, M., John, E., Kaerger, J., 2008. Influence of fine lactose and magnesium stearate on low dose dry powder inhaler formulations. *International Journal of Pharmaceutics* 348 (1-2), 10–17.
- Hagedoorn, P., Grasmeijer, F., Noort, M.v.d., Frijlink, H.W., de Boer, A.H., 2011. The effect of mixing time on dispersion performance of carrier based mixtures in relation to initial carrier payload. *Drug Delivery To The Lungs* 22, 149–152.
- Hartmann, T., 2004. Pulverinhalation - Einfluss des Mischverfahrens auf die Feinpartikelfraktion: Diplomarbeit, 87 pp.
- Hartmann, T., Müller, B.W., Steckel, H., 2008. Apparatus and Method for Continuous Production of Spherical Powder Agglomerates.
- Hartmann, T., Steckel, H., 2004. Influence of mixer type and mixing conditions on delivery efficiency from flowcaps, a capsule-based dry powder inhaler. *Drug Delivery To The Lungs* 15, 178–181.

- Hersey, J.A., 1975. Ordered mixing: A new concept in powder mixing practice. *Powder Technology* 11 (1), 41–44.
- HOSOKAWA MICRON B.V. instruction manual: picomix.
- Islam, N., Stewart, P., Larson, I., Hartley, P., 2004. Lactose Surface Modification by Decantation: Are Drug-Fine Lactose Ratios the Key to Better Dispersion of Salmeterol Xinafoate from Lactose-Interactive Mixtures? *Pharm Res* 21 (3), 492-499.
- Jashnani, R.N., Byron, P.R., Dalby, R.N., 1995. Testing of dry powder aerosol formulations in different environmental conditions. *Int J Pharm* 113 (1), 123–130.
- Jones, M.D., Price, R., 2006. The Influence of Fine Excipient Particles on the Performance of Carrier-Based Dry Powder Inhalation Formulations. *Pharmaceutical Research* 23 (8), 1665–1674.
- Jones, M.D., Price, R., Hooton, J., Dawson, M., Ferrie, A., 2005. Using afm to investigate how fines improve dpi performance. *Drug Delivery To The Lungs* 16, 11–14.
- Kamin, W., Erdnüss, F., Krämer, I., 2013. Inhalation solutions — Which ones may be mixed? Physico-chemical compatibility of drug solutions in nebulizers — Update 2013. *J Cyst Fibros*.
- Kaye, B.H., Gratton-Liimatainen, J., Faddis, N., 1995. Studying the Avalanching Behaviour of a Powder in a Rotating Disc. *Part. Part. Syst. Charact.* 12 (5), 232–236.
- Khassawneh, B.Y., Al-Ali, M.K., Alzoubi, K.H., Batarseh, M.Z., Al-Safi, S.A., Sharara, A.M., Alnasr, H.M., 2008. Handling of Inhaler Devices in Actual Pulmonary Practice: Metered-Dose Inhaler Versus Dry Powder Inhalers. *Respiratory Care* 53 (3), 324–328.
- Labiris, N.R., Dolovich, M.B., 2003. Pulmonary drug delivery. Part I: Physiological factors affecting therapeutic effectiveness of aerosolized medications. *Brit J Clin Pharmacol* 56 (6), 588–599.
- Lacey, P.M.C., 1954. Developments in the theory of particle mixing. *J. Appl. Chem.* 4 (5), 257–268.
- Le, V.N.P., Robins, E., Flament, M.P., 2010. Air permeability of powder: A potential tool for Dry Powder Inhaler formulation development.

- European Journal of Pharmaceutics and Biopharmaceutics 76 (3), 464–469.
- Learoyd, T.P., Burrows, J.L., French, E., Seville, P.C., 2008. Chitosan-based spray-dried respirable powders for sustained delivery of terbutaline sulfate. *European Journal of Pharmaceutics and Biopharmaceutics* 68 (2), 224–234.
- Lewis, D.A., Young, P.M., Buttini, F., Church, T., Colombo, P., Forbes, B., Haghi, M., Johnson, R., O’Shea, H., Salama, R., Traini, D., 2013. Towards the bioequivalence of pressurised metered dose inhalers 1: Design and characterisation of aerodynamically equivalent beclomethasone dipropionate inhalers with and without glycerol as a non-volatile excipient. *European Journal of Pharmaceutics and Biopharmaceutics*.
- Lindberg, N., Pålsson, M., Pihl, A., Freeman, R., Freeman, T., Zetzener, H., Enstad, G., 2004. Flowability Measurements of Pharmaceutical Powder Mixtures with Poor Flow Using Five Different Techniques. *Drug Development and Industrial Pharmacy* 30 (7), 785–791.
- Littringer, E.M., Mescher, A., Schröttner, H., Achelis, L., Walzel, P., Urbanetz, N.A., 2012. Spray dried mannitol carrier particles with tailored surface properties – The influence of carrier surface roughness and shape. *Eur J Pharm Biopharm* 82 (1), 194–204.
- Louey, M.D., Razia, S., Stewart, P.J., 2003. Influence of physico-chemical carrier properties on the in vitro aerosol deposition from interactive mixtures. *International Journal of Pharmaceutics* 252 (1-2), 87–98.
- Louey, M.D., Stewart, P.J., 2002. Particle Interactions Involved in Aerosol Dispersion of Ternary Interactive Mixtures. *Pharmaceutical Research* 19 (10), 1524–1531.
- Lucas, P., Anderson, K., Staniforth, J.N., 1998a. Protein Deposition from Dry Powder Inhalers: Fine Particle Multiplets as Performance Modifiers. *Pharmaceutical Research* 15 (4), 562–569.
- Lucas, P., Clarke, M.J., Anderson, K., Tobyn, M.J., Staniforth, J.N., 1998b. The role of fine particle excipients in pharmaceutical dry powder aerosoles. *Respiratory Drug Delivery VI*, 243–250.
- Markefka, P., 2004. Oberflächeneigenschaften von Laktose als Hilfsstoff in der pulmonalen Applikation. Christian-Albrechts-Universität zu Kiel.

- Mitchell, J., Newman, S., Chan, H.-K., 2007. In vitro and in vivo aspects of cascade impactor tests and inhaler performance: A review. *AAPS PharmSciTech* 8 (4), 237–248.
- Mutschler, E., Geisslinger, G., Kroemer, H.K., Ruth, P., Schäfer-Korting, M., 2008. *Mutschler Arzneimittelwirkungen: Lehrbuch der Pharmakologie und Toxikologie ; mit einführenden Kapiteln in die Anatomie, Physiologie und Pathophysiologie ; 264 Tabellen, 9., vollst. neu bearb. und erw. Aufl ed. Wiss. Verl.-Ges., Stuttgart, XXVI, 1244 S.*
- Mutschler, E., Thews, G., Schaible, H.-G., Vaupel, P., 2007. *Anatomie, Physiologie, Pathophysiologie des Menschen: 140 Tabellen, 6., völlig überarb. und erw. Aufl ed. Wiss. Verl.-Ges., Stuttgart, XXI, 981 S.*
- Navaneethan, C.V., Missaghi, S., Fassihi, R., 2005. Application of powder rheometer to determine powder flow properties and lubrication efficiency of pharmaceutical particulate systems. *AAPS PharmSciTech* 6 (3), E398.
- Newman, S.P., 2004. Spacer Devices for Metered Dose Inhalers. *Clin Pharmacokinet* 43 (6), 349-360.
- Ng, B., Kwan, C., Ding, Y., Ghadiri, M., Fan, X., 2007. Solids motion in a conical frustum-shaped high shear mixer granulator. *Chemical Engineering Science* 62 (3), 756–765.
- Onoue, S., Yamada, S., 2013. Pirfenidone in respirable powder form for the treatment of pulmonary fibrosis: a safer alternative to the current oral delivery system? *Therapeutic Delivery* 4 (8), 887–889.
- Ph. Eur., 2011. 2.9.18 Zubereitungen zur Inhalation: Aerodynamische Beurteilung feiner Teilchen, 7th ed. *Europäisches Arzneibuch 7.0, amtliche deutsche Ausgabe*, 384–399.
- Phipps, P.R., Gonda, I., 1990. Droplets produced by medical nebulizers. Some factors affecting their size and solute concentration. *CHEST* 97 (6), 1327.
- Pilcer, G., Amighi, K., 2010. Formulation strategy and use of excipients in pulmonary drug delivery. *Int J Pharm* 392 (1-2), 1–19.
- Pitcairn, G., Reader, S., Pavia, D., Newman, S., 2005. Deposition of Corticosteroid Aerosol in the Human Lung by Respimat® Soft Mist™ Inhaler Compared to Deposition by Metered Dose Inhaler or by Turbuhaler® Dry Powder Inhaler. *J Aerosol Med* 18 (3), 264–272.

- 
- Podczeczek, F., 1996. Assessment of the mode of adherence and the deformation characteristics of micronized particles adhering to various surfaces. *International Journal of Pharmaceutics* 145 (1-2), 65–76.
- Price, D., Bosnic-Anticevich, S., Briggs, A., Chrystyn, H., Rand, C., Scheuch, G., Bousquet, J., 2013. Inhaler competence in asthma: Common errors, barriers to use and recommended solutions. *Resp Med* 107 (1), 37–46.
- Price, R., 2009. The fluidisation behaviour of pharmaceutical powders and their influence on particle deaggregation. *Powderflow 2009*, 16 December 2009, London.
- Price, R., 2010. Low and High Energy Blending, 19 October 2010, Parma.
- Price, R., Shur, J., 2010. Powder Rheology: A New Technique to Predict the Performance of Inhaled Powder Formulations. *RDD* (1), 331–340.
- Price, R., Young, P.M., Edge, S., Staniforth, J.N., 2002. The influence of relative humidity on particulate interactions in carrier-based dry powder inhaler formulations. *Int J Pharm* 246 (1-2), 47–59.
- Rahimpour, Y., Kouhsoltani, M., Hamishehkar, H., 2013. Alternative carriers in dry powder inhaler formulations. *Drug Discov Today*.
- Rasenack, N., Müller, B.W., 2004. Micron-Size Drug Particles: Common and Novel Micronization Techniques. *Pharm Dev Technol* 9 (1), 1–13.
- Riley, T., Christopher, D., Arp, J., Casazza, A., Colombani, A., Cooper, A., Dey, M., Maas, J., Mitchell, J., Reiners, M., Sigari, N., Tougas, T., Lyapustina, S., 2012. Challenges with Developing In Vitro Dissolution Tests for Orally Inhaled Products (OIPs). *AAPS PharmSciTech* 13 (3), 978–989.
- Schulze, D., 2008. *Powders and bulk solids: Behavior, characterization, storage and flow*. Springer, Berlin, New York, 1 online resource (xvi, 511).
- Shaw, R.J.S., Waller, J.F., Hetzel, M.R., Clark, T.J.H., 1982. Do oral and inhaled terbutaline have different effects on the lung? *Brit J Dis Chest* 76 (0), 171–176.
- Shur, J., Harris, H., Jones, M.D., Kaerger, J., Price, R., 2008. The Role of Fines in the Modification of the Fluidization and Dispersion Mechanism Within Dry Powder Inhaler Formulations. *Pharmaceut Res* 25 (7), 1631–1640.

- Smith, I.J., Parry-Billings, M., 2003. The inhalers of the future? A review of dry powder devices on the market today. *Pulmonary Pharmacology & Therapeutics* 16 (2), 79–95.
- Soh, J.L.P., Liew, C.V., Heng, Paul W. S., 2006. New Indices to Characterize Powder Flow Based on Their Avalanching Behavior. *Pharmaceutical Development and Technology* 11 (1), 93–102.
- Staniforth, J.N., 1995. Performance-Modifying Influences in Dry Powder Inhalation Systems. *Aerosol Science and Technology* 22 (4), 346–353.
- Staniforth, J.N., 1996. Pre-Formulation Aspects of Dry Powder Aerosols. *Respiratory Drug Delivery V*, 65–73.
- Stank, K., 2014. Oberflächenmodifizierung von Wirkstoffen zur Inhalation. Christian-Albrechts-Universität zu Kiel, Kiel.
- Steckel, H., Bolzen, N., 2004. Alternative sugars as potential carriers for dry powder inhalations. *International Journal of Pharmaceutics* 270 (1–2), 297–306.
- Steckel, H., Eskandar, F., 2003. Factors affecting aerosol performance during nebulization with jet and ultrasonic nebulizers. *Eur J Pharm Sci* 19 (5), 443–455.
- Tay, T., Das, S., Stewart, P., 2010. Magnesium stearate increases salbutamol sulphate dispersion: What is the mechanism? *International Journal of Pharmaceutics* 383 (1-2), 62–69.
- Tee, S., Marriott, C., Zeng, X.-M., Martin, G., 2000. The use of different sugars as fine and coarse carriers for aerosolised salbutamol sulphate. *Int J Pharm* 208 (1-2), 111–123.
- Telko, M.J., Hickey, A.J., 2005. Dry Powder Inhaler Formulation. *Respiratory Care* 50 (9), 1209–1227.
- Thalberg, K., Lindholm, D., Axelsson, A., 2004. Comparison of different flowability tests for powders for inhalation. *Powder Technology* 146 (3), 206–213.
- Traini, D., Young, P.M., Thielmann, F., Acharya, M., 2008. The Influence of Lactose Pseudopolymorphic Form on Salbutamol Sulfate–Lactose Interactions in DPI Formulations. *Drug Dev Ind Pharm* 34 (9), 992–1001.

- 
- Trofast, E.A.C., Falk, E.J., 1994. AGGLOMERATION OF FINELY DIVIDED POWDERS.
- USP, 2013a. <1174>POWDER FLOW. The United States Pharmacopeia USP 37, The National Formulary NF 32.
- USP, 2013b. <601> AEROSOLS, NASAL SPRAYS, METERED-DOSE INHALERS; AND DRY POWDER INHALERS. The United States Pharmacopeia USP 37, The National Formulary NF 32.
- Wachtel, H., 2009. 2.9.18: Zubereitungen zur Inhalation: Aerodynamische Beurteilung feiner Teilchen, in: Böhme, H., Hartke, K., Hartke, H., Wichtl, M., Bracher, F. (Eds.), Arzneibuch-Kommentar, 32 ed. Wissenschaftliche Verlagsgesellschaft mbH, Stuttgart.
- Winkler, R., 2013. Konzept eines aktiven Pulverinhalators. Johannes Gutenberg-Universität, Mainz.
- Wittmann, R., Schwarz, E., Steckel, H., 2012. The Influence of Amorphous Content in Lactose on the De-agglomeration Behavior of Powders for Inhalation. *Drug Delivery To The Lungs* 23.
- Young, P.M., Chan, H.-K., Chiou, H., Edge, S., Tee, T.H.S., Traini, D., 2007. The influence of mechanical processing of dry powder inhaler carriers on drug aerosolization performance. *J. Pharm. Sci* 96 (5), 1331–1341.
- Young, P.M., Edge, S., Triani, D., Jones, M., Price, R., Elsabawi, D., Urry, C., Smith, C., 2005. The influence of dose on the performance of dry powder inhalation systems. *Int J Pharm* 296 (1-2), 26–33.
- Young, P.M., Price, R., 2004. The influence of humidity on the aerosolisation of micronised and SEDS produced salbutamol sulphate. *Eur J Pharm Sci* 22 (4), 235–240.
- Young, P.M., Tobyn, M.J., Price, R., Buttrum, M., Dey, F., 2006. The use of colloid probe microscopy to predict aerosolization performance in dry powder inhalers: AFM and in vitro correlation. *J. Pharm. Sci.* 95 (8), 1800–1809.
- Zeng, X.-M., Martin, G.P., Marriott, C., Pritchard, J., 2001. Lactose as a carrier in dry powder formulations: The influence of surface characteristics on drug delivery. *J. Pharm. Sci.* 90 (9), 1424–1434.
- Zeng, X.-M., Martin, G.P., Tee, S.-K., Marriott, C., 1998. The role of fine particle lactose on the dispersion and deaggregation of salbutamol sulphate in an
-

- air stream in vitro. *International Journal of Pharmaceutics* 176 (1), 99–110.
- Zhou, Q., Qu, L., Gengenbach, T., Denman, J.A., Larson, I., Stewart, P.J., Morton, D.A., 2011. Investigation of the extent of surface coating via mechanofusion with varying additive levels and the influences on bulk powder flow properties. *International Journal of Pharmaceutics* 413 (1-2), 36–43.
- Zhou, Q.T., Qu, L., Larson, I., Stewart, P.J., Morton, D.A., 2010. Improving aerosolization of drug powders by reducing powder intrinsic cohesion via a mechanical dry coating approach. *International Journal of Pharmaceutics* 394 (1-2), 50–59.
- Zhu, K., Tan, R.B., Kiong Ng, W., Shen, S., Zhou, Q., Heng, P.W., 2008. Analysis of the influence of relative humidity on the moisture sorption of particles and the aerosolization process in a dry powder inhaler. *J Aerosol Sci* 39 (6), 510–524.

## **DANKSAGUNG**

Am Ende dieser Arbeit bleibt mir noch allen zu danken, die bei der Entstehung dieser Arbeit direkt oder indirekt mitgewirkt haben und meine Jahre am Institut zu einer lehrreichen und schönen Zeit gemacht haben!

Ein herzlicher Dank gilt dabei zunächst meinem Doktorvater, Herrn Prof. Dr. Hartwig Steckel, für die Überlassung des interessanten und herausfordernden Forschungsthemas und der freundlichen Aufnahme in seinen Arbeitskreis. Er hat mir viele Freiräume bei der Ausgestaltung meines Themas eingeräumt, auf der anderen Seite aber auch immer mit Rat und Tat - und vor allem unkomplizierter Hilfe - zur Seite gestanden.

Ein weiterer Dank gilt Herrn Prof. Dr. H.W. Frijlink von der Universität in Groningen, der mir die Möglichkeit gab, vier Wochen innerhalb seines Arbeitskreises die Grundlagen für den ersten Teil dieser Arbeit zu legen. Die Expertise und große Gastfreundlichkeit, vor allem von Floris Grasmeijer und Dr. Anne de Boer, machten den Aufenthalt in Groningen zu einer wertvollen Erfahrung für mich. Doch auch den weiteren Bekanntschaften aus dem Arbeitskreis (Anne Lexmond, Wouter Tonnis, Marcel Hoppentocht, Hans de Waard und Paul Hagedoorn) möchte ich für die nette Zeit dort danken.

Des Weiteren möchte ich mich bei Jamie Clayton, Dr. Brian Armstrong und Tim Freeman von Freeman Technology bedanken. Sie standen mir immer mit schneller und umfänglicher Hilfe bei sämtlichen Fragen rund um das FT4 Pulverrheometer zur Seite.

Dr. Anna Giulia Balducci und Dr. Francesca Buttini von der Universität Parma danke ich für Durchführung der Dissolutionstests.

Was wäre die Arbeit ohne Kollegen?! Simon und Lars – wir haben viele fachliche und manchmal vielleicht auch etwas weniger fachliche Diskussionen geführt, uns aber stets gegenseitig vorangetrieben. Ähnliches gilt für Kirsten, Katha, Ronja, Sabrina, Sven S. und Gereon. Wir haben gemeinsam viel erlebt – sei es bei der Arbeit, im Praktikum, auf Dienstreisen oder auch privat – danke dafür! Sabrina danke ich zudem für das Korrekturlesen dieser Arbeit und Regina S. für ihre stetige Diskussionsbereitschaft und wertvollen Tipps und Anregungen.

Ein weiterer Dank geht an Marieke, Maren K. und Christian, die mir geholfen haben, die ersten Hürden der Promotionszeit zu meistern. Besonders Christian danke ich zudem für seine Ratschläge, die bis zum Ende meiner Doktorandenzeit angehalten haben.

Schließlich möchte ich einen großen Dank an alle alten und neuen Kollegen des Arbeitskreises richten, die für ein durchweg positives Arbeitsumfeld gesorgt haben.

Hierzu haben auch maßgeblich Regina K., Maren R., Hanna, Simone, Arne, Volkmar, Detlef, Dirk, Rüdi, Kalle, Rebecca und Denissa beigetragen. Ich konnte mich während meiner Promotionszeit immer auf Eure versierte und schnelle Hilfe bei diversen technischen und nicht-technischen Problemen verlassen! Rüdi, vielen Dank zudem für die spannenden Einblicke in das Kieler Kulturleben – ich habe die abwechslungsreichen Gespräche mit Dir immer sehr genossen.

Schließlich möchte ich mich von ganzem Herzen bei Ricarda für ihre unermüdliche Unterstützung während der Zeit in Kiel bedanken! Ich konnte in jeder Situation auf Dich zählen und Du hast mir über so manches Tief erfolgreich hinweggeholfen.

Meinen Eltern und meinem Bruder danke ich besonders für ihren stetigen Rückhalt und für das Interesse an meinen Vorhaben - nicht nur während der Promotionszeit! Sie haben dadurch maßgeblich dazu beigetragen, dass ich diese Arbeit erfolgreich beenden konnte.



# **LEBENS LAUF**

## **Persönliche Daten**

Nachname	Cordts
Vorname	Eike
Geburtsdatum	17. Dezember 1984
Geburtsort	Rotenburg (Wümme)
Staatsangehörigkeit	deutsch

## **Promotion**

Seit 2010	Wissenschaftlicher Mitarbeiter in der Arbeitsgruppe von Herrn Prof. Dr. Hartwig Steckel am Pharmazeutischen Institut der Christian-Albrechts-Universität zu Kiel
-----------	--

## **Studium der Pharmazie**

2010	Dritter Abschnitt der Pharmazeutischen Prüfung und Approbation als Apotheker
2009 -2010	Pharmaziepraktikant, Welfenhof-Apotheke, Wiesbaden
2008 - 2009	Pharmaziepraktikant, Boehringer Ingelheim Pharma GmbH & Co. KG, Ingelheim
2008	Zweiter Abschnitt der Pharmazeutischen Prüfung
2006	Erster Abschnitt der Pharmazeutischen Prüfung
2004 - 2008	Westfälische Wilhelms-Universität Münster

## **Schulbildung**

2004	Abitur
2001 – 2002	Squalicum High School, Bellingham, WA, USA
1997 – 2004	Ratsgymnasium Rotenburg (Wümme)
1991 – 1997	Grundschule und Orientierungsstufe Visselhövede

## Erklärung nach § 8 der Promotionsordnung

Hiermit erkläre ich gemäß § 8 der Promotionsordnung der Mathematisch-Naturwissenschaftlichen Fakultät der Christian-Albrechts-Universität zu Kiel, dass ich die vorliegende Arbeit, abgesehen von der Beratung durch meinen Betreuer, selbstständig und ohne fremde Hilfe verfasst habe. Ich habe keine anderen als die angegebenen Quellen oder Hilfsmittel verwendet und die den benutzten Werken wörtlich oder inhaltlich entnommenen Stellen als solche kenntlich gemacht. Die vorliegende Arbeit ist unter Einhaltung der Regeln guter wissenschaftlicher Praxis entstanden und wurde bisher bei keiner anderen Universität zur Begutachtung eingereicht.

Eike Cordts